Parameter Estimation from Polymerization Reactor and Product Property Data: Missing Data Approach

by

Anouk M. Tremblay

A thesis submitted to the Department of Chemical Engineering
in partial fulfilment of the requirements for the degree of
Master of Science (Engineering)

Queen's University
Kingston, Ontario
January, 1999

ABSTRACT

Kinetic rate parameters were fitted successfully, for a dynamic mechanistic model describing ethylene homopolymerization in a laboratory-scale semi-batch reactor, using data sets with missing data structure. The response-variable data consisted of reactor operating data, collected at regular time intervals throughout each experimental run, and product property data, measured only at the end of each experimental run. Hence, the resulting response-variable data structure for 16 experimental runs was block rectangular. There were a total of 1920 polymerization rate observations (operating data) in the first block and 16 observations of both weight and number average molecular weight (product property data) in the second block. This type of data was available at each of the three different operating temperatures.

The three-response model that was fitted described non-isothermal polymerization using a Ziegler-Natta catalyst with two types of sites. Successful parameter estimation was achieved using the parameter estimation subroutine GREG, assuming a known diagonal covariance matrix for the response measurements. The estimated polydispersities, ranging from 3 to 5, were consistently lower than the corresponding observed polydispersities. Assessment of the validity of the model revealed that predictions of the polymerization rates and weight average molecular weights were satisfactory, while the number average molecular weights were consistently overpredicted.

Acknowledgements

To my supervisors, Drs. K. B. McAuley and D. W. Bacon, I express my gratitude for their invaluable ideas, support, and constructive criticisms, without which this project would not have taken life.

I would like to acknowledge Dr. Hsu for giving me access to the valuable experimental data that became the foundation of this work and for our enlightening conversations at the onset of my project.

Many thanks to Dr. Bain for his assistance in obtaining the FORTRAN subroutine, GREG, used during my thesis. His time and interest were much appreciated.

Most of all, I thank my parents and sisters, Julie and Marie-Claude, for their words of encouragement and Jon for his patience during the numerous revisions. To all my family and friends, thank you for your support.

Table of Contents

Chapter 1: Introduction 1

Chapter 2: Literature Review 4
2.1 Introduction 4
2.2 Free Radical Polymerization 6
2.2.1 Methyl Methacrylate Polymerization 6
2.2.2 Free Radical Ethylene Polymerization 7
2.3 Ziegler-Natta and Metallocene Catalyzed Polymerization 10
2.3.1 Propylene Polymerization 11
2.3.2 Ethylene Ziegler-Natta and Mettalocene (Co)Polymerization 12
2.4 Ziegler-Natta Catalyst Properties 18
2.4.1 Broad Molecular Weight Distribution 18
2.4.2 Number of Potential Catalyst Sites 19
2.5 Parameter Transformations 20
2.6 Missing Data 21

Chapter 3: Parameter Estimation 25
3.1 Data Structure 25
3.1.1 Homopolymerization Data 26
3.2 Objective Functions 26
3.2.1 Single Response 26
3.2.2 Multiresponse (m responses) 27
3.2.3 Maximum-density Algorithm for Parameter Estimation 29
3.3 Differential and Algebraic Equation Solver 31
3.4 General Application to Case Studies 32

Chapter 4: Development of a One Type of Site Model for Homopolymerization of Ethylene 34
4.1 Experimental Design 34
4.2 Kinetic Model for Ziegler-Natta Catalyst with One Type of Site 36
4.2.1 Number of Potential Active Sites 39
4.2.2 Parameter Effects 40
4.2.3 Ordinary Differential Equation Tolerances 41
4.3 Model with One Type of Catalyst Site and No Monomer Diffusion 43
4.3.1 Fitting a Single Response Model 44
4.3.2 Three-response Model with Unknown Diagonal Covariance Matrix 44
4.3.3 Sample Variances of Response Measurements 47
4.3.4 Fitting a Two-Response Model with Known Diagonal Covariance Matrix 49
4.3.5 Fitting a Three-Response Model with Known Diagonal Covariance Matrix 50

Chapter 5: Models for Ziegler-Natta Catalyst with Two Types of Sites 57
5.1 Model with Two Types of Sites and Monomer Diffusion 57
5.1.1 Parameter Transformations 61
5.2 Single Response Model 62
5.3 Multiresponse Model with Known Diagonal Covariance Matrix 63
5.4 Non-isothermal Multiresponse Model 67
5.5 Model Validation 74

Chapter 6: Conclusions and Recommendations 78

References 81

Nomenclature 86

Appendix A 89

Appendix B 90

Appendix C 93

Appendix D 96

Appendix E 97

Appendix F 106

Appendix G 107

Vitae 114

List of Figures

Figure 4.1 Fitted molecular weight values from the three-response model (R_p, $\overline{M}_n$, and $\overline{M}_w$) assuming an unknown diagonal covariance matrix 46
Figure 4.2 Fitted values from the two-response model (R_p and $\overline{M}_w$) assuming a known diagonal covariance matrix 50
Figure 4.3 Fitted values from the two-response model (R_p and $\overline{M}_n$) assuming a known diagonal covariance matrix 50
Figure 4.4 Block rectangular data used in parameter estimation 51
Figure 4.5 Fitted values from the three-response model (R_p, $\overline{M}_n$, and $\overline{M}_w$) assuming a known diagonal covariance matrix 53
Figure 4.6 Fitted polymerization rate values for replicate runs at 70°C from a three-response model (R_p, $\overline{M}_n$, and $\overline{M}_w$) assuming a known diagonal covariance matrix 54

Figure 5.1 Temperature dependence of rate constants for the three-response model (R_p, $\overline{M}_n$, and $\overline{M}_w$) 68
Figure 5.2 Fitted MW response values for the non-isothermal three-response model (R_p, $\overline{M}_n$, and $\overline{M}_w$) with two active site types and monomer diffusion, assuming a known diagonal covariance matrix 73
Figure 5.3 Three-response predictions for two experimental runs at each temperature group (62, 70, and 78°C) 75
Figure C1. Fitted and observed polymerization rate values for the single response model with one type of site and no monomer diffusion at 70°C 93
Figure E1. Fitted polymerization rate response values for the non-isothermal three-response model (R_p, M_n, and M_w) with two active site types and monomer diffusion, assuming a known diagonal covariance matrix 97
Figure G1. Predicted polymerization rate values for the non-isothermal three-response model (R_p, M_n, and M_w) with monomer diffusion, assuming a known diagonal covariance matrix 107
Figure G2. Predicted molecular weight values for the non-isothermal three-response model (R_p, M_n, and M_w) with monomer diffusion, assuming a known diagonal covariance matrix 113

List of Tables

Table 3.1 Complete, block rectangular, and irregular data structures 25
Table 3.2 Schematic representation of the ethylene homopolymerization data structure 26

Table 4.1 Experimental design factors and actual settings for ethylene homopolymerization experiments (Shariati, 1996) 35
Table 4.2 Catalyst composition 35
Table 4.3 Kinetics for a single type of site model 36
Table 4.4 Material balances and initial conditions 37
Table 4.5 Correlation matrix for parameter estimates for all three fixed values of k_p 40
Table 4.6 Tolerance array for DDASAC with the one type of active site model 42
Table 4.7 Performance comparison 43
Table 4.8 Parameter estimates from a single response model with one active site type and no monomer diffusion (GREG *level* 10) 44
Table 4.9 Parameter estimates from a three-response model (R_p, $\overline{M}_n$, and $\overline{M}_w$) with one type of active sites and no monomer diffusion, assuming an unknown diagonal covariance matrix (GREG *level* 32) 45
Table 4.10 Sample variances of response measurements with their 95% confidence intervals 49
Table 4.11 Parameter estimates from a three-response model (R_p, $\overline{M}_n$, and $\overline{M}_w$) with one type of active sites and no monomer diffusion, assuming a known diagonal covariance matrix (GREG *level* 22) 51
Table 4.12 Approximate 95% confidence intervals for the observed polydispersity values for a three-response model (R_p, $\overline{M}_n$, and $\overline{M}_w$) with one type of active sites and no monomer diffusion, assuming a known diagonal covariance matrix (GREG *level* 32) 56

Table 5.1 Kinetics for a two types of sites model 58
Table 5.2 Material balances and initial conditions for the two types of sites model 60
Table 5.3a Parameter estimates from a single response model at 70°C with two active site types and monomer diffusion (GREG *level* 10) 63
Table 5.3b Parameter estimates from a single response model at 62°C with two active site types and monomer diffusion (GREG *level* 10) 63
Table 5.4a Parameter estimates from a three-response model (R_p, $\overline{M}_n$, and $\overline{M}_w$) at 78°C with two active site types and monomer diffusion (GREG *level* 22) 64
Table 5.4b Parameter estimates from a three-response model (R_p, $\overline{M}_n$, and $\overline{M}_w$) at 70°C with two active site types and monomer diffusion (GREG *level* 22) 64
Table 5.4c Parameter estimates from a three-response model (R_p, $\overline{M}_n$,

and $\overline{M}_w$) at 62°C with two active site types and monomer diffusion (GREG *level* 22) 65
Table 5.5a Correlation matrix for the parameter estimates at 78°C (corresponding to Table 5.4a) 65
Table 5.5b Correlation matrix for the parameter estimates at 70°C (corresponding to Table 5.4b) 65
Table 5.5c Correlation matrix for the parameter estimates at 62°C (corresponding to Table 5.4c) 66
Table 5.6 Observed and estimated polydispersities from the fitted models for individual temperature groups 67
Table 5.7a Parameter estimates from the non-isothermal three-response model (R_p, $\overline{M}_n$, and $\overline{M}_w$) with two active site types and monomer diffusion, assuming a known diagonal covariance matrix (GREG *level* 22) 69
Table 5.7b Correlation matrix for the parameter estimates 70
Table 5.8 Observed polydispersity values along with their approximate 95% confidence intervals and corresponding estimated polydispersity values from the fitted non-isothermal three-response model (R_p, $\overline{M}_n$, and $\overline{M}_w$) with two active site types and monomer diffusion, assuming a known diagonal covariance matrix 71
Table 5.9 Parameter estimates for the model validation with 30 runs and a non-isothermal three-response model (R_p, $\overline{M}_n$, and $\overline{M}_w$) with two active site types and monomer diffusion, assuming a known diagonal covariance matrix (GREG *level* 22) 74
Appendix B1. Polymerization conditions for the experimental runs at 62°C 90
Appendix B2. Polymerization conditions for the experimental runs at 70°C 91
Appendix B3. Polymerization conditions for the experimental runs at 78°C 92
Appendix D1. Correlation matrix for the parameter estimates from a single response model at 70°C with two types of sites and monomer diffusion 96
Appendix D2. Correlation matrix for the parameter estimates from a single response model at 62°C with two types of sites and monomer diffusion 96

Chapter 1: Introduction

In some experimental situations observations of the response variables are not always available at the same frequency. This creates a missing data structure. Semibatch polymerization experiments fall into this category when the reactor is not fitted with equipment to remove polymer samples throughout the experiment. Professor Stewart and his coworkers at the University of Wisconsin-Madison have developed GREG, a FORTRAN subroutine for general regression analysis (Stewart, 1995), which can estimate parameters in systems with missing data. GREG has many options that gives the user the flexibility to properly define the type of missing data structure and the status of the covariance matrix for the response variables, which in turn determine the objective function to be minimized for parameter estimation.

The objectives of the current study are as follows:

- to estimate rate constants in an ordinary differential equation model from a missing data structure;
- to make use of combined reactor operating data and product property data in parameter estimation; and
- to assess the validity of the fitted model.

The proposed kinetic model of interest involved three responses describing the non-isothermal behavior of a Ziegler-Natta catalyst with two types of sites and monomer diffusion. The proposed model for the parameter estimation consisted of a set of ordinary differential equations along with three algebraic equations (one for each response

variable: polymerization rate, weight average molecular weight, and number average molecular weight). As a starting point for estimating parameters in the proposed model, a simplified model involving fewer parameters was fitted first. The simplified model, involving only a single response (polymerization rate) describing the isothermal behavior of a one type of site Ziegler-Natta catalyst and no monomer diffusion, contained three parameters (rate constants).

The reactor operating data and product property data were collected from experimental homopolymerization reactions of ethylene over a multi-sited Ziegler-Natta catalyst. Polymerization rate data (operating data) were available at regular time intervals during the one-hour experimental runs, while molecular weight properties (product property data) were available only at the end of each experimental run. Combining the polymerization rate data with the molecular weight properties data (three-response model) for parameter estimation resulted in a missing data structure. For each experimental run the missing data structure had 120 polymerization rate observations, one number average molecular weight observation, and one weight average molecular weight observation.

Parameter estimates from the simplified single response model were used as initial values for the parameters in a simplified three-response model. The simplified three-response model, involving the polymerization rate and the molecular weight response variables, described the isothermal behavior of a one type of Ziegler-Natta catalyst site with no monomer diffusion limitation. Since the kinetic model must include

at least two types of catalyst sites in order to properly predict the observed broad molecular weight distribution, the estimates from the simplified three-response model were used as initial values for the parameters in the model with two types of sites.

The validity of the proposed kinetic model was assessed by fitting it to 30 experimental runs and using that fitted model to predict the values of the three responses for the remaining 18 experimental runs.

Chapter 2 contains a literature review of some of the relevant published polymerization research involving different approaches used to deal with full or missing data structures, the number of parameters estimated, and the objective function used to fit the empirical model. The problems of determining the initial number of potential catalyst sites, parameter transformations, and missing data outside the polymerization field are also addressed. Chapter 3 briefly describes the FORTRAN subroutine GREG used for parameter estimation. Parameter estimation results from the models that assume a one type of Ziegler-Natta catalyst site are presented in Chapter 4, while Chapter 5 deals with both isothermal and non-isothermal two types of Ziegler-Natta catalyst sites models. Conclusions and recommendations regarding the model and parameter estimation results are presented in Chapter 6.

Chapter 2: Literature Review

2.1 Introduction

The most common types of data collected for kinetic modeling of polymerization reactions are polymer quantity (polymerization rate data) and polymer quality (molecular weight data). The former are usually recorded frequently throughout the reaction. To obtain molecular weight data, a sample must be removed from the reactor and analyzed. If it is not possible to remove samples throughout an experimental run, a sample is taken at the end of the run. Ideally, polymerization reactions could be run for various lengths of time to characterize the polymer quality with respect to time, but that procedure is impractical in many cases due to the cost and time involved. The parameter estimation problem is then how to combine data collected over time with measured values obtained only at the end point of the reaction. Since no papers in the polymerization literature deal directly with ways to combine on-line and off-line data, published techniques for handling missing data are presented in Section 2.6.

Kinetic modeling in the current study was performed using experimental data collected from a 0.5 L semi-batch reactor by Shariati (1996). The semi-batch ethylene slurry homopolymerization experiments used a polymer-supported heterogeneous Ziegler-Natta catalyst. Polymerization rate data were available throughout the reaction; however, it was impossible to remove polymer samples from the apparatus during an experimental run. Polymer samples collected at the end of each experimental run were analyzed using gel permeation chromatography (GPC) to determine their molecular

weight distributions (MWDs), from which the number and weight average molecular weights ($\overline{M}_n$ and $\overline{M}_w$, respectively) were obtained.

The following two sections contain brief reviews of approaches to kinetic modeling and parameter estimation for polymerization reactions. Section 2.2 deals with free radical polymerization, while Ziegler-Natta and metallocene catalyst reactions are considered in Section 2.3. Free radical and Ziegler-Natta polymerizations are discussed separately, because it is considerably more difficult to determine kinetic parameters for Ziegler-Natta polymerizations than it is for free radical polymerizations. In the propagation step of free radical polymerization, the polymer grows away from the initiator. Once propagation has started, the initiator does not affect the reaction rate and it is therefore possible to determine kinetic parameters without considering the type of initiator used. As such, values of kinetic parameters for free radical polymerization reactions are tabulated in the literature. In Ziegler-Natta and metallocene polymerizations, however, the catalyst site is coordinated to the propagating end of the polymer chain. The rates of propagation and other reactions then depend on the type of catalyst site employed for polymerization. Since there are many types of active catalyst sites that can be used for Ziegler-Natta polymerization, and each catalyst can contain multiple types of sites, determining appropriate rate constants for use in kinetic models of Ziegler-Natta catalyzed polymerizations can be very difficult. Methods for determining the number of potential catalyst sites and the use of parameter transformations in kinetic modeling are discussed in Sections 2.4 and 2.5, respectively.

2.2 Free Radical Polymerization

2.2.1 Methyl Methacrylate Polymerization

Ponnuswamy and Penlidis (1988) performed batch solution polymerization of methyl methacrylate in a 5.0 L pilot plant reactor. The experiments were conducted at various temperatures (65 – 75°C) and initiator concentrations (0.05 – 0.1 mol/L). Three response variables, conversion, $\overline{M}_n$ and $\overline{M}_w$, were measured throughout the polymerization.

Ponnuswamy and Penlidis used kinetic constants from the literature to obtain predictions with their kinetic model. After comparison of model predictions with their experimental data, they decided that two parameters should be re-estimated. Both parameters were expressed in Arrhenius form using a centering transformation about the mean temperature (Pritchard and Bacon, 1978). Weighted least squares estimation of the parameters was done using the Levenberg-Marquardt method (Bard, 1974) with the ordinary differential equations being solved by a subroutine based on Gear's approach (1971). The entries in the diagonal weighting matrix, **W**, in the objective function (equation 2.1) were the reciprocals of the measurement variances.

The objective function which was minimized to obtain estimates of the parameters θ, was:

$$S(\theta) = \sum_{i=1}^{n} e_i^T W e_i^T \qquad (2.1)$$

where $e_i = Y_i^{exp} - Y_i^{mod}$, with Y_i^{exp} is the i^{th} experimental value of the response variable Y and Y_i^{mod} is the corresponding fitted value of the same response variable, i=1, 2, ..., n.

Since it was possible to get simultaneous measurements of polymer quantity and quality throughout a polymerization run, traditional multiresponse estimation procedures (Bard, 1974) could be used to obtain the parameter estimates.

2.2.2 Free Radical Ethylene Polymerization

Lorenzini et al. (1992) studied high temperature (180 – 280°C) and high pressure (1500 – 1950 bar) free radical ethylene polymerization in a 0.9 L bench-scale continuously-stirred-tank reactor (CSTR). After measuring the quantity of polymer produced at the end of an experimental run, a sample was analyzed to determine the structural properties of the polymer. MWD, $\overline{M}_n$, $\overline{M}_w$, z-average molecular weight ($\overline{M}_z$), and long chain branching index were determined by GPC and viscosity, while other indices for branching and double bonds were analyzed by infrared spectroscopy (IR).

Although all of the data were collected at the end of each experimental run, parameter estimation was performed in two steps: first using polymer quantity data, and then using polymer quality data. The two parameters that were required to predict the polymer production rate varied with temperature and pressure according to equation 2.2:

$$\theta_i = \theta_i^0 \exp\left(-\frac{E_i + P\Delta v_i}{RT}\right) \qquad (2.2)$$

where θ_i represents a temperature and pressure-dependent kinetic parameter, θ_i^0 is the frequency factor, E_i is the activation energy of θ_i, and Δv_i is the activation volume of θ_i. Consequently, six parameters (θ_i^0, E_i, and, Δv_i, i=1, 2) were estimated.

The ten parameters used in modeling the polymer property data also varied with temperature and pressure according to equation 2.2, giving a total of 30 parameters to be estimated. The objective function used by Lorenzini et al. (1992) to estimate the parameters for the structural characteristics listed above was:

$$F = \sum_{r=1}^{n}\left(\sum_{j=1}^{N_c}\delta_j\left(\frac{Y_j^{exp}-Y_j^{mod}}{Y_j^{exp}}\right)_r^2\right)+\sum_{r=1}^{n}\left(\sum_{k=1}^{N_{p,i}}\delta_{MWD,k}\left(w^{exp}(k)-w^{mod}(k)\right)_r^2\right) \qquad (2.3)$$

where n is the number of experimental runs and N_c is the number of structural characteristics, Y_j, that were measured. The superscript 'exp' denotes an experimental value while 'mod' refers to a model prediction. $N_{p,i}$ is the number of points used in the MWD for run i, w(k) is the weight fraction of polymer in the k^{th} fraction of the MWD, and δ_j and δ_{MWD} are weighting coefficients. Weighting factors in the objective function were chosen to emphasize the peak of the MWD rather than its tails. The optimization routines used were Box's Complex method (Box, 1965) and Comet's method (Staha, 1973).

Brandolin et al. (1988) used a plug flow reactor at high pressure for free radical ethylene polymerization with an oxygen initiator. One of the proposed model's assumptions was that the reaction mixture's physical properties changed along the length of the reactor. Consequently, the temperature profile was recorded and temperatures were used as response variables. At the end of each experimental run, samples from the outlet of the reactor were analyzed by GPC and intrinsic viscosity to determine MWD.

The authors used values of kinetic constants from the literature to determine which rate constants most affected the response variables. It was found that the rate constants for initiation, propagation, and termination determined temperature whereas those for thermal degradation, transfer to solvent, and transfer to polymer strongly affected properties of the MWD. Therefore, estimation of the seven parameters was carried out in two steps.

The first step involved minimizing an objective function, F, to fit the temperature profile changes along the reactor:

$$F = \sum_{j=0}^{n} \sum_{i=0}^{f} \left(1 - \frac{T_j^{\mathrm{mod}}(z_i)}{T_j^{\mathrm{exp}}(z_i)} \right)^2 \qquad (2.4)$$

where n is the number of experimental runs, z_i is the axial position for temperature measurement i, $T_j^{mod}(z_i)$ is the predicted temperature at $z = z_i$ for run j, and 'exp' denotes an experimental value. The parameters (order of the oxygen initiation reaction, rate constants for initiation, propagation, and termination) required to produce the calculated temperatures in equation 2.4 were estimated using Powell's method (1964).

A second objective function, G, involving the polymer quality data was then minimized:

$$G = \sum_{r=1}^{n} \left(\sum_{j=1}^{Nc} \left(\frac{Y_j^{\mathrm{exp}} - Y_j^{\mathrm{mod}}}{Y_j^{\mathrm{exp}}} \right)_r^2 \right) \qquad (2.5)$$

where n is the number of experimental runs, Y_j represents the remaining response variables: number and weight average degrees of polymerization and weight-average

branch point number. The parameters in this case were the rate constants for chain transfer to polymer, chain transfer to solvent, and thermal degradation. G was minimized using the Levenberg-Marquardt algorithm. It should be noted that G is the first term on the right hand side of equation 2.3 used by Lorenzini et al. (1992), with equal weighting coefficients. Also, the objective function of Brandolin et al. involved three structural characteristics of the polymer, whereas the objective function of Lorenzini et al. involved eight.

2.3 Ziegler-Natta and Metallocene Catalyzed Polymerization

Although Ziegler-Natta catalysts were developed in the 1950's (Kim et al., 1991; Lorenzini et al., 1991) many aspects of their kinetic behavior are still not well understood (deCarvalho et al., 1989; Rincon-Rubio et al., 1990; Vela Estrada and Hamielec, 1994). The polymerization models reviewed in this chapter result from kinetic mechanisms that include initiation, propagation, and deactivation reactions (Kim et al., 1991) as well as chain transfer and site transformation reactions (deCarvalho et al., 1989; Rincon-Rubio et al., 1990; McAuley et al., 1990; Lorenzini et al., 1991; Vela Estrada and Hamielec, 1994; Shariati, 1996).

In polymerization reactions involving heterogeneous catalysts, monomers adsorb onto the catalyst and the reaction occurs at the catalyst's surface. Since different catalysts have different properties, including the number and type of potential catalyst sites (discussed in Section 2.4), finding appropriate values for kinetic parameters in the literature for specific Ziegler-Natta catalysts can be extremely difficult.

2.3.1 Propylene Polymerization

Rincon-Rubio et al. (1990) investigated the slurry polymerization of propylene over a $TiCl_4/MgCl_2$ catalyst, with triethylaluminum (TEA) as a cocatalyst, in a 2.0 L stirred autoclave at a constant temperature of 70°C. Propylene pressure was kept at 4 atm by continuously feeding propylene into the reactor.

Polymerization rates were determined from the rate of monomer consumption, whereas the MW and polydispersities ($\overline{M}_w/\overline{M}_n$) were determined by GPC at various times during the course of the reaction. The polymerization rates did not exhibit an acceleration period in the initial stage of the reaction, but simply decayed throughout the reaction.

The proposed model accounted for two types of active catalyst sites, and two arbitrary assumptions were made regarding these sites:

1. half of the most active sites (type 1) were transformed to type 2 sites while the rest of the type 1 sites deactivated; and
2. the propagation rate constant for type 1 sites was ten times that for type 2 sites.

Although the authors did not give explicit details about their parameter estimation techniques, they did outline the procedure they followed. As a starting point, orders of magnitude for the concentrations of active sites and propagation and chain transfer rate constants were taken from the literature and then the model was fitted to the experimental data. The site transformation and deactivation rate constants for the two sites were also

estimated (applying the assumptions above), giving a total of 18 kinetic parameters. The fit showed good agreement between observed and fitted polymerization rates and molecular weight distribution curves.

The model's ordinary differential equations, developed from mass balances and the method of moments, were solved numerically with the LSODE solver (Hindmarsh, 1982). Although the model fitted the instantaneous rates and average molecular weights well, the assumptions made were specific to the catalyst used in the experimental study.

2.3.2 Ethylene Ziegler-Natta and Metallocene (Co)Polymerization

Lorenzini et al. (1991) studied the gas-phase copolymerization of ethylene and 1-butene in a 0.9 L CSTR under high pressure (800 bar) and in a high temperature range (200 – 260°C). A suspended catalyst ($TiCl_3$, $^1/_3AlCl_3$, $MgCl_2$, $Al(Et)_3$) was used for the seventeen experimental runs.

Polymer samples were weighed only at the end of the reaction. They were analyzed by GPC to determine their MWDs and average molecular weights ($\overline{M}_n$, $\overline{M}_w$, and $\overline{M}_z$) and by IR to determine short-chain branching indices and double bond indices. Those quantities, along with the polymer mass flow rate and the concentrations of ethylene, butene-1, and hydrogen, were the response variables (Y_j) involved in the objective function:

$$F = \sum_{r=1}^{n}\left(\sum_{j=1}^{N_c}\delta_j\left(\frac{Y_j^{\exp}-Y_j^{\mathrm{mod}}}{Y_j^{\exp}}\right)_r^2\right)+\sum_{r=1}^{n}\left(\sum_{k=1}^{N_{p,i}}\delta_{MWD,k}\left(w^{\exp}(k)-w^{\mathrm{mod}}(k)\right)_r^2\right) \qquad (2.6)$$

δ_j and δ_{MWD} were weighting parameters. This objective function, minimized using Comet's method, involved only quantities measured at the end of each experimental run. Since the model accounted for three types of catalyst sites and the rate constants were assumed to follow Arrhenius relationships, a sensitivity analysis was carried out on predictions of each response variable, Y_j, to determine whether certain elementary reactions were negligible (in an attempt to reduce the number of parameters). For the three-site model this resulted in the number of chemical mechanisms considered in the model being reduced from 28 to 14, giving 28 parameters for estimation. The authors concluded that three types of sites were necessary and sufficient to fit the data.

Kim et al. (1991) used a 1.0 L semi-batch reactor at constant high pressure to study slurry polymerization of ethylene over $TiCl_4/MgCl_2/SiO_2$ catalyst. Experiments were performed by varying three factors: temperature (50 – 80°C) and concentrations of ethylene (128 – 428 mmol/L) and aluminum alkyl (0.92 – 4.35 mmol/L). For each one-hour experiment, the instantaneous polymerization rates were determined from the measured monomer mass flowrate. The rate of monomer consumption decreased with time, most likely due to catalyst deactivation. No analyses were performed on the polymer to determine its properties.

The chain transfer reaction rate constants and the deactivation rate constant were estimated using a method described by Kim and Woo (1990b). During the first twenty minutes of the experimental run the polymerization rate increased quickly to a maximum

before it decreased. For that initial period, Kim et al. (1991) assumed that deactivation and termination were negligible compared to activation and propagation. Consequently, the pseudo-rate constant of active center formation ($k_i^{'}$, s^{-1}) and the propagation rate constant (k_p, L/mol s)) were estimated by Powell's method (1964) with data from the initial stage of the polymerization using the following polymerization rate model:

$$R_p = k_p[M]\left(1-\exp\left(-k_i^{'}t\right) MW\,(3.6)[S_0]/Ti\right) \qquad (2.7)$$

where $[S_0]/Ti = 0.019$ from (Kim et al., 1990a), MW is the ethylene molecular weight, and [M] is the monomer concentration.

Values of four kinetic rate constants for deactivation and termination were taken from the literature. Using the two previously estimated parameters and the rate constants taken from the literature, the nonlinear ordinary differential equations in the model describing the polymerization rate were solved using Gear's method (1971).

Sensitivities of the two estimated parameters to each of the three factors (temperature, concentration of ethylene, and concentration of aluminum alkyl) were determined. It was found that k_p depended only on temperature. $k_i^{'}$ was dependent not only on temperature, but also on the concentrations of monomer and aluminum alkyl when either of these concentrations was at a high setting. Kim et al. (1991) concluded that the latter two dependencies were most likely due to the fact that catalyst deactivation was neglected during the estimation of k_p and $k_i^{'}$.

Vela Estrada and Hamielec (1994) also used a 1.0 L semi-batch reactor for the polymerization of ethylene over a soluble metallocene catalyst (Cp_2ZrCl_2/MAO). The three operating variables of interest were: temperature (50 and 71°C), concentration of zirconocene dichloride (6.54E-3 and 13.08E-3 mmol/L), and concentration of methylaluminoxane (13.18 and 21.08 mmol/L). During the one-hour experimental runs ethylene polymerization rates were recorded with a mass flowmeter. The rate decrease with time was attributed to the catalyst deactivation. At the end of the polymerization, the molecular weights were measured by GPC.

This experimental situation, like the one considered in this thesis, involved reactor data collected throughout the reaction and polymer property data determined only at the end of the reaction. However, Vela Estrada and Hamielec did not attempt to estimate all the parameters in one step. The polymerization rate was modeled as:

$$R_p = \left[\theta_1 \exp(-k_c t) + \frac{k_c \theta_2}{k_c - k_{d2}}\left(\exp(-k_{d2} t) - \exp(-k_c t)\right)\right] P \qquad (2.8a)$$

$$\theta_1 = k_{p1}' N_{10}^{\bullet}$$
$$\theta_2 = k_{p2}' N_{10}^{\bullet} \qquad (2.8b)$$

where k_{pi}', i=1, 2, are the pseudo rate constants for species of types 1 and 2 (min^{-1} psi^{-1}), k_{d2} is the deactivation constant of species 2 (min^{-1}), k_c is the transformation rate constant (from site type 1 to site type 2, min^{-1}), P is the ethylene pressure (psi), and $N_{10}^{\bullet}$ is the initial molar mass of active species of type 1.

The parameters θ_1 (mol/min psi), θ_2 (mol/min psi), k_c, and k_{d2} were estimated by a least squares with an objective function of the form:

$$F = \sum \left(rate^{\exp} - rate^{\mathrm{mod}} \right)^2 \qquad (2.9)$$

where superscripts 'exp' and 'mod' correspond to experimental rate values and fitted rate values, respectively.

The estimated parameters, $\hat{\theta}_1$ and $\hat{\theta}_2$, were substituted into a set of model equations used to predict $\overline{M}_n$ and $\overline{M}_w$. The system of ordinary differential equations and algebraic equations was solved using LSODAR (Petzold, 1980). Parameter $N_{10}^{\bullet}$ and the chain transfer rate constants for site types 1 and 2 were adjusted until the calculated $\overline{M}_n$ and $\overline{M}_w$ values were in good agreement with the corresponding experimental values. Consequently, parameter $N_{10}^{\bullet}$ and the chain transfer rate constants for site types 1 and 2 are not statistical estimates. Then, using the relationships in equation 2.8b, $k_{p1}^{\cdot}$ and $k_{p2}^{\cdot}$ were calculated.

The MWD was found to be bimodal. From further analyses of the molecular weights it was postulated that two types of sites were present. The ratio of θ_1 to θ_2 was found to be dependent on the three operating variables and all of their pairwise interactions. k_c, the rate constant for the transformation of site type 1 to site type 2, was affected only by temperature, whereas k_{d2}, the rate constant for the deactivation of site type 2, was independent of all factors and interactions. The authors used the rate data to

estimate a set of parameters, then empirically adjusted a second set of parameters until the calculated polymer properties agreed with the experimental values.

Shariati (1996) also used a two-stage approach to estimate the kinetic parameters in his model. As mentioned in the introduction of this chapter, the experiments involved a slurry ethylene polymerization with a polymer-supported Ziegler-Natta catalyst in a semi-batch reactor. Rate data were recorded throughout one-hour experimental runs and $\overline{M}_n$ and $\overline{M}_w$ were measured by GPC from samples obtained at the end of each run.

Shariati considered two models, a rate model and a molecular weight model. Three parameters appeared only in the molecular weight model and the remaining sixteen parameters were common to both models. Shariati's approach was to estimate the common parameters using the rate data alone, using a nonlinear least squares analysis. After fixing those estimates in the molecular weight model, the $\overline{M}_w$ data were fitted to get estimates of the other three parameters. The predicted values of $\overline{M}_n$ were then calculated using the estimated values of all nineteen parameters. The same procedure was applied using only the $\overline{M}_n$ data to obtain the three parameters. No convergence was reached when estimating the three parameters with $\overline{M}_n$ and $\overline{M}_w$ data simultaneously.

From this review it is apparent that when polymer quantity and product property data were available in past investigations, the tendency has been to separate the rate constants to be estimated into two groups (Lorenzini et al., 1992; Vela Estrada and Hamielec, 1994; Shariati, 1996). If the data collected contained gaps, resulting in a

missing data structure (described in Chapter 3), the set of rate constants describing the polymer quantity was estimated first, and then those estimates were used in the molecular-weight model to obtain estimates of the remaining parameters. The investigation in the current thesis is focused on finding a way to use both rate data and polymer property data simultaneously to estimate all the parameters in kinetic models that describe Ziegler-Natta polymerizations.

2.4 Ziegler-Natta Catalyst Properties

Many different types of Ziegler-Natta catalysts have been used for olefin polymerization (Xie et al., 1994). Even similar Ziegler-Natta catalysts can have different properties, such as the number of catalyst site types and the number of potential catalyst sites of each type per unit mass of catalyst, that allow them to behave differently from one another. Each type of catalyst site is characterized by its initiation, propagation, deactivation, and chain transfer rate constants.

2.4.1 Broad Molecular Weight Distribution

The causes of broad MWDs produced by Ziegler-Natta catalysts have been debated for many years. The two proposed theoretical explanations are diffusion effects and multiple active catalyst site types. Hoel et al. (1994) developed a model in which diffusion was responsible for the broad MWD. To confirm their model, they used data obtained from a copolymerization over a single-site metallocene catalyst. However, most researchers agree that diffusion alone cannot explain the occurrence of the broad MWDs observed in Ziegler-Natta catalyzed olefin polymerizations (Galvan and Tirrell, 1986;

Floyd et al., 1987; deCarvalho et al., 1989; Rincon-Rubio et al., 1990; Hoel et al., 1994) but diffusional limitations could be a contributing factor.

Most models encountered in this literature review used multiple catalyst sites to describe the MWDs found in experimental Ziegler-Natta polymerization data (deCarvalho et al., 1989; McAuley et al., 1990; Rincon-Rubio et al., 1990; Lorenzini et al., 1991; Vela Estrada and Hamielec, 1994). Since a single type of active site cannot predict the broad MWD seen in this study (described in Chapter 4), the final proposed model includes two types of active catalyst sites and a monomer concentration gradient, based on Shariati's proposal (1996).

2.4.2 Number of Potential Catalyst Sites

A common method used to determine the number of active sites on a catalyst is a radioactive quenching technique using carbon monoxide or carbon dioxide as the quenching agent (Bukatov et al., 1982; Chien and Hsieh, 1976; Marques et al., 1988; Zakharov et al., 1983). Marques et al. (1988) found great disagreement between active site concentrations obtained from a radioactive technique and those obtained from a kinetic method. If radioactive quenching experiments are not performed, it is difficult to simultaneously estimate the initial number of potential active sites and the propagation rate constant from polymerization data, since the two parameters are highly correlated and, together, control the maximum height of the polymerization rate curve. Shariati (1996) did not measure the number of potential active catalyst site on his catalyst, and so this number will need to be estimated from kinetic data in the current study.

2.5 Parameter Transformations

Parameter transformations are used to ensure that the kinetic rate constants are positive (to make physical sense). The natural logarithms of the rate constants, rather than the rate constants themselves, are more likely, *a priori*, to have uniform local distributions (Box and Draper, 1965; Box and Draper, 1972) and consequently to satisfy the assumptions in the parameter estimation subroutine GREG (Stewart, 1995) used in this thesis. Furthermore, logarithmic transformations ensure that the estimated parameters have similar orders of magnitude (Biegler et al., 1986).

Kinetic rate constants are known to be temperature dependent; this dependence is usually described using Arrhenius relationships (Pritchard and Bacon, 1978; Bates and Watts, 1988; Watts, 1994; Shariati, 1996). Pritchard and Bacon (1978) suggested centering temperatures in an Arrhenius relationship about a reference temperature to improve the convergence in parameter estimation.

Watts (1994) suggested that the best approach to estimating nonlinear kinetic rate constants is to perform a logarithmic transformation on a centered Arrhenius relationship. Such transformations can improve the convergence of the optimized parameters (Bilardello et al., 1993) and can also ensure linear dependence of the transformed rate constants on the inverse temperatures (Bates and Watts, 1988). This procedure is as follows:

$$k = k_0 \exp\left[-\left(\frac{E}{R}\right)\left(\frac{1}{T}-\frac{1}{T_0}\right)\right]$$

$$\theta = \ln(k) \tag{2.10}$$

where k_0 is the rate constant at the centering temperature, T_0.

2.6 Missing Data

When collecting and analyzing experimental data it is not unusual that an observation, Y_i, is not measured or not available at the same time as observations of the other response variables. In such cases, Y_i is called a missing observation. Two structures for missing data are illustrated in Tables 3.1b and 3.1c. Table 3.1b represents a block rectangular data structure where response variables Y_1 and Y_2 form one block of measured values during the time interval from observation 1 to observation 3 and response variable Y_3 forms another block of measured values for the time span from observations 4 to 6. The missing observations for the response variables in Table 3.1c form a random pattern through time.

Box et al. (1970) dealt with missing data by treating them as additional parameters to be estimated. The response vector is represented by $\mathbf{Y}^T = (\mathbf{Y}^{exp,T} : \mathbf{Y}^{mis,T})$ where superscripts 'exp' and 'mis' denote an experimental observation and a missing data point, respectively. The probability density function for the total number of observations (observed and missing) is:

$$(2\pi)^{-nm/2}\left|\Sigma^{-1}\right|^{n/2}\exp\left(-\frac{1}{2}\sum_{i=1}^{m}\sum_{j=1}^{m}\sigma^{ij}\upsilon_{ij}\right) \tag{2.11}$$

where $\upsilon_{ij} = \sum_{u=1}^{n} \left(Y_{ui} - f_i(x_u, \theta)\right)\left(Y_{uj} - f_j(x_u, \theta)\right)$ are the sums of squares and cross products of errors, x_u are the values of the independent variables for the u^{th} experimental run (total of n experimental runs), m is the number of response variables, σ^{ij} are the elements of the inverse of the covariance matrix Σ of the response variables, and θ is the vector of unknown parameters to be estimated.

Box and Draper (1965) used Bayes' theorem to obtain a posterior density function, $p(\theta,\Sigma|\mathbf{Y})$, for the parameters θ and the unknown covariance matrix Σ for the responses. The posterior density function is the product of the prior density function for θ and Σ, $p(\theta,\Sigma)$, and the likelihood function, $\ell(\theta,\Sigma|\mathbf{Y})$. The prior density function can be separated into two parts, a uniform prior density for θ (that describes the anticipated behaviour of unknown θ before collecting data) and a non-informative prior density for the m(m+1)/2 elements of Σ (Box and Draper, 1965; Box and Tiao, 1973; Stewart, 1995):

$$p(\theta,\Sigma) \cong p(\theta)p(\Sigma) \qquad (2.12)$$

with

$$p(\theta) \propto \text{constant} \qquad \text{and} \qquad p(\Sigma) \propto \left|\Sigma^{-1}\right|^{(m+1)/2}.$$

Box et al. (1970) applied Bayes' theorem, following the work of Box and Draper (1965), to obtain the joint posterior distribution, which results in the following marginal distribution of θ and $\mathbf{Y}^{mis}$ when the σ^{ij} are integrated out:

$$p\left(\theta, Y^{mis}\middle|Y^{exp}\right) \propto \left|\upsilon_{ij}\right|^{-n/2} \qquad (2.13)$$

where $|\upsilon_{ij}|$ represents the determinant of the error matrix. Point estimates can be found by maximizing the marginal posterior distribution (expression 2.13) or by minimizing the determinant with respect to θ and $\mathbf{Y}^{mis}$. Box et al. showed, using an example with one parameter and one missing data point, that these two approaches are equivalent.

However, if the number of missing data points is large, it becomes impractical to treat all missing values as additional parameters. One example presented by Stewart and Sørensen (1981) deals specifically with a large number of missing observations. The first response variable had 25 missing observations from a total of 41 observation points, whereas response variables two and three each had 16 missing observations. Response variable four had no missing values.

The approach taken to solve this problem was to modify the likelihood function used in Bayes' theorem to account for the missing data. The methodology, which is applied in the parameter estimation subroutine GREG (Stewart, 1995), can handle problems that range from complete sets of data to those with many missing observations. Chapter 3 is dedicated to a description of this subroutine that is used in this thesis.

The posterior density function used by Stewart and Sørensen (1981) to deal with missing data is:

$$p(\theta,\sigma|Y) \propto |\sigma|^{-(m+1)/2}\left[\prod_{u=1}^{n}|\sigma_u|^{-1/2}\right]\exp\left\{-\frac{1}{2}\sum_{u=1}^{n}\sum_{i=1}^{m}\sum_{j=1}^{m}\sigma_u^{ij}\upsilon_{ij}\right\} \qquad (2.14)$$

where n is the number of experiments and the matrix σ_u is formed by substituting the corresponding elements of the unit matrix into corresponding positions in the full-order covariance matrix where there is a missing observation, while a zero is inserted into the corresponding position in the vector of errors. Point estimates of θ and σ can be found by maximizing expression 2.14 or by minimizing:

$$(m+1)\ln|\sigma| + \ln|\sigma_u| + \sum_{u=1}^{n}\sum_{i=1}^{m}\sum_{j=1}^{m}\sigma_u^{ij}\upsilon_{ij} \qquad (2.15)$$

Stewart and Sørensen (1981) successfully estimated thirteen parameters and seven elements of the covariance matrix using the data from example 2 of Fuguitt and Hawkins (1945) involving four response variables by fixing a fourteenth parameter at a given value and setting three other elements of the covariance matrix at zero.

Chapter 3: Parameter Estimation

GREG, a FORTRAN 77 subroutine for generalized regression analysis developed by Stewart (1995), can solve nonlinear parameter estimation problems for three types of data structures (Table 3.1): complete, block rectangular, and irregular data. In the GREG subroutine, the variable *level* identifies the data structure that will be employed, the form of the objective function to be minimized, and whether analytical expressions or numerical approximations for the derivatives in the proposed kinetic model are to be used.

Table 3.1. Complete, block rectangular, and irregular data structures. An observation for a response Y_u is indicated by a '+', whereas a missing observation is left blank.

a)

Time	Y_1	Y_2	Y_3
1	+	+	+
2	+	+	+
3	+	+	+
4	+	+	+
5	+	+	+
6	+	+	+

b)

Time	Y_1	Y_2	Y_3
1	+	+	
2	+	+	
3	+	+	
4			+
5			+
6			+

c)

Time	Y_1	Y_2	Y_3
1	+	+	
2	+	+	+
3	+		+
4		+	
5	+		
6		+	+

3.1 Data Structure

Three values of the variable *level* were used in this study. *Level 10* is used when dealing with a single response model and a full data structure (for example, data represented by Y_1 alone in Table 3.1a); *level 22* deals with a multiresponse model with block rectangular data (Table 3.1b) and a known diagonal covariance matrix for the responses; *level 32* solves a multiresponse model with irregular block data (Table 3.1c) and an unknown diagonal covariance matrix for the responses. Minor changes to the GREG subroutine were required to solve the ordinary differential equations numerically

using a differential-algebraic equation solver (DDASAC) at *level 22* (see Appendix A for details).

3.1.1 Homopolymerization Data

During the homopolymerization of ethylene, Shariati (1996) recorded polymerization rate data at half-minute intervals throughout the one-hour experimental runs, whereas molecular weight data were obtained only at the end of each run. Table 3.2 illustrates this data structure; a plus sign indicates an observation, whereas a blank space implies a missing data point. The data structure in Table 3.2 is block rectangular.

Table 3.2. Schematic representation of the ethylene homopolymerization data structure

Time (min)	Rate (mol/min)	Weight average molecular weight (g/mol)	Number average molecular weight (g/mol)
0.25	+		
0.75	+		
⋮	⋮		
59.75	+		
60.00		+	+

3.2 Objective Functions

3.2.1 Single Response

When estimating parameters in Shariati's (1996) polymerization model using the rate data alone (*level 10*), the following objective function was minimized:

$$S(\theta) = \sum_{u=1}^{n} \left(Y_u - f(\mathbf{x}_u, \theta) \right)^2 \qquad (3.1)$$

where Y_u is a measured value of the response variable at time u, $\mathbf{x}_u$ are the independent variables (temperature, monomer partial pressure, hydrogen-to-monomer ratio, catalyst

loading, cocatalyst loading, and catalyst particle size), and θ is the model parameter vector. Since the values of Y_u and $\mathbf{x}_u$ are known, $S(\theta)$ is a function of the parameter vector θ only (Draper and Smith, 1981).

3.2.2 Multiresponse (m responses)

Bayes' theorem, as described in Section 2.6, is used to obtain the posterior density function for θ and Σ. When the data structure is complete (Table 3.1a), the likelihood function can be expressed as follows.

$$\ell(\theta, \Sigma|Y) \propto \left|\Sigma^{-1}\right|^{n/2} \exp\left(-\frac{1}{2} \sum_{u=1}^{n} \sum_{i=1}^{m} \sum_{j=1}^{m} \sigma^{ij} e_{ui} e_{uj} \right) \tag{3.2}$$

where n is the number of experimental runs and the errors $e_{ui} = Y_{ui} - f_i(x_u, \theta)$ are random variables assumed to have a multivariate normal distribution with expected value $\mathbf{0}$ and covariance matrix Σ, and $\{\sigma^{ij}\}$ are the elements of Σ^{-1} (Stewart and Sørensen, 1981). Using the prior density function for θ and Σ described in Section 2.6, the posterior density function is:

$$p(\theta, \Sigma|Y) \propto \left|\Sigma^{-1}\right|^{(n+m+1)/2} \exp\left(-\frac{1}{2} \sum_{u=1}^{n} \sum_{i=1}^{m} \sum_{j=1}^{m} \sigma^{ij} e_{ui} e_{uj} \right) \tag{3.3}$$

and the values of θ and Σ that maximize this expression are called highest posterior density estimates.

However, if the data structure is irregular (Table 3.1c), additional terms are required in the likelihood function. When there is a missing observation, a zero is

inserted into the vector of errors $[e_{u1},\ldots, e_{um}]^T$ and the element from the unit matrix, δ_{ij}, is placed in the full-order covariance matrix to form the missing data covariance matrix Σ_u.

The Jeffreys prior density function for Σ ($|\Im(\Sigma)|^{1/2}$), where $\Im$ denotes Fisher's Information Matrix (Box and Tiao, 1973), has been modified by Stewart (1995) so that GREG can deal with missing data. Combining the likelihood function (equation 3.2) with the Jeffreys prior, and assuming an unknown diagonal covariance matrix (uncorrelated responses), gives the objective function to be minimized for *level 32*:

$$S(\psi) = \sum_{i=1}^{m} \left((n_i + 2)\log\sigma_{ii} + \frac{\sum_{u=1}^{n} e_{ui}^2(\theta)}{\sigma_{ii}} \right) \tag{3.4}$$

where $\{\sigma_{ii}\}$ are the diagonal elements of the unknown covariance matrix. The parameter vector ψ is comprised of the p parameters in the proposed model plus the m diagonal elements in Σ.

When the data structure is block rectangular (Table 3.1b) and the variances of the response measurements are known, the objective function essentially reduces to the sum of weighted sums of squares for the blocks (*level 22*):

$$S(\theta) = \sum_{i=1}^{m} \left(\frac{\sum_{u=1}^{n} e_{ii}^2(\theta)}{\sigma_{ii}} \right) \tag{3.5}$$

GREG requires a subroutine called MODEL to calculate the model predictions given a candidate set of values for the model parameters. The MODEL subroutine required, however, is different when using *level 22* with a block rectangular data structure. In this situation the matrix $\mathbf{F} = \{f(\mathbf{x}_u,\theta)\}$ holds the residuals rather than the predictions, and the user must specify the block to which each response belongs. An IF statement is used to set a residual to zero if the corresponding observation is missing.

To summarize, *levels 22* and *32* are used for multiresponse analyses with missing data, assuming diagonal covariance matrices for the responses. *Level 22* only estimates the model parameter vector (θ), whereas *level 32* estimates both the model parameter vector and the diagonal covariance matrix (Σ) for the responses. *Level 32* is only used in the initial stage of estimation to see how efficiently GREG can estimate the response variances.

3.2.3 Maximum-density Algorithm for Parameter Estimation

The maximum-density algorithm combines successive quadratic programming and line searches to minimize the objective function, $S(\theta)$ or $S(\psi)$. A feasible region for the model parameter vector is defined as the intersection of a trust region (defined by the maximum allowable change at every iteration for each parameter (CHMAX)) and the upper and lower bounds for each parameter (BNDUP and BNDLW, respectively). If there are no restrictions on the parameters, the boundaries are set at ±1E30. However, if the user does not wish to set boundaries, but a parameter has a physical restriction (such as that it needs to be positive), a parameter transformation may be applied (e.g. k =

exp(θ), as described in Section 2.5). This allows the estimated parameter, θ, to take any real value as well as satisfying GREG's assumption of a constant prior density.

The objective function is approximated by a quadratic expression that is minimized over the feasible region (Stewart and Sørensen, 1981; Stewart, 1995). Assuming that θ_0 is the initial parameter vector, the minimum of the quadratic expression is found at θ_1 using a negative directional derivative (to ensure a reduction in the objective function). Then a line search between θ_0 and θ_1 is performed to find a value of the relaxation factor, λ, that produces a positive definite covariance matrix and minimizes S(θ) according to the Armijo criterion (1966):

$$S(\theta_c + \lambda\Delta\theta) \leq S(\theta_c) + \alpha\lambda\nabla S(\theta_c)^T\Delta\theta \qquad (3.6)$$

where θ_c represents the current parameter vector and α is the Armijo constant $\in(0,1]$. The halving mechanism is chosen for the line search:

$$\lambda_{new} = \frac{1}{2}\lambda_{old} \qquad (3.7)$$
$$\text{with} \quad \lambda \in (0,1]$$

GREG allows accelerated searches to be performed (when the endpoint satisfies the Armijo criterion) by expanding the feasible region and increasing λ by a factor of two. The acceleration, repeated until the criterion is not satisfied, allows the objective function to decrease more quickly without having to solve a new quadratic expression.

Grippo et al. (1986) developed a non-monotone line search that can accelerate the convergence by allowing longer steps to be taken. The concept, which is programmed in GREG, is that the objective function is not forced to decrease at every point, but rather at every n^{th} step (in GREG n=MGLL is selected by the user). If MGLL=4, then the objective function at a search point must be less than the maximum of the objective functions at the previous four search points (Zhou and Tits, 1993; Stewart, 1995).

Minimization of the objective function continues until one or both convergence criteria are met at iteration k. The first convergence criterion is based on the step size becoming sufficiently small:

$$\text{stop if} \quad |\Delta\theta_i| \le \max\left(RPTOL \cdot |\theta_i|, 10^{-8}\right), \tag{3.8}$$

while the second is based on convergence of the objective function using the quadratic approximation:

$$\text{stop if} \quad \left|\Delta S_k^{pred}\right| \le RSTOL^2 . \tag{3.9}$$

Both the tolerance for the step size (RPTOL) and the tolerance for the objective function (RSTOL) can be specified, giving the user discretion as to which criterion, if either, is more important.

3.3 Differential and Algebraic Equation Solver

DDASAC, **D**ouble precision **D**ifferential-**A**lgebraic Sensitivity **A**nalysis **C**ode, an extension of the implicit integrator DDASSL (Brenan et al., 1989) modified by Stewart et al. (1994), is designed to perform sensitivity analyses and solve nonlinear initial value problems using a backward difference formula. Also, the implicit integrator can deal

with stiff, coupled ordinary differential equation systems; it uses a variable-order, variable-step predictor-corrector approach developed by Gear (1971).

For the three levels used in this study, the ordinary differential equations were solved numerically with DDASAC by setting the problem identification variable, IDPROB, to 2 in the main program, informing GREG that the system of differential equations is to be solved by DDASAC. Since there are also algebraic equations to be solved, the variable INFO(13) is set to –1, which implies that the equation system is a combination of algebraic and differential equations. The subroutine ESUB is used to specify which equations are algebraic and which are differential. To avoid scaling problems, DDASAC is designed to use tolerance arrays for the state variables by setting the variable INFO(2) to 1. Further details on the choices of tolerances and their effects on performance are given in Section 4.2.3.

At *level 22* parametric sensitivities are required for the response variables. These are calculated by DDASAC when the variable INFO(12) is set equal to the parameter NSPAR (in this case NSPAR is equal to the number of parameters). Also, the choice of method for calculating the Jacobian is controlled by the variables INFO(5) and INFO(6). In this study, all Jacobians were approximated by finite differences.

3.4 General Application to Case Studies

Parameter estimation for this research began with a simplified model, which describes homopolymerization of ethylene with a one type of Ziegler-Natta catalyst site

and no monomer diffusion limitation (see Section 4.3), to obtain reasonable initial guesses for the parameters to be estimated in a more complicated and realistic model. The approach taken was to start with a single response variable (*level 10*) to find reasonable initial estimates of some of the parameters, which could then be used as initial guesses in the multiresponse model (*level 22*).

Chapter 4: Development of a One Type of Site Model for Homopolymerization of Ethylene

The experimental design used to obtain the response data analyzed in this study is discussed in Section 4.1. Section 4.2 describes simplifications made to the kinetic model and defines the system of ordinary differential equations used in the initial stage of the parameter estimation. In Section 4.3 the results from fitting the single and three-response models are presented.

4.1 Experimental Design

The ethylene homopolymerization experiments conducted by Shariati (1996) will only be briefly described. Complete description of the catalyst preparations and experimental procedures can be found in Shariati's thesis. Semibatch slurry ethylene polymerization was carried out in a 500 mL stirred stainless steel reactor. The experimental design, which was based on a central composite design, involved six polymerization variables (presented in Table 4.1 along with their actual settings) and three response variables: rate of polymerization (R_p), weight average molecular weight ($\overline{M}_w$), and number average molecular weight ($\overline{M}_n$). For the present analysis, data collected at three temperature settings (62, 70, and 78°C) are used. There are sixteen runs in each of the three temperature groups, including six replicate runs at the center point conditions for all variables.

Table 4.1. Experimental design factors and actual settings for ethylene homopolymerization experiments (Shariati, 1996)

Temperature (°C)	50.0	62.0	70.0	78.0	90.0
Monomer partial pressure (atm)	1.0	1.6	2.0	2.4	3.0
Hydrogen to monomer ratio	0.05	0.09	0.12	0.16	0.20
Catalyst loading (mg)	5.0	8.0	10.0	12.0	15.0
Cocatalyst loading (mL)	0.4	0.9	1.2	1.5	2.0
Catalyst particle size (μm)	125.0	177.0	250.0	325.0	420.0

A heterogeneous Ziegler-Natta catalyst was used with a triisobutylaluminum cocatalyst. The reaction temperature was controlled by passing cooling water through an internal coil. A pressure regulator on the ethylene cylinder maintained the total pressure at the desired setting, by allowing fresh ethylene to flow into the reactor to make up for ethylene consumed by reaction. The ethylene flow rate (a direct indication of polymerization rate) was measured with a mass flow meter (reported by Shariati in moles of ethylene per mole titanium per minute, every 30 seconds during each one-hour reaction). Upon completion of the experimental runs, polymer samples were analyzed by gel permeation chromatography (GPC) to determine their molecular weight distributions, and consequently $\overline{M}_w$ and $\overline{M}_n$, which were reported by Shariati (1996).

For each particle size the catalyst composition was measured; the results are summarized in Table 4.2. The titanium content is required to convert the polymerization rate from (mol C_2/mol Ti/min) to (mol C_2/min).

Table 4.2. Catalyst composition

Catalyst Particle Size (μm)	Ti (%)	Mg (%)	Al (%)
125	3.6	6.4	22.9
177	3.5	6.6	24.0
250	3.6	6.2	23.0
325	3.4	6.4	22.2
420	3.6	6.8	23.8

4.2 Kinetic Model for Ziegler-Natta Catalyst with One Type of Site

When dealing with a complex mechanistic model, it is often wise to simplify the model first to reduce the number of parameters to be estimated (Stewart, 1995). Once a simplified model has been fitted, the estimated parameter values can be used as initial guesses in a more complex model. In this case, the simplified model consists of a homopolymerization model with one type of site Ziegler-Natta catalyst and no monomer diffusion. The reactions involved in this simplified kinetic model are summarized in Table 4.3.

Table 4.3 Kinetics for a single type of site model

Reaction Type	Description	Reaction Mechanism
Activation	Cocatalyst activates potential active sites	$C + [A] \xrightarrow{k_a} C_0^*$ (1)
Initiation	Monomer initiates active sites	$C_0^* + [M] \xrightarrow{k_p} [P_1^*]$ (2)
Propagation	Propagation of polymer chains	$[P_n^*] + [M] \xrightarrow{k_p} [P_{n+1}^*]$ (3)
Deactivation	Hydrogen deactivates polymer chains	$[P_n^*] + [H] \xrightarrow{k_d} C_d + [D_n]$ (4)
Chain Transfer	Hydrogen causes chain transfer	$[P_n^*] + [H] \xrightarrow{k_t} C_0^* + [D_n]$ (5)

The model includes: activation of potential active sites (C) by the cocatalyst (A); initiation of active sites (C^*_0) and propagation of growing polymer chains of length n (P^*_n) with the monomer (M); deactivation of polymer chains by hydrogen (H); and chain transfer to hydrogen. D_n represents a dead polymer chain and C_d refers to a deactivated catalyst site. The rate constants are named for the reaction type (k_a is for activation, k_d for deactivation, etc.). Böhm (1978a) recommended that the number of catalyst sites be expressed in moles rather than in moles per liter. Furthermore, it is assumed that the

initiation of active sites occurs at the same rate as the propagation (k_p); the rate constant assigned to those steps is the propagation rate constant.

Ordinary differential equations describing the material balances on the potential and active catalyst sites are listed in Table 4.4. To model the molecular weights the method of moments is applied. The i^{th} moments of the live and the dead polymer chains are, respectively, (deCarvalho et al., 1989; Rincon-Rubio et al., 1990):

$$\lambda_i = \sum_{n=1}^{\infty} n^i P_n^* \tag{4.1}$$

$$\Lambda_i = \sum_{n=2}^{\infty} n^i D_n \tag{4.2}$$

Table 4.4. Material balances and initial conditions

Material Balances on Sites and Polymer Chains		Initial conditions (mol/min)
$\frac{dC}{dt} = -k_a C[A]$	(1)	Varies, see Appendix B
$\frac{d\sum P_n^*}{dt} = k_a C[A] - k_d \sum P_n^*[H]$	(2)	2E-14
$\frac{dC_0^*}{dt} = k_a C[A] - k_p C_0^*[M] + k_t \lambda_0 [H]$	(3)	2E-14
$\frac{d\lambda_0}{dt} = k_p C_0^*[M] - k_d \lambda_0 [H] - k_t \lambda_0 [H]$	(4)	2E-10
$\frac{d\lambda_1}{dt} = k_p (C_0^* + \lambda_0)[M] - k_d \lambda_1 [H] - k_t \lambda_1 [H]$	(5)	2E-12
$\frac{d\lambda_2}{dt} = k_p (C_0^* + \lambda_0 + 2\lambda_1)[M] - k_d \lambda_2 [H] - k_t \lambda_2 [H]$	(6)	2E-14
$\frac{d\Lambda_0}{dt} = k_d \lambda_0 [H] + k_t \lambda_0 [H]$	(7)	2E-10
$\frac{d\Lambda_1}{dt} = k_d \lambda_1 [H] + k_t \lambda_1 [H]$	(8)	2E-12
$\frac{d\Lambda_2}{dt} = k_d \lambda_2 [H] + k_t \lambda_2 [H]$	(9)	2E-14

Material balances are performed on the zeroth, first, and second moments of the MWD for both live and dead polymer chains (Table 4.4, equations 4 through 9). R_p (equation 4.3) is computed as the product of the propagation rate constant, k_p, the total number of active sites, C^*, and the monomer concentration, [M]. It is assumed that C^* and [M] are of first order.

$$R_p = k_p\, C^* [M] \tag{4.3}$$

$\overline{M}_n$ (equation 4.4) is proportional to the ratio of the first moment to the zeroth moment (including live and dead chains), whereas $\overline{M}_w$ (equation 4.5) is proportional to the ratio of the second moment to the first moment; the proportionality constant is the monomer molecular weight, MW.

$$\overline{M}_n = MW \frac{\lambda_1 + \Lambda_1}{\lambda_0 + \Lambda_0} \tag{4.4}$$

$$\overline{M}_w = MW \frac{\lambda_2 + \Lambda_2}{\lambda_1 + \Lambda_1} \tag{4.5}$$

In the single response model (required to predict R_p) there are two differential equations (1 and 2 in Table 4.4) and one algebraic equation (4.3) to solve, involving three parameters (k_a, k_d, k_p). The polymerization rate data and molecular weight data can be combined in a multiresponse model involving seven ordinary differential equations (1, 3 through 8 in Table 4.4) and three algebraic equations (4.3 through 4.5), containing four parameters (k_a, k_d, k_p, k_t). The initial conditions for the ordinary differential equations are also given in Table 4.4; values of 2E-10 and smaller are effectively zero but are chosen to be the values shown to avoid division by zero in the equation solver, DDASAC

(Stewart et al., 1994). The initial conditions for the three algebraic equations are all 2E-14, again effectively zero.

The initial condition for the number of potential active sites varies but is not measured experimentally. The procedure to obtain this initial condition value is described in Section 4.2.1.

4.2.1 Number of Potential Active Sites

The experiments performed by Shariati did not include the determination of the initial number of potential active sites (C). Consequently, C must be estimated from the polymerization rate data. As discussed in Section 2.4, estimates for C and k_p are highly negatively correlated and thus estimating both simultaneously would be difficult. To overcome this barrier, it was assumed that C is proportional to the catalyst load (M_c), which is the mass of catalyst used in a polymerization run:

$$C = \zeta M_c \tag{4.6}$$

The proportionality constant, ζ (mol/mg-catalyst), was estimated (along with k_a and k_d) by solving the simplified model (equations 1 and 2 in Table 4.4) with the propagation rate constant fixed at a reasonable value in equation 4.3. A survey of the literature revealed that the propagation rate constant for ethylene polymerization with Ziegler-Natta catalysts at 70°C is in the range of 6E4 to 6E5 L/mol/min (Bukatov et al., 1982; Floyd et al., 1987; and Dusseault and Hsu, 1993). Therefore, k_p was set successively at values of 1.2E5, 1.8E5, and 3.0E5 L/mol/min to determine the effect of

the assumed value of k_p on the value of the objective function used for parameter estimation and on the parameter estimates themselves.

The final value of the objective function (equation 3.1) was the same in all three cases. Neither the estimate of the activation rate constant (135.0 L/mol/min) nor the estimate of the deactivation rate constant (5.6 L/mol/min) was affected by varying the propagation rate constant, k_p, used to estimate ζ . Also, the correlation matrix for the estimates of the parameters k_a, k_d, and C (Table 4.5) was unaffected. The proportionality constant, ζ ,decreased from 1.06E-7 to 7.06E-8 to 4.24E-8 moles per mg-catalyst as the propagation rate constant increased; the value of 7.06E-8 moles per mg-catalyst was chosen for subsequent parameter estimation in all proposed models.

Table 4.5 Correlation matrix for parameter estimates for all three fixed values of k_p

	k_a	k_d	C
k_a	1.00		
k_d	-0.40	1.00	
C	-0.44	0.86	1.00

4.2.2 Parameter Effects

In polymerization reactions involving Ziegler-Natta catalysts, the rate of polymerization can follow different patterns over time. For a heterogeneous Ziegler-Natta-catalyzed polymerization reaction, the initial rate of polymerization often shows an acceleration period, followed by a decay period after the maximum rate has been achieved (Kissin, 1985). Such was the behavior of the homopolymerization rate data gathered by Shariati.

The acceleration period is governed by activation of the catalyst sites, whereas the rate decay is caused by the deactivation of the catalyst sites. A catalyst with a greater activation rate constant will produce an acceleration pattern with a steeper slope and a higher maximum rate than a catalyst with a lower activation rate constant. Similarly, larger deactivation rate constants will produce faster decreases in the polymerization rate.

A simplified representation of the rate of polymerization, R_p, is:

$$R_p = k_p[M]C^* \tag{4.7}$$

Naturally, any increase in the propagation rate constant (k_p) would directly increase the rate of polymerization. The same effect is observed in $\overline{M}_w$ and $\overline{M}_n$ since they are also directly proportional to k_p.

The chain transfer rate constant, k_t, only affects $\overline{M}_w$ and $\overline{M}_n$ and does so in an inversely proportional manner. Since chain transfer to hydrogen is generally the dominant mechanism for producing dead chains, any effect of k_d on $\overline{M}_w$ and $\overline{M}_n$ will generally be small.

4.2.3 Ordinary Differential Equation Tolerances

It is important to properly scale the DDASAC tolerances of the response variables and the variables in the ordinary differential equations. By doing so, a response variable having a small numerical value will not be deemed insignificant when compared to another response variable having a much larger numerical value. The highest order of magnitude for anticipated values of the variables (Table 4.6) is used to set the relative

tolerance (RTOL) and absolute tolerance (ATOL) arrays (Stewart et al., 1994). A rule of thumb, suggested by Brenan et al. (1989), is to denote m_i as the number of significant digits needed to describe a response variable Y_i. Consequently, $RTOL_i$ equals $10^{-(m_i+1)}$ and $ATOL_i$ is set to the order of magnitude at which the variable is essentially insignificant.

Initially the system of differential equations for the single-site three-response model (Section 4.3.5) using data collected during the one-hour experimental runs was solved with scalar tolerances (RTOL = 1E-6 and ATOL = 1E-8) and took five minutes of simulation time on a network. The same model was then solved using the tolerance arrays in Table 4.6 and took two minutes since fewer calculations were required (as shown in Table 4.7).

Table 4.6. Tolerance array for DDASAC with the one type of active site model

Variables	RTOL	ATOL
C (mol)	1E-10	1E-11
C (mol)	1E-14	1E-14
λ_0 (mol)	1E-10	1E-11
λ_1 (mol)	1E-7	1E-8
λ_2 (mol)	1E-2	1E-3
Λ_0 (mol)	1E-8	1E-9
Λ_1 (mol)	1E-4	1E-5
Λ_2 (mol)	1.0	1E-1
R_p (mol/L)	1E-6	1E-7
$\overline{M}_w$ (g/mol)	1E1	1.0
$\overline{M}_n$ (g/mol)	1E1	1.0

Table 4.7. Performance comparison

	Scalar tolerances	Array tolerances
Number of steps taken	412	153
Number of function calls	2960	1104
Number of Jacobian calls	424	159
Number of error test failures	7	3
Number of convergence failures	0	0

Array tolerances were used in DDASAC for all reported simulations.

4.3 Model with One Type of Catalyst Site and No Monomer Diffusion

In the single response problem (wherein only R_p was predicted) for the simplified model, three rate constants were estimated: activation, deactivation, and propagation. In the multiresponse analysis (wherein R_p, $\overline{M}_n$, and $\overline{M}_w$ were predicted) for the simplified model, there was one extra rate constant to estimate, the chain transfer rate constant. The parameters were estimated with data from the sixteen experimental runs carried out at 70°C. There were 120 observations of the polymerization rate per experimental run, spaced evenly over time, and only one observation for each of the molecular weight responses ($\overline{M}_n$ and $\overline{M}_w$), available at the end of each experimental run.

At the beginning of the reaction, the polymerization rate increased rapidly to a maximum, then slowly decreased for the remainder of the reaction. This initial increase is attributed to the activation of potential sites, while the decrease is most likely due to the deactivation of active sites (Kissin, 1985). For simplicity, no monomer diffusion effects were included in the simplified model at this point.

4.3.1 Fitting a Single Response Model

The analysis began by using only the polymerization rate data to estimate the three rate constants. GREG estimated the parameters while DDASAC solved the first two ordinary differential equations in Table 4.4 and equation 4.3. The fitted polymerization rates from the simplified single response model (GREG *level* 10, see Section 3.2.1) agreed well with the data (see Appendix C). The estimated parameters, along with their 95% highest posterior density (HPD) confidence intervals and correlation matrix are given in Table 4.8.

Table 4.8. Parameter estimates from a single response model with one active site type and no monomer diffusion (GREG *level* 10)

			Correlation matrix		
Parameter (L/mol/min)	Estimated value	95% confidence interval	k_a	k_d	k_p
k_a	135.3	● 11.3	1.00		
k_d	5.62	± 0.41	-0.455	1.00	
k_p	1.8E5	± 2.5E3	-0.462	0.869	1.00

As none of the confidence intervals includes zero and the pairwise correlations among the parameter estimates are not too large, these estimated parameter values were used as reasonable initial guesses for the multiresponse model.

4.3.2 Three-response Model with Unknown Diagonal Covariance Matrix

Shariati (1996) used a central composite experimental design to collect data for three responses, R_p, $\overline{M}_n$, and $\overline{M}_w$. Parameter estimation was carried out assuming that the covariance matrix for the measured responses was diagonal but unknown (GREG *level* 32, see Section 3.2.2). The three-response model, described by equations 1 and 3

through 9 of Table 4.4 and equations 4.3 through 4.5, was also fitted using GREG and DDASAC. Since there were a total of 1920 polymerization rate observations and only sixteen $\overline{M}_n$ and sixteen $\overline{M}_w$ observations, the capabilities of the parameter estimation code to estimate variances can be evaluated in this extreme case of missing data.

As shown in Table 4.9, estimates for parameters k_a, k_d, and k_p converged at approximately the same values as in the single response model; consequently, the fitted polymerization rates are similar to those from the previously fitted single response model. The 95% confidence intervals and correlations among those parameters also remained essentially unchanged.

Table 4.9. Parameter estimates from a three-response model (R_p, $\overline{M}_n$, and $\overline{M}_w$) with one type of active sites and no monomer diffusion, assuming an unknown diagonal covariance matrix (GREG *level* 32)

			Correlation matrix						
Parameter	Estimated value	95% confidence interval	k_a	k_d	k_p	k_t	σ^2_{rate}	σ^2_{Mw}	σ^2_{Mn}
k_a (L/mol/min)	135.3	± 10.2	1.00						
k_d (L/mol/min)	5.62	± 0.41	-0.40	1.00					
k_p (L/mol/min)	1.8E5	± 2.4E3	-0.44	0.86	1.00				
k_t (L/mol/min)	9.4E3	± 1.3E3	-0.04	0.08	0.10	1.00			
σ^2_{rate} $(L/min)^2$	3.9E-6	± 2.5E-7	-7E-4	-4E-4	-3E-4	8E-5	1.00		
σ^2_{Mw} $(g/mol)^2$	6.1E10	±4.1E10	2E-5	-6E-5	8E-4	0.22	2E-5	1.00	
σ^2_{Mn} $(g/mol)^2$	4.0E8	± 2.7E8	-8E-5	2E-4	-7E-4	-0.22	-2E-5	-5E-2	1.00

Figure 4.1 shows that the fitted values of $\overline{M}_n$, determined using the parameter estimates in Table 4.9, fall near the corresponding observations, whereas observed values of $\overline{M}_w$ are grossly underestimated. It is well known that a one type of site model, as described in Table 4.4, can only result in a polydispersity ($\overline{M}_w / \overline{M}_n$) of 2.

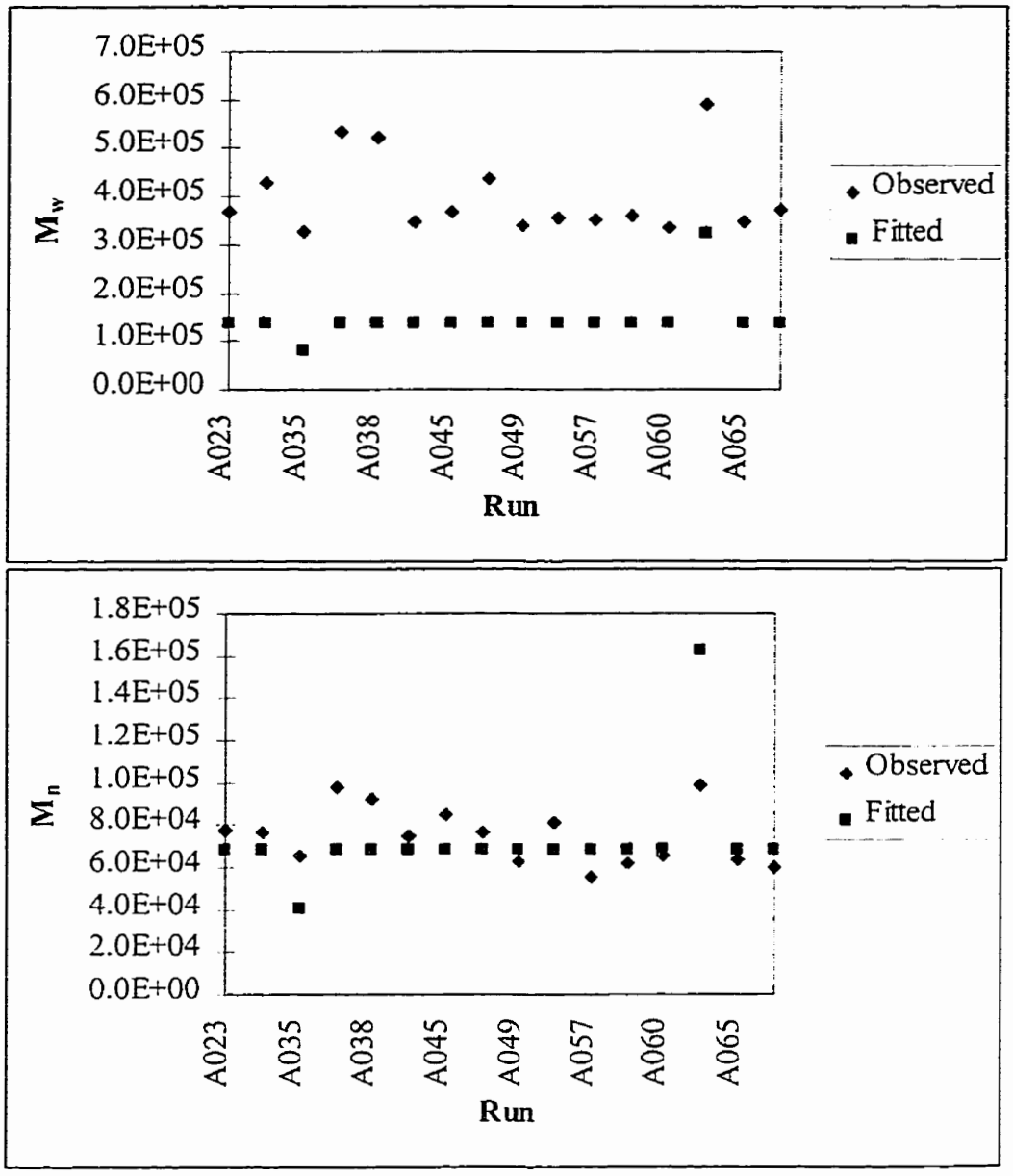

Figure 4.1 Fitted molecular weight values from the three-response model (R_p, $\overline{M}_n$ and $\overline{M}_w$) assuming an unknown diagonal covariance matrix (see Appendix B for operating conditions)

Consequently, in the simultaneous fit of $\overline{M}_w$ and $\overline{M}_n$, it was assumed that GREG had concentrated much more on fitting $\overline{M}_n$ since the estimate of σ^2_{Mw} was larger than the estimate of σ^2_{Mn}. To investigate this problem, two further fits were performed (see Section 4.3.4) each assuming known measurement variances (GREG *level* 22, see Section 3.2.2) with two responses:

1) R_p with $\overline{M}_w$ and

2) R_p with $\overline{M}_n$.

4.3.3 Sample Variances of Response Measurements

Sample variances, s^2, for the measurements of each of the three response variables were calculated from the six replicate runs contained within the sixteen experimental runs at 70°C, according to:

$$s^2 = \frac{1}{6-1}\sum_{i=1}^{6}\left(Y_i - \overline{Y}\right)^2 \qquad (4.8)$$

where $\overline{Y}$ is the average of the 6 measured values Y_i from the replicate runs for response variable Y. The sample variances for R_p, $\overline{M}_n$, and $\overline{M}_w$ each have 5 degrees of freedom.

For the polymerization rate data, equation (4.8) was applied at each time step, resulting in 120 sample variances each having 5 degrees of freedom. Bartlett's test (Bartlett, 1937) was used to determine whether the variance of the measured rates was constant through time. If so, the 120 sample variances can be pooled to form a more reliable estimate, s_p^2. Bartlett's test statistic U can be expressed as:

$$U = \frac{1}{C}\left[\left(\left\{\sum_{t=1}^{k} n_t\right\} - k\right)\ln s_p^2 - \sum_{t=1}^{k}(n_t - 1)\ln s_t^2\right] \tag{4.9}$$

$$\text{where } C = 1 + \frac{\left[\sum_{t=1}^{k}\frac{1}{n_t} - \frac{1}{\sum_{t=1}^{k} n_k}\right]}{3k-3} \tag{4.10}$$

and k is the number of groups of measurements (120), n_t is the number of measurements in each group (6), n_k is the total number of measurements (720), and s_t^2 is the sample variance for group t.

The data yield a value of 26.03 for U and, since the value of $\chi^2_{0.95,119}$ (145.46) is greater than the test statistic U, the group variances can be assumed to be homogenous, indicating that the replication variance is constant through time. 95% confidence intervals are also calculated (equation 4.11) for the replication variances of the three response variables, assuming that each of the samples is composed of random observations from a normal distribution (Montgomery and Runger, 1994):

$$\frac{\nu s^2}{\chi^2_{\nu,0.025}} \leq \sigma^2 \leq \frac{\nu s^2}{\chi^2_{\nu,0.975}} \tag{4.11}$$

where ν denotes the number of degrees of freedom associated with the sample variance s^2. $\nu = 5$ for $\overline{M}_w$ and $\overline{M}_n$ and $\nu = (120)(5) = 600$ for the measured rate. Table 4.10 displays the sample variances and their 95% confidence intervals.

Table 4.10. Sample variances of response measurements with their 95% confidence intervals

	Sample Variance	95% confidence interval	
σ^2_{rate}	2.98E-6	2.68E-6	3.36E-6
σ^2_{Mn}	6.54E7	2.55E7	3.94E8
σ^2_{Mw}	1.87E8	7.29E7	1.13E9

4.3.4 Fitting a Two-Response Model with Known Diagonal Covariance Matrix

Fitting a two-response model (rate data with one of the MW responses) will determine whether acceptable fitted molecular weight values can be obtained using sample variances calculated from replicate runs as "known" variances and assuming all measured response values to be uncorrelated. In both cases 1) and 2) (defined at the end of Section 4.3.2), the estimates of the parameters k_a, k_d, and k_p converged at approximately the same values as before (Table 4.9). When R_p and $\overline{M}_w$ were used as the two response variables, the converged estimate of k_t decreased drastically from 9.4E3 (Table 4.9) to 3.6E3 and the fitted response values showed better agreement with the observations (Figure 4.2). However, when $\overline{M}_n$ was used as the second response variable with R_p, the converged estimate of k_t increased only slightly to 9.8E3 and the fitted values of $\overline{M}_n$ (Figure 4.3) were largely unchanged from those shown in Figure 4.1. Therefore, the two-response models were capable of fitting the MW response variables to the observations by adjusting the estimate of k_t.

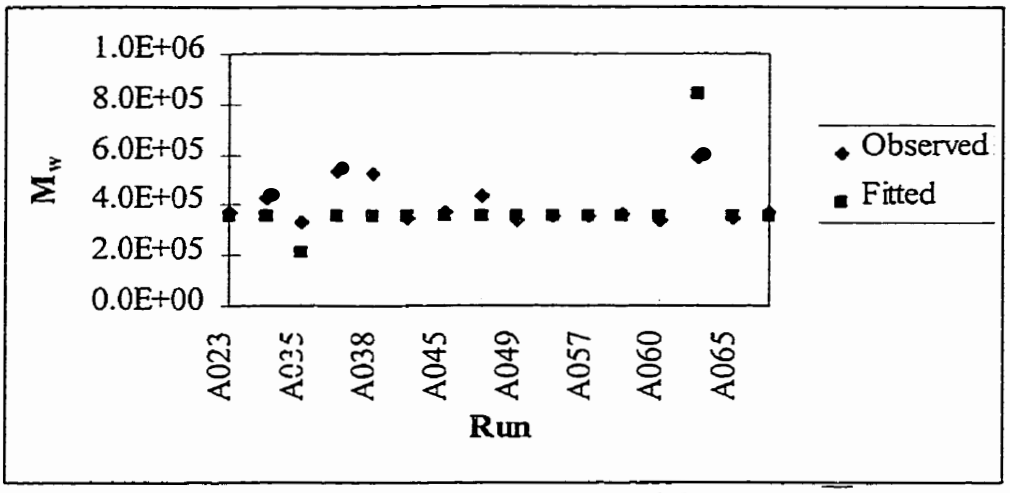

Figure 4.2 Fitted values from the two-response model (Rp and $\overline{M}_w$) assuming a known diagonal covariance matrix (see Appendix B for operating conditions)

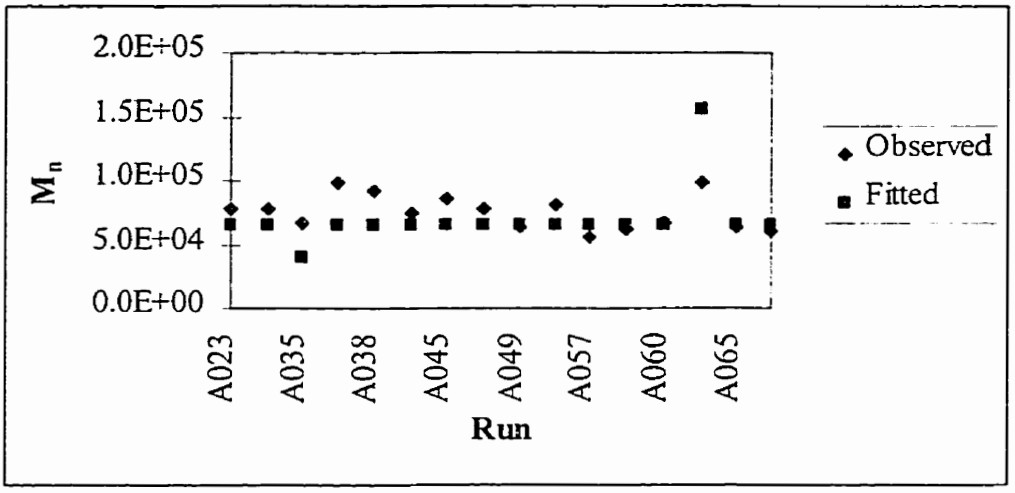

Figure 4.3 Fitted values from the two-response model (Rp and $\overline{M}_n$) assuming a known diagonal covariance matrix (see Appendix B for operating conditions)

4.3.5 Fitting a Three-Response Model with Known Diagonal Covariance Matrix

The three-response model described in Section 4.3.2 was refitted using the response variance estimates calculated from the data as the elements of a known diagonal covariance matrix (GREG *level* 22, see Section 3.2.2). The data structure is block rectangular, as described in the introduction of Chapter 3 and illustrated here in Figure

4.4. Again, an observation is represented by a plus sign while a blank space implies a missing data value. Results from this parameter estimation are reported in Table 4.11.

Event	R_p (mol/min)	$\overline{M}_w$ (g/mol)	$\overline{M}_n$ (g/mol)
1	+		
2	+		
:	:		
:	:		
1920	+		
1921		+	+
1922		+	+
:		:	:
:		:	:
1936		+	+

Figure 4.4. Block rectangular data used in parameter estimation

Table 4.11. Parameter estimates from a three-response model (R_p, $\overline{M}_n$, and $\overline{M}_w$) with one type of active sites and no monomer diffusion, assuming a known diagonal covariance matrix (GREG *level* 22)

			Correlation matrix			
Parameter (L/mol/min)	Estimated value	95% confidence interval	k_a	k_d	k_p	k_t
k_a	135.3	± 7.9	1.000			
k_d	5.61	± 0.19	-0.090	1.000		
k_p	1.8E5	± 297.6	-0.173	0.249	1.000	
k_t	4.9E3	± 86.7	-0.016	0.023	0.093	1.000

Although the widths of all of the confidence intervals are smaller than the corresponding intervals in Table 4.9, those for k_p and k_t are significantly reduced, by ±2100 L/mol/min and ±1200 L/mol/min, respectively. Also, all of the off-diagonal elements of the parameter correlation matrix are smaller, with no strong correlation between any two parameter estimates. These results indicate that there is enough information in the data to estimate all four parameters, so that they can be used as initial guesses for parameter estimation in a more complex model.

A comparison between the results obtained in Section 4.3.2 and the results of this fit indicates that the estimated values for k_a, k_d, and k_p are similar to those in Table 4.9, whereas the value for k_t decreases by almost one-half. This suggests that the polymer chains propagate for a longer period before terminating, resulting in higher average molecular weights. Figure 4.5 confirms the higher fitted values for $\overline{M}_w$ and $\overline{M}_n$, $\overline{M}_w$ being consistently underestimated while $\overline{M}_n$ is consistently overestimated. Fitted rate values for the six replicate runs are pictured in Figure 4.6. The fitted values are lower than the observations for experimental runs A056 and A060 while good agreement is achieved for the other four runs. The observed maximum polymerization rates for experimental runs A056 and A060 are higher than those of the other four replicate runs. A higher activation rate constant would be needed to reach the higher maxima.

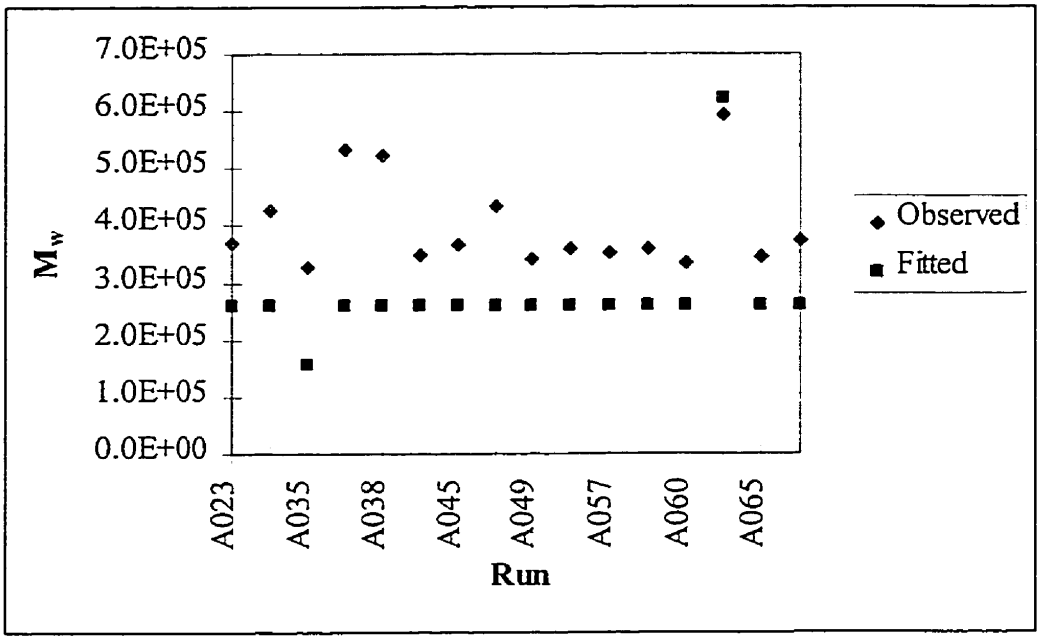

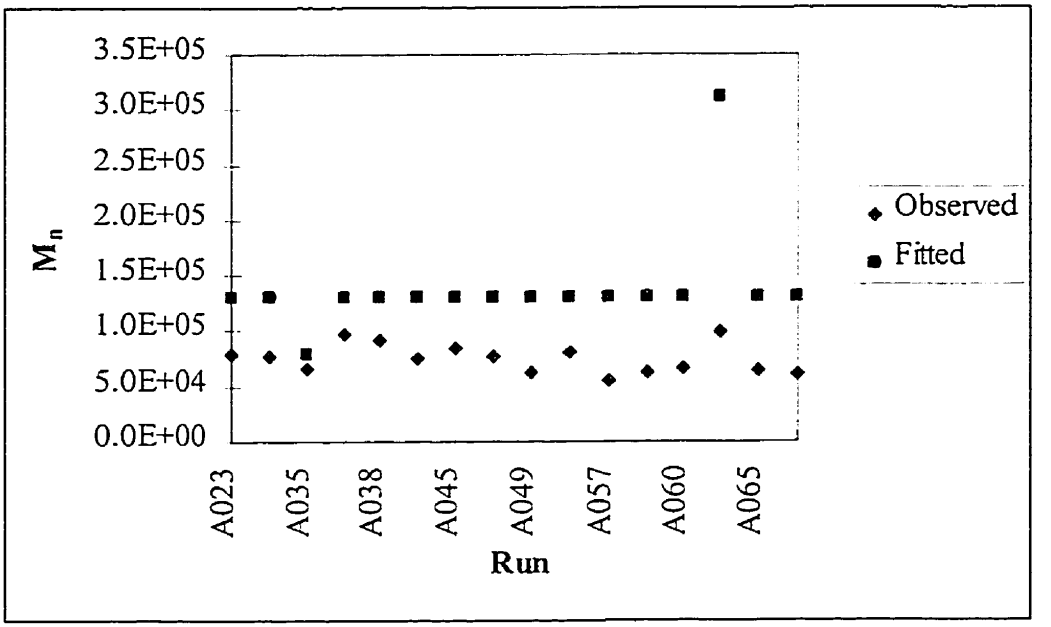

Figure 4.5 Fitted values from the three-response model (R_p, $\overline{M}_n$, and $\overline{M}_w$) assuming a known diagonal covariance matrix (see Appendix B for operating conditions)

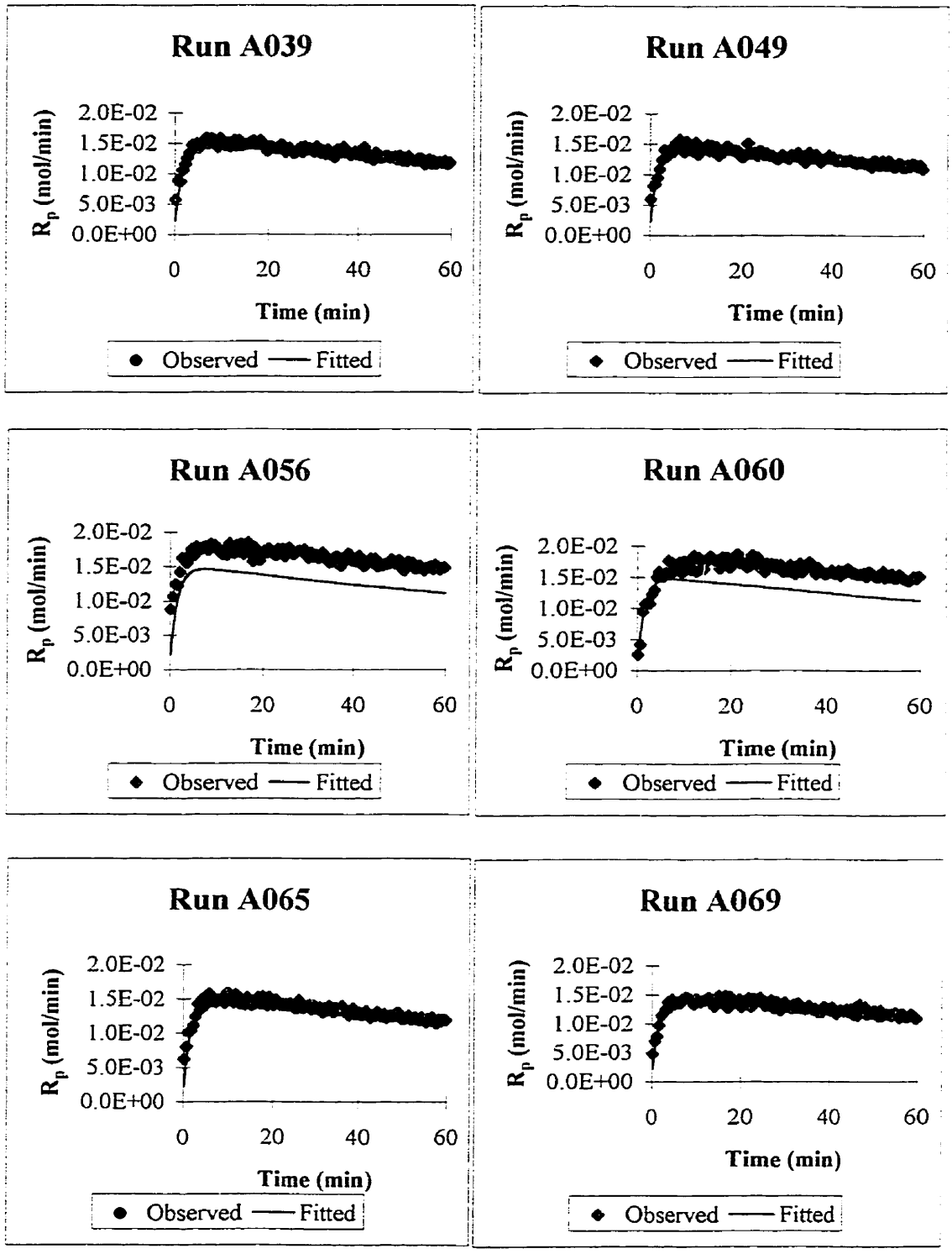

Figure 4.6. Observed and fitted polymerization rate values for replicate runs at 70^0C from the three-response model (R_p, M_w, M_n) assuming a known diagonal covariance matrix (operating condition: 10 mg-catalyst, 1.2 mL-cocatalyst, 2 atm monomer partial pressure, 0.24 atm hydrogen partial pressure, 250 μm particle size)

The last elements to be verified are the polydispersities, which are the ratios of $\overline{M}_w$ to $\overline{M}_n$. Using the fitted values of molecular weights to calculate fitted values of polydispersities yields values of 2, whereas the observed polydispersities range from 4 to 7. Approximate 95% confidence intervals for the observed polydispersity values can be calculated according to the following expression:

$$\text{observed } PD \pm t_{\nu,0.025}\, s_{PD} \tag{4.12}$$

where ν is the number of degrees of freedom associated with the estimated standard deviation of the observed polydispersity values, s_{PD}, and $t_{5,0.025} = 2.571$. The degrees of freedom are assumed to be the same as the degrees of freedom for the sample variances of the measured values of $\overline{M}_n$ and $\overline{M}_w$. An expression for the polydispersity variance can be derived from a first order Taylor series expansion:

$$PD = \frac{\overline{M}_{w,0}}{\overline{M}_{n,0}} + \left(\overline{M}_w - \overline{M}_{w,0}\right)\left.\frac{\partial\left(\frac{\overline{M}_w}{\overline{M}_n}\right)}{\partial \overline{M}_w}\right|_{\overline{M}_{w,0},\overline{M}_{n,0}} + \left(\overline{M}_n - \overline{M}_{n,0}\right)\left.\frac{\partial\left(\frac{\overline{M}_w}{\overline{M}_n}\right)}{\partial \overline{M}_n}\right|_{\overline{M}_{w,0},\overline{M}_{n,0}} \tag{4.13}$$

$$\sigma^2_{PD} = \left(\frac{1}{\overline{M}_{n,0}}\right)^2 \sigma^2_{\overline{M}_w} + \left(\frac{-\overline{M}_{w,0}}{\left(\overline{M}_{n,0}\right)^2}\right)^2 \sigma^2_{\overline{M}_n} \tag{4.14}$$

where $\overline{M}_{n,0}$ and $\overline{M}_{w,0}$ are point estimates of $\overline{M}_n$ and $\overline{M}_w$. From Table 4.12 it can be seen that none of the approximate 95% confidence intervals for the observed polydispersity values contain the fitted polydispersity values of 2, thereby confirming the inadequacy of this model as a predictor of polydispersity.

Table 4.12. Approximate 95% confidence intervals for the observed polydispersity values from a three-response model (R_p, $\overline{M}_n$, and $\overline{M}_w$) with one type of active sites and no monomer diffusion, assuming a known diagonal covariance matrix (GREG *level* 22)

Run number	Estimated PD	Observed PD	95% confidence interval
A023	2.00	4.74	± 1.34
A024	2.00	5.56	± 1.57
A035	2.00	4.95	± 1.65
A036	2.00	5.45	± 1.21
A038	2.00	5.67	± 1.34
A039	2.00	4.67	± 1.38
A045	2.00	4.32	± 1.13
A048	2.00	5.65	± 1.59
A049	2.00	5.40	± 1.87
A056	2.00	4.42	± 1.22
A057	2.00	6.40	± 2.50
A059	2.00	5.81	± 2.03
A060	2.00	5.08	± 1.69
A064	2.00	5.98	± 1.31
A065	2.00	5.41	± 1.84
A069	2.00	6.22	± 2.23

In summary, an acceptable fit to this set of data containing a large number of missing values could not be obtained with the three-response (R_p, $\overline{M}_w$, and $\overline{M}_n$) model assuming an unknown diagonal covariance matrix. With a known diagonal covariance matrix there was enough information in the data to estimate four parameters, but the fitted response values were still unsatisfactory. This was expected because the single-site structure of the model given in Table 4.4 is known to give polydispersity predictions near 2.0, no matter what parameter values are used. To resolve this problem, a model with two active site types was then considered. The results from this model are reported in Chapter 5.

Chapter 5: Models for Ziegler-Natta Catalyst with Two Types of Sites

A similar approach to parameter estimation was taken to deal with the two-types-of-sites model as was used with the one type of site model. Material balances and single- and three-response models are described in Section 5.1. New parameters involved in the proposed model are also introduced in Section 5.1. Parameter estimation results for the single and three-response models are presented in Sections 5.2 and 5.3, respectively. Temperature dependence of the rate constants is investigated in Section 5.4. The validity of the model is assessed in Section 5.5.

5.1 Model with Two Types of Sites and Monomer Diffusion

The two-types-of-sites model is a natural extension of the one-type-of-site model presented in Chapter 4. The research done by Shariati (1996) suggested the presence of two types of catalyst sites: Ti^{+3} (hereafter referred as type 1) and Ti^{+2} (hereafter referred as type 2). Consequently, the potential sites were assumed to be activated by the cocatalyst to form sites of type 1 or type 2.

The initiation and propagation steps were again assumed to have the same rate constant. There is also a possibility of site transformation; a site of type 1 could react with the cocatalyst in the initiation and propagation stages and reduce to a site of type 2, and a site of type 2 could react with hydrogen after activation to form a site of type 1. The rate constants associated with the two site transformation reactions are denoted as k_{st} and k_{ah}, respectively.

Monomer diffusion limitations within a polymer particle can lead to a monomer concentration gradient and contribute to a broad MWD. Therefore, the average monomer concentration within a particle (equation 5.2) was used in the initiation and propagation reaction and in the rate equation 5.3. Two types of site deactivation were considered: a site could deactivate by itself (k_{sd}) or by reacting with hydrogen (k_d). Hydrogen is used to control the molecular weight by chain transfer reactions. The kinetic reactions considered in the two types of sites model are presented in Table 5.1 while the material

Table 5.1 Kinetics for a two types of sites model

Reaction Type	Description	Reaction Mechanism
Activation	Cocatalyst activates potential sites of type 1	$C+[A]\xrightarrow{k_{a1}}C_{01}^{*}$
	Cocatalyst activates potential sites of type 2	$C+[A]\xrightarrow{k_{a2}}C_{02}^{*}$
Initiation	Monomer initiates active sites of type 1	$C_{01}^{*}+[\overline{M}]\xrightarrow{k_{p1}}[P_{11}^{*}]$
	Monomer initiates active sites of type 2	$C_{02}^{*}+[\overline{M}]\xrightarrow{k_{p2}}[P_{12}^{*}]$
Propagation	Propagation of polymer chains at sites of type 1	$[P_{n,1}^{*}]+[\overline{M}]\xrightarrow{k_{p1}}[P_{n+1,1}^{*}]$
	Propagation of polymer chains at sites of type 2	$[P_{n,2}^{*}]+[\overline{M}]\xrightarrow{k_{p2}}[P_{n+1,2}^{*}]$
Site Transformation	Cocatalyst transforms type 1 to type 2	$C_{01}^{*}+[A]\xrightarrow{k_{st}}C_{02}^{*}$
	Cocatalyst transforms type 1 to type 2	$[P_{n,1}^{*}]+[A]\xrightarrow{k_{st}}[P_{n,2}^{*}]$
	Hydrogen transforms type 2 to type 1	$C_{02}^{*}+[H]\xrightarrow{k_{ah}}C_{01}^{*}$
Deactivation	Hydrogen deactivates polymer chains at sites of type 1	$[P_{n,1}^{*}]+[H]\xrightarrow{k_{d1}}C_{d}+[D_{n}]$
	Hydrogen deactivates polymer chains at sites of type 2	$[P_{n,2}^{*}]+[H]\xrightarrow{k_{d2}}C_{d}+[D_{n}]$
	Spontaneous deactivation at sites of type 1	$[P_{n,1}^{*}]\xrightarrow{k_{sd1}}C_{d}+[D_{n}]$
	Spontaneous deactivation at sites of type 2	$[P_{n,2}^{*}]\xrightarrow{k_{sd2}}C_{d}+[D_{n}]$
Chain Transfer	Hydrogen causes chain transfer at sites of type 1	$[P_{n,1}^{*}]+[H]\xrightarrow{k_{t1}}C_{01}^{*}+[D_{n}]$
	Hydrogen causes chain transfer at sites of type 2	$[P_{n,2}^{*}]+[H]\xrightarrow{k_{t2}}C_{02}^{*}+[D_{n}]$

balances and their initial conditions are found in Table 5.2.

The growth of polymer particles (equation 2 of Table 5.2) was modeled according to the work described in Shariati (1996). Again, the method of moments was applied to determine the molecular weights. The ordinary differential equations (ODEs) solved for the single response model (which predicts R_p alone) were equations 1 through 4 of Table 5.2 along with equation 5.3, involving ten parameters (k_{a1}, k_{a2}, k_{d1}, k_{d2}, k_{p1}, k_{p2}, k_{st}, k_{ah}, k_{sd1}, and k_{sd2}). For the three-response model (which predicts R_p, $\overline{M}_w$, and $\overline{M}_n$) equations 1, 2, and 5 through 15 of Table 5.2 along with equations 5.3 through 5.5 were solved simultaneously to estimate twelve parameters (the ten parameters from the single response model plus k_{t1} and k_{t2}).

Shariati used the equation group 5.1 to simplify some of the ordinary differential equations described in Table 5.2 and the average monomer concentration (equation 5.2).

$$C^* = C_1^* + \frac{k_{p2}}{k_{p1}} C_2^*$$

$$C_j^* = C_{0j}^* + \lambda_0^j \qquad (5.1)$$

$$a = \exp\left(\sqrt{\frac{k_{p1} C^*}{D_m}} r_p \right)$$

$$\left[\overline{M}\right] = [M]_0 \left(\frac{a-1}{(a+1) r_p \sqrt{\frac{k_{p1} C^*}{D_m}}} \right) \qquad (5.2)$$

Table 5.2 Material balances and initial conditions for the two types of sites model

Material Balances and Methods of Moments		Initial Conditions
$\frac{dC}{dt} = -(k_{a1} + k_{a2})C[A]$	(1)	Varies, see Appendix B
$\frac{dr_p}{dt} = \frac{MW M_0 D_m}{\rho_p r_p}\left(\sqrt{\frac{k_{p1} C^*}{D_m}} r_p \frac{a^2+1}{a^2-1} - 1\right)$	(2)	Varies, see Appendix B
$\frac{dC_1^*}{dt} = k_{a1} C[A] - C_1^*\{k_{st}[A] + k_{sd1} + k_{d1}[H]\} + k_{aH} C_2^*[H]$	(3)	2E-14
$\frac{dC_2^*}{dt} = k_{a2} C[A] + k_{st} C_1^*[A] - C_2^*\{k_{aH}[H] + k_{sd2} + k_{d2}[H]\}$	(4)	2E-14
$\frac{dC_{01}^*}{dt} = k_{a1} C[A] - C_{01}^*\{k_{st}[A] + k_{p1}[\overline{M}]\} + k_{aH} C_{02}^*[H] + k_{t1}\lambda_0^1[H]$	(5)	2E-14
$\frac{dC_{02}^*}{dt} = k_{a2} C[A] + k_{st} C_{01}^*[A] - C_{02}^*\{k_{aH}[H] + k_{p2}[\overline{M}]\} + k_{t2}\lambda_0^2[H]$	(6)	2E-14
$\frac{d\lambda_0^1}{dt} = k_{p1} C_{01}^*[\overline{M}] - \lambda_0^1\{k_{d1}[H] + k_{st}[A] + k_{t1}[H] - k_{sd1}\}$	(7)	2E-10
$\frac{d\lambda_1^1}{dt} = k_{p1}(C_{01}^* + \lambda_0^1)[\overline{M}] - \lambda_1^1\{k_{d1}[H] + k_{t1}[H] + k_{st}[A] + k_{sd1}\}$	(8)	2E-12
$\frac{d\lambda_2^1}{dt} = k_{p1}(C_{01}^* + \lambda_0^1 + 2\lambda_1^1)[\overline{M}] - \lambda_2^1\{k_{d1}[H] + k_{t1}[H] + k_{st}[A] + k_{sd1}\}$	(9)	2E-14
$\frac{d\lambda_0^2}{dt} = k_{p2} C_{02}^*[\overline{M}] - \lambda_0^2\{k_{d2}[H] - k_{st}[A] + k_{t2}[H] + k_{sd2}\}$	(10)	2E-10
$\frac{d\lambda_1^2}{dt} = k_{p2}(C_{02}^* + \lambda_0^2)[\overline{M}] - \lambda_1^2\{k_{d2}[H] + k_{t2}[H] - k_{st}[A] + k_{sd2}\}$	(11)	2E-12
$\frac{d\lambda_2^2}{dt} = k_{p2}(C_{02}^* + \lambda_0^2 + 2\lambda_1^2)[\overline{M}] - \lambda_2^2\{k_{d2}[H] + k_{t2}[H] - k_{st}[A] + k_{sd2}\}$	(12)	2E-14
$\frac{d\Lambda_0}{dt} = \{k_{d1}\lambda_0^1 + k_{d2}\lambda_0^2 + k_{t1}\lambda_0^1 + k_{t2}\lambda_0^2\}[H] + k_{sd1}\lambda_0^1 + k_{sd2}\lambda_0^2$	(13)	2E-10
$\frac{d\Lambda_1}{dt} = \{k_{d1}\lambda_1^1 + k_{d2}\lambda_1^2 + k_{t1}\lambda_1^1 + k_{t2}\lambda_1^2\}[H] + k_{sd1}\lambda_1^1 + k_{sd2}\lambda_1^2$	(14)	2E-12
$\frac{d\Lambda_2}{dt} = \{k_{d1}\lambda_2^1 + k_{d2}\lambda_2^2 + k_{t1}\lambda_2^1 + k_{t2}\lambda_2^2\}[H] + k_{sd1}\lambda_2^1 + k_{sd2}\lambda_2^2$	(15)	2E-14

The equations describing the rate of polymerization, number average molecular weight, and weight average molecular weight are:

$$R_p = k_{p1} C^*[\overline{M}] \qquad (5.3)$$

$$\overline{M}_n = MW \frac{\lambda_1^1 + \lambda_1^2 + \Lambda_1}{\lambda_0^1 + \lambda_0^2 + \Lambda_0} \tag{5.4}$$

$$\overline{M}_w = MW \frac{\lambda_2^1 + \lambda_2^2 + \Lambda_2}{\lambda_1^1 + \lambda_1^2 + \Lambda_1} \tag{5.5}$$

The initial conditions for equations 3 through 15 in Table 5.2 were set at a small number (effectively zero but chosen to avoid division by zero in DDASAC (Stewart et al., 1994)), whereas the initial conditions for equations 1 and 2 had the values listed in Appendix B. The polyethylene density (used to calculate the rate of change of the radius of the growing polymer particle, equation 2 of Table 5.2), ρ_p, was set at 960 g/L, which is at the high end of the high-density polyethylene density range. The monomer diffusivity constant D_m was fixed at a mid-range value of 6E-5 cm^2/min suggested by Floyd et al. (1987).

5.1.1 Parameter Transformations

Parameter transformations were applied to all parameters for a number of reasons. Transformations were used to prevent the parameters from taking on meaningless values (such as a negative number) and also to provide appropriate scaling. When parameter transformations were applied to only some of the parameters, convergence was not always attained. Consequently, for the rest of the study all parameters were transformed during the parameter estimation, but the parameter estimates are reported in their original untransformed forms. The transformations applied to the rate constants were described in Section 2.5. The logarithmic transformation given in equation 2.10 can be rewritten as:

$$k_i = \exp(\theta_i) \tag{5.6}$$

Since it was assumed that the activation energy of k_{i2} was the same as the activation energy of k_{i1}, a ratio of rate constants at the two site types ($\gamma_i = k_{i2}/k_{i1}$, where i represents a, d, p, or t) was estimated. The transformation applied to the ratios, to ensure positive values, was:

$$\gamma_i = \theta_i^2 \qquad (5.7)$$

5.2 Single Response Model

The single and three-response models for a catalyst having two types of sites (Sections 5.2 and 5.3, respectively) were fitted to the data from the 16 experimental runs at 70°C (as was done with the one type of site catalyst in Chapter 4). Parameter estimation was also performed using the data from the sets of 16 experimental runs at 62 and 78°C, respectively. Fitting the single response model (which predicts R_p alone) involved estimation of nine parameters in equations 1 through 4 in Table 5.2 and equation 5.3 since, at these three temperatures, it was impossible to obtain separate estimates of both k_{sd1} and k_{sd2}. Whenever the parameter k_{sd2} was included in the set of parameters to be estimated no convergence was achieved, since GREG would oscillate about an arbitrary parameter vector and not meet the convergence criteria after more than 100 iterations. Therefore, only one spontaneous deactivation rate constant, k_{sd}, was estimated for both site types. Results at 78°C are not reported here since the estimated value for k_{sd} was 6.7E-24 with a 95% confidence interval of (exp(-3.4E4), exp(3.4E4)). The results at 70 and 62°C can be found in Tables 5.3a and 5.3b, respectively.

Table 5.3a. Parameter estimates from a single response model at 70°C with two active site types and monomer diffusion (GREG *level* 10)

Parameter	Estimate	95% confidence interval	
k_{a1} (L/mol/min)	114.54	105.96	123.79
γ_a	1.2E-4	3.9E-5	7.9E-4
k_{d1} (L/mol/min)	5.19	4.45	6.06
γ_d	0.64	0.15	1.48
k_{p1} (L/mol/min)	4.7E5	4.61E5	4.78E5
γ_p	1.5E-4	1.1E-4	1.25E-3
k_{sd} (min^{-1})	9.5E-12	2.1E-17	4.2E-6
k_{ah} (L/mol/min)	7.1E-4	1.5E-4	3.5E-3
k_{st} (L/mol/min)	0.47	0.42	0.51

Table 5.3b. Parameter estimates from a single response model at 62°C with two active site types and monomer diffusion (GREG *level* 10)

Parameter	Estimate	95% confidence interval	
k_{a1} (L/mol/min)	94.16	88.85	99.80
γ_a	2.44	2.21	2.68
k_{d1} (L/mol/min)	4.76	4.42	5.13
γ_d	20.66	20.13	21.19
k_{p1} (L/mol/min)	3.81E5	3.77E5	3.85E5
γ_p	1.5E-3	2.1E-5	5.4E-3
k_{sd} (min^{-1})	6.4E-12	8.9E-15	4.6E-9
k_{ah} (L/mol/min)	4.0E-4	1.3E-4	1.3E-3
k_{st} (L/mol/min)	0.10	0.08	0.13

The estimated parameters were used as reasonable initial guesses in the multiresponse model. Estimated parameters at 70°C were used as initial values for fitting the multiresponse model to the data at 78°C. The parameter correlation matrices are in Appendix D.

5.3 Multiresponse Model with Known Diagonal Covariance Matrix

The multiresponse model (which predicts R_p, $\overline{M}_w$, and $\overline{M}_n$) simultaneously solves the differential equations 1, 2, and 5 through 15 of Table 5.2 and the three algebraic equations 5.3 through 5.5. Initially, eleven parameters (k_{a1}, γ_a, k_{d1}, γ_d, k_{p1}, γ_p,

k_{st}, k_{tl}, γ_t, k_{ah}, and k_{sd}) were included in the model. However, no convergence was attained (iterations were oscillating in a small region) since the parameter estimates for k_{ah} and k_{sd} were becoming extremely small (3E-7 and 4E-8, respectively). At 70°C the orders of magnitude for the terms in the differential equations involving those two parameters were compared to the other terms. Since the terms with k_{ah} and k_{sd} were always four to five orders of magnitude smaller than the other terms in equations 1, 2, and 5 through 15 of Table 5.2, those two parameters were set to zero and removed from the model. Results for the three temperature groups are reported in Tables 5.4a-5.4c and the respective correlation matrices for the parameters are presented in Tables 5.5a-5.5c. The objective function tolerance (RSTOL) was set to 5 for all reported simulations.

Table 5.4a. Parameter estimates from a three-response model (R_p, $\overline{M}_w$, and $\overline{M}_n$) at 78°C with two active site types and monomer diffusion (GREG *level* 22)

Parameter	Estimated value	95% confidence interval	
k_{al} (L/mol/min)	169.81	156.77	183.94
k_{dl} (L/mol/min)	1.88	1.39	2.55
k_{pl} (L/mol/min)	5.34E5	5.26E5	5.42E5
γ_p	9.0E-3	5.7E-3	1.3E-2
k_{st} (L/mol/min)	2.23	2.09	2.39
γ_d	2.84	1.39	4.79
γ_a	4.2E-2	3.8E-2	4.7E-2
k_{tl} (L/mol/min)	7.28E3	7.18E3	7.38E3
γ_t	10.82	8.31	13.66

Table 5.4b. Parameter estimates from a three-response model (R_p, $\overline{M}_w$, and $\overline{M}_n$) at 70°C with two active site types and monomer diffusion (GREG *level* 22)

Parameter	Estimated value	95% confidence interval	
k_{al} (L/mol/min)	112.29	105.24	119.81
k_{dl} (L/mol/min)	5.29	4.67	6.00
k_{pl} (L/mol/min)	4.91E5	4.85E5	4.98E5
γ_p	7.3E-3	6.0E-3	8.7E-3
k_{st} (L/mol/min)	0.48	0.36	0.64
γ_d	1.28	0.68	2.06
γ_a	4.4E-2	4.1E-2	4.7E-2
k_{tl} (L/mol/min)	6.98E3	6.89E3	7.07E3
γ_t	19.42	15.21	24.14

Table 5.4c. Parameter estimates from a three-response model (R_p, $\overline{M}_w$, and $\overline{M}_n$) at 62°C with two active site types and monomer diffusion (GREG *level* 22)

Parameter	Estimated value	95% confidence interval	
k_{a1} (L/mol/min)	94.04	87.88	100.62
k_{d1} (L/mol/min)	4.74	4.15	5.41
k_{p1} (L/mol/min)	3.95E5	3.89E5	4.01E5
γ_p	7.0E-3	5.7E-3	8.3E-3
k_{st} (L/mol/min)	0.14	0.06	0.32
γ_d	1.12	0.54	1.91
γ_a	5.1E-2	4.7E-2	5.5E-2
k_{t1} (L/mol/min)	5.48E3	5.40E3	5.55E3
γ_t	26.22	21.54	31.35

Table 5.5a. Correlation matrix for the parameter estimates at 78°C (corresponding to Table 5.4a)

Parameter	k_{a1}	k_{d1}	k_{p1}	γ_p	k_{st}	γ_d	γ_a	k_{t1}	γ_t
k_{a1}	1.00								
k_{d1}	-0.10	1.00							
k_{p1}	-0.36	0.22	1.00						
γ_p	0.03	-0.06	-0.26	1.00					
k_{st}	-0.14	-0.77	0.30	0.06	1.00				
γ_d	-0.06	-0.57	0.02	0.29	0.57	1.00			
γ_a	-0.04	0.10	0.25	-0.93	-0.13	-0.08	1.00		
k_{t1}	-0.39	0.21	0.97	-0.29	0.32	0.02	0.25	1.00	
γ_t	-1E-3	0.02	-0.01	0.02	-0.03	0.09	-8E-5	-0.01	1.00

Table 5.5b. Correlation matrix for the parameter estimates at 70°C (corresponding to Table 5.4b)

Parameter	k_{a1}	k_{d1}	k_{p1}	γ_p	k_{st}	γ_d	γ_a	k_{t1}	γ_t
k_{a1}	1.00								
k_{d1}	-0.14	1.00							
k_{p1}	-0.43	0.32	1.00						
γ_p	-0.05	-0.16	-0.09	1.00					
k_{st}	-0.13	-0.77	0.24	0.22	1.00				
γ_d	-0.15	-0.30	0.16	0.34	0.42	1.00			
γ_a	0.02	0.20	0.09	-0.91	-0.28	-0.04	1.00		
k_{t1}	-0.47	0.30	0.97	-0.11	0.26	0.17	0.09	1.00	
γ_t	4E-3	0.02	-5E-3	0.05	-0.02	0.12	-0.02	-0.01	1.00

Table 5.5c. Correlation matrix for the parameter estimates at 62°C (corresponding to Table 5.4c)

Parameter	k_{al}	k_{dl}	k_{pl}	γ_p	k_{st}	γ_d	γ_a	k_{tl}	γ_t
k_{al}	1.00								
k_{dl}	-0.16	1.00							
k_{pl}	-0.44	0.34	1.00						
γ_p	-0.02	-0.14	-0.19	1.00					
k_{st}	-0.16	-0.69	0.30	0.18	1.00				
γ_d	-0.17	-0.23	0.24	0.15	0.43	1.00			
γ_a	0.01	0.16	0.18	-0.96	-0.23	0.03	1.00		
k_{tl}	-0.47	0.33	0.98	-0.20	0.32	0.25	0.19	1.00	
γ_t	-1E-3	0.02	-0.01	0.03	-0.02	0.11	-0.01	-0.01	1.00

The highest pairwise correlations are between parameters k_{pl} and k_{tl} (0.97 and 0.98) and between parameters γ_p and γ_a (-0.91 and –0.96). The pairwise correlation between k_{pl} and k_{tl} is highly positive since increasing both k_{pl} and k_{tl} can lead to a constant molecular weight. The pairwise correlation between γ_p and γ_a is strongly negative since an increase in γ_p and a decrease in γ_a will maintain a constant polymerization rate. Although these correlation values are high, no parameters were eliminated from the model until the three temperature groups were combined, in hope that the correlations would decrease. The estimated polydispersities (PD), calculated from the fitted molecular weights, are presented in Table 5.6. Although most of the estimated polydispersities are greater than 3, they are still consistently lower than the observed values.

Table 5.6. Observed and estimated polydispersities from the fitted models for individual temperature groups

62°C		70°C		78°C	
Estimated	Observed	Estimated	Observed	Estimated	Observed
3.39	5.68	3.20	4.74	3.29	5.50
3.31	6.03	3.08	5.56	3.32	4.86
3.59	5.29	2.93	4.95	3.01	5.86
3.76	7.04	3.09	5.45	3.06	4.93
3.76	5.92	3.04	5.67	2.95	5.38
3.65	5.39	3.12	4.67	3.06	5.47
3.81	5.90	3.00	4.32	3.28	6.38
3.46	5.57	3.16	5.65	3.10	5.53
3.43	5.54	3.12	5.40	2.98	5.37
3.76	5.34	3.12	4.42	2.78	5.78
3.69	6.13	3.14	6.40	2.86	4.95
3.69	5.92	3.18	5.81	3.01	6.25
3.36	6.04	3.12	5.08	2.92	5.93
3.46	6.31	3.43	5.98	2.88	6.02
3.31	6.42	3.12	5.41	3.36	5.65
3.48	5.95	3.12	6.22	2.99	5.19

5.4 Non-isothermal Multiresponse Model

Figure 5.1, depicting ln k (from Tables 5.4a-5.4c) versus 1/T, shows that parameters k_{al}, k_{pl}, k_{tl}, and k_{st} have a strong linear temperature dependency and so they should be modeled with an Arrhenius relationship. There is no apparent linear relationship between estimates of ln k_{dl} and 1/T, and so it was assumed that k_{dl} is relatively insensitive to temperature effects over the range of interest. As discussed in Section 2.5, to facilitate parameter estimation the Arrhenius relationships are centered about a reference temperature T_0:

$$k_i = k_{i0} \exp\left[-\frac{E_i}{R}\left(\frac{1}{T}-\frac{1}{T_0}\right)\right] \tag{5.8}$$

In this case the reference temperature was chosen to be 70°C.

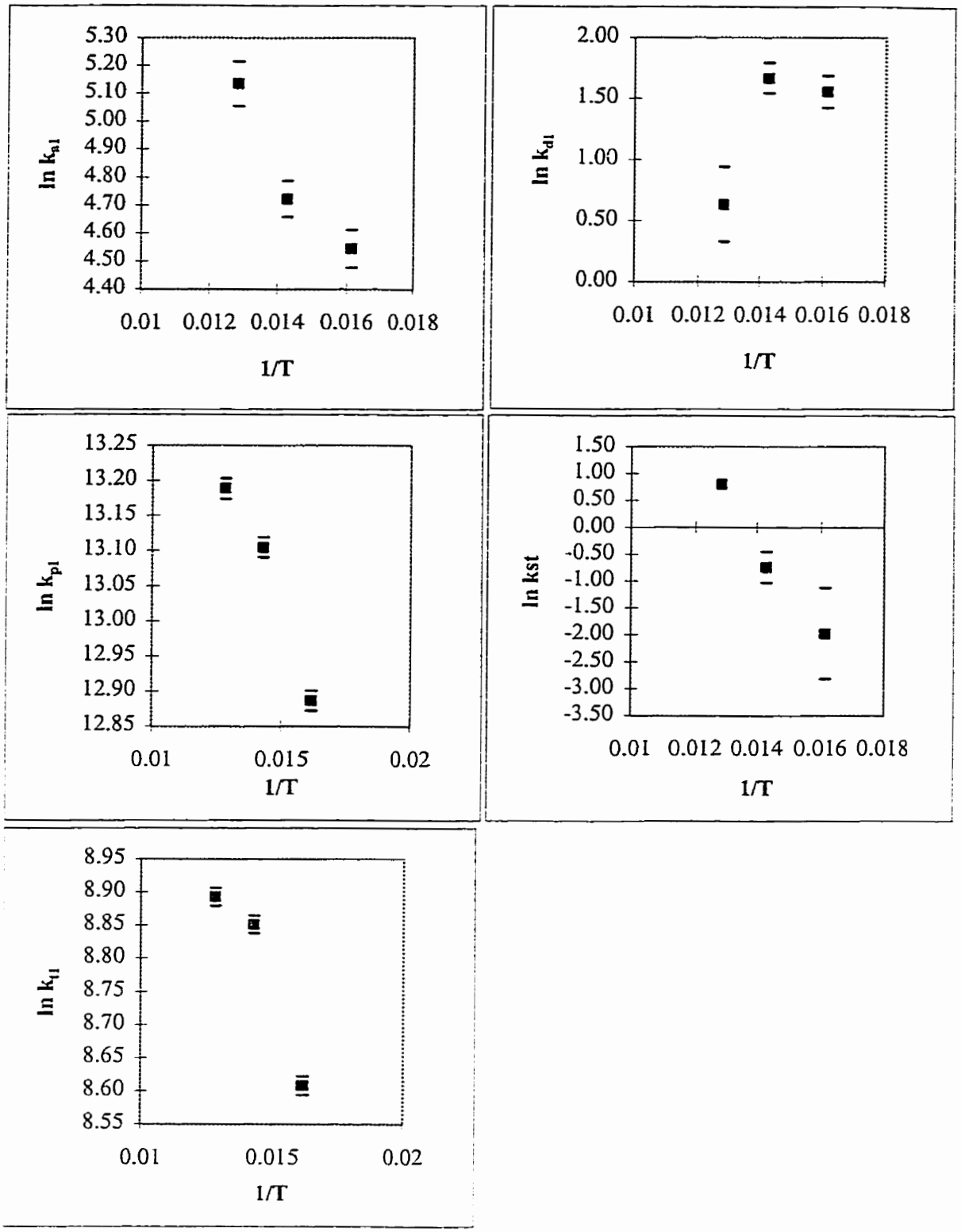

Figure 5.1. Temperature dependence of rate constants for the three-response model (R_p, M_w, and M_n

Both types of sites were assumed to have the same activation energy for each reaction type. No reasonable value could be obtained for the site transformation activation energy (E_{st}) with a model having thirteen parameters (k_{a0}, E_a, γ_a, k_{p0}, E_p, γ_p, k_{d1}, γ_d, k_{st0}, E_{st}, k_{t0}, E_t, and γ_t) since the estimated transformed parameter value was –6E3 (E_{st}=exp(-6E3)); therefore the Arrhenius relationship was removed for that parameter. In an attempt to increase the estimated polydispersities, the assumption that the propagation activation energy for sites of type 1 was the same as that for sites of type 2 was removed and separate estimates were obtained for E_{p1} and E_{p2}. With the transformation included, the Arrhenius equation for the ratio of the propagation rate constants (the subscript $_0$ refers to parameters at the centering temperature, 70°C) is:

$$\gamma_p = \gamma_{p0} \exp\left[\frac{\left(E_{p1} - E_{p2}\right)}{R}\left(\frac{1}{T} - \frac{1}{T_0}\right)\right] \qquad (5.9)$$

The parameter estimation results are presented in Tables 5.7a and 5.7b. All model fittings presented in this section converged with an RSTOL of 5.

Table 5.7a. Parameter estimates from the non-isothermal three-response model (R_p, $\overline{M}_w$, and $\overline{M}_n$) with two active site types and monomer diffusion, assuming a known diagonal covariance matrix (GREG *level* 22)

Parameter	Estimated value	95% confidence interval	
k_{a0} (L/mol/min)	1.17E2	1.12E2	1.22E2
E_a (cal/mol)	1.69E4	1.57E4	1.83E4
γ_a	7.7E-3	7.2E-3	8.3E-3
k_{p0} (L/mol/min)	4.52E5	4.49E5	4.55E5
E_{p1} (cal/mol)	1.74E3	1.59E3	1.91E3
E_{p2} (cal/mol)	6.11E2	4.93E2	7.58E2
γ_{p0}	0.89	0.86	0.92
k_{d1} (L/mol/min)	5.53	5.28	5.79
γ_d	2.69	2.59	2.80
k_{st} (L/mol/min)	0.58	0.55	0.60
k_{t0} (L/mol/min)	6.84E3	6.79E3	6.89E3
E_t (cal/mol)	2.64E3	2.49E3	2.80E3
γ_t	5.2E-4	3.7E-4	7.0E-4

Table 5.7b. Correlation matrix for the parameter estimates

	k_{a0}	E_a	γ_a	k_{p0}	E_{p1}	E_{p2}	γ_{p0}
k_{a0}	1.00						
E_a	0.48	1.00					
γ_a	-0.06	-0.05	1.00				
k_{p0}	-0.37	-0.06	0.09	1.00			
E_{p1}	-0.06	-0.19	0.11	0.16	1.00		
E_{p2}	-0.07	-0.32	0.20	0.12	0.77	1.00	
γ_{p0}	0.06	0.05	-0.98	-0.17	-0.11	-0.18	1.00
k_{d1}	-0.31	-0.08	0.14	0.71	0.17	0.11	-0.15
γ_d	0.19	0.05	-0.20	-0.51	-0.14	0.01	0.26
k_{st}	-0.03	0.03	-0.30	0.12	-0.06	-0.01	0.20
k_{t0}	-0.42	-0.07	0.12	0.96	0.15	0.15	-0.17
E_t	-0.06	-0.27	0.14	0.12	0.91	0.88	-0.13
γ_t	-4E-3	3E-3	-1E-3	7E-3	-0.01	-0.01	-0.02

	k_{d1}	γ_d	k_{st}	k_{t0}	E_t	γ_t
k_{a0}						
E_a						
γ_a						
k_{p0}						
E_{p1}						
E_{p2}						
γ_{p0}						
k_{d1}	1.00					
γ_d	-0.83	1.00				
k_{st}	-0.37	0.47	1.00			
k_{t0}	0.71	-0.47	0.09	1.00		
E_t	0.15	-0.11	-0.07	0.15	1.00	
γ_t	-0.03	-0.04	0.07	3E-3	-0.01	1.00

Since the confidence interval for E_{p1} did not include the estimate for E_{p2} and the pairwise correlation between those two estimates was not too high, both parameters were kept in the model. The greatest pairwise correlations are between estimates of parameters γ_a and γ_{p0} (-0.98) and between estimates of parameters k_{p0} and k_{t0} (0.96). The former correlation is strongly negative since a decrease in the activation rate constants would

require an increase in the propagation rate constants to maintain the same polymerization rate. As for the latter positive correlation, the molecular weight is maintained by increasing both k_{p0} and k_{t0}. Almost all of the estimated polydispersity values (Table 5.8) are larger than the corresponding values from the fitted models at individual temperatures (Table 5.6). As in Section 4.3.5, the observed polydispersity sample variances were calculated according to equation 4.14 while the approximate 95% confidence intervals for the observed polydispersity values were calculated according to equation 4.12. The results of these calculations are shown in Table 5.8.

Table 5.8. Observed polydispersity values along with their approximate 95% confidence intervals and corresponding estimated polydispersity values from the fitted non-isothermal three-response model (R_p, $\overline{M}_n$, and $\overline{M}_w$) with two active site types and monomer diffusion, assuming a known diagonal covariance matrix

62°C		70°C		78°C	
Estimated	Observed	Estimated	Observed	Estimated	Observed
4.32	5.68 ± 1.54	4.21	4.74 ± 1.34	4.15	5.50 ± 1.46
4.02	6.03 ± 2.10	3.86	5.56 ± 1.57	4.11	4.86 ± 1.34
2.97	5.29 ± 1.18	4.39	4.95 ± 1.65	3.40	5.86 ± 1.61
3.43	7.04 ± 1.86	3.16	5.45 ± 1.21	4.69	4.93 ± 2.01
2.99	5.92 ± 1.35	3.57	5.67 ± 1.34	3.88	5.38 ± 1.43
3.64	5.39 ± 1.38	3.88	4.67 ± 1.38	4.24	5.47 ± 2.33
3.66	5.90 ± 1.37	3.89	4.32 ± 1.13	3.59	6.38 ± 2.50
4.05	5.57 ± 1.57	3.94	5.65 ± 1.59	4.21	5.53 ± 2.67
3.43	5.54 ± 1.85	3.88	5.40 ± 1.87	4.66	5.37 ± 2.17
3.11	5.34 ± 1.23	3.89	4.42 ± 1.21	4.41	5.78 ± 2.46
3.13	6.13 ± 1.72	4.30	6.40 ± 2.50	3.99	4.95 ± 1.98
3.46	5.92 ± 1.44	3.88	5.81 ± 2.03	3.91	6.25 ± 2.21
3.46	6.04 ± 1.89	3.88	5.08 ± 1.69	4.49	5.93 ± 2.17
4.29	6.31 ± 2.12	3.00	5.98 ± 1.31	5.02	6.02 ± 2.50
3.64	6.42 ± 2.12	3.88	5.41 ± 1.84	3.61	5.65 ± 1.66
3.66	5.95 ± 2.22	3.89	6.22 ± 2.23	3.42	5.19 ± 1.51

The two types of sites, non-isothermal three-response model greatly improved the estimated polydispersities and was preferred to the one type of site, isothermal three-response model (at 70°C, Section 4.3.5). 50% of the estimated polydispersity values fell

within the estimated 95% confidence interval for the corresponding observed polydispersity values. Despite this substantial improvement this model still produced estimated polydispersity values that were consistently lower than the corresponding observed ones. Therefore, a centered Arrhenius relationship was applied to the chain transfer rate constant, E_{t2}. Since the 95% confidence interval for E_{t2} (420, 1.7E5) included the confidence interval for E_{t1} (2.9E3, 3.2E3) and no improvements were observed in the estimated polydispersities, the parameter E_{t2} (estimated value of 2.3E3) was not included in the final model and the full results are not presented here. That is, only one activation energy for the chain transfer rate constant, E_t, was estimated.

Most of the polymerization rate data were fitted rather well (Appendix E) and the fits are similar to those obtained by Shariati (1996). Figure 5.2 shows the fitted and observed MWs. Although these results are superior to those from previous models, the proposed model still had difficulty fitting both $\overline{M}_w$ and $\overline{M}_n$ simultaneously. The 95% confidence intervals for the estimated parameters in Table 5.7a are all much smaller than the corresponding 95% confidence intervals found in Shariati's Tables 6.9 and 6.11, indicating that the estimates of the current study are more precise. However, it was concluded that non-isothermal, three-response model based on the kinetics from Shariati's two types of sites model was incapable of fitting the three-response variables simultaneously, without a consistent bias. As mentioned in Section 2.3.2, Shariati (1996) solved two single response models, one for the polymerization rate and the other for one of the molecular weight response variables. It is not always possible to separate a kinetic model in such a manner (McAuley et al., 1990). The approach taken in this study could

be applied to different models that cannot be separated and fitted to missing data structures.

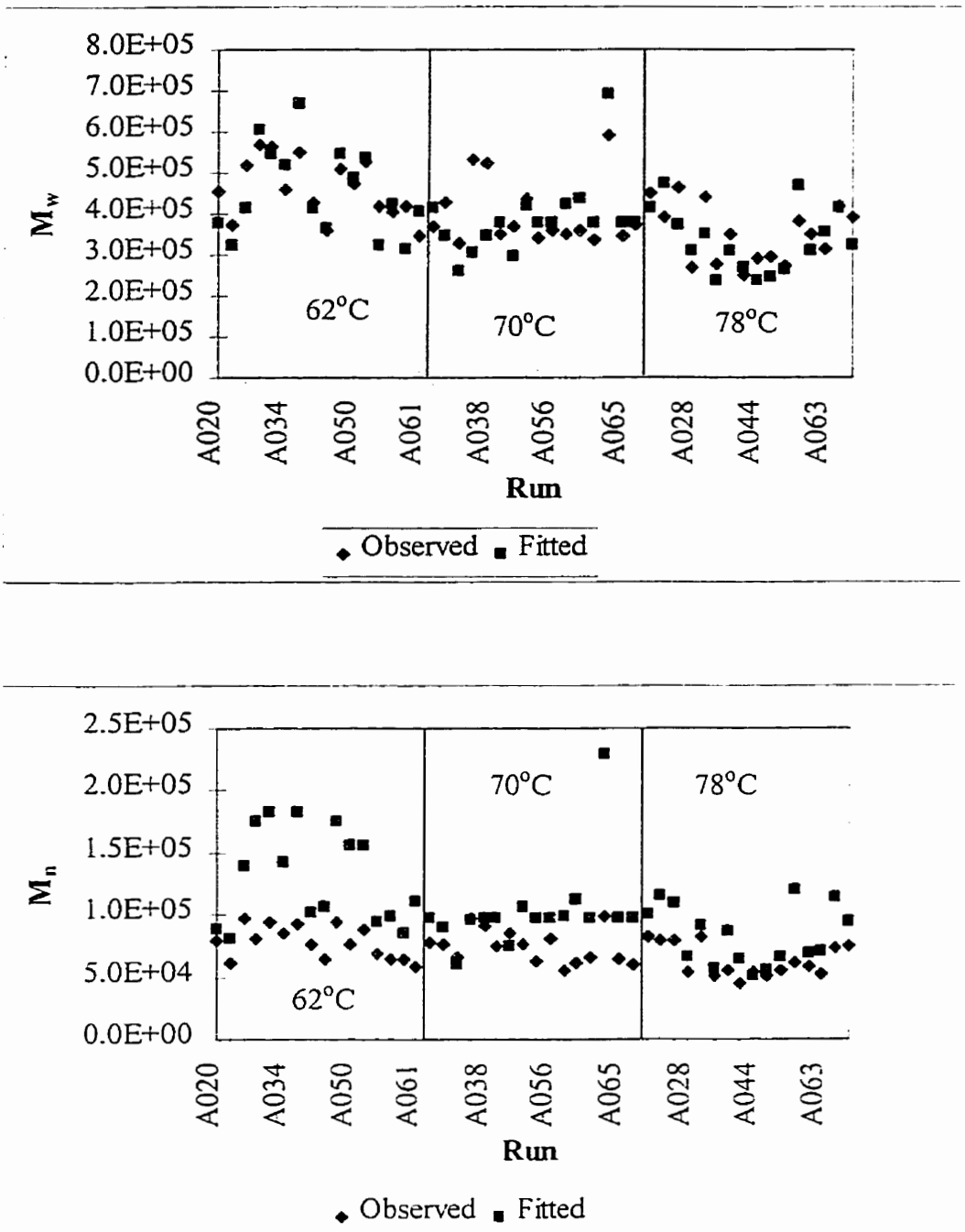

Figure 5.2 Fitted molecular weight response values for the non-isothermal three-response model (R_p, $\overline{M}_n$, and $\overline{M}_w$) with two active site types and monomer diffusion, assuming a known diagonal covariance matrix (see Appendix B for operating conditions)

5.5 Model Validation

To test the predictive capabilities of the model, parameter estimation was carried out with 30 experimental runs consisting of ten experimental runs randomly chosen from each of the three temperature groups (see Appendix F). The results are presented in Table 5.9. Using those estimated parameters the model equations were then solved to predict response values for the remaining eighteen experimental runs.

Table 5.9. Parameter estimates for the model validation using 30 runs and a non-isothermal three-response model (R_p, $\overline{M}_w$, and $\overline{M}_n$) with two active site types and monomer diffusion, assuming a known diagonal covariance matrix (GREG *level* 22)

Parameter	Estimated value	95% confidence interval	
k_{a0} (L/mol/min)	99.01	94.33	103.93
E_a (cal/mol)	1.64E4	1.49E4	1.80E4
γ_a	1.5E-2	1.2E-2	1.8E-2
k_{p0} (L/mol/min)	4.76E5	4.72E5	4.81E5
E_{p1} (cal/mol)	2.51E3	2.30E3	2.74E3
E_{p2} (cal/mol)	1.88E3	1.69E3	2.10E3
γ_{p0}	0.52	0.47	0.58
k_{d1} (L/mol/min)	6.34	6.00	6.70
γ_d	0.99	0.92	1.07
k_{st} (L/mol/min)	0.45	0.42	0.49
k_{t0} (L/mol/min)	6.48E3	6.42E3	6.55E3
E_t (cal/mol)	3.60E3	3.40E3	3.82E3
γ_t	2.6E-4	9.3E-5	5.0E-4

Figure 5.3 compares the predicted responses with the experimental values for two runs in each temperature group. The predicted responses for each of the 18 experimental runs are found in Appendix G. It was not possible to obtain confidence intervals for the predicted responses from GREG. Therefore, 95% confidence intervals for the observed MW responses were calculated (equation (4.12)) and indicated on Figure G2. The fitted model provides marginally acceptable predictions of the polymerization rate data.

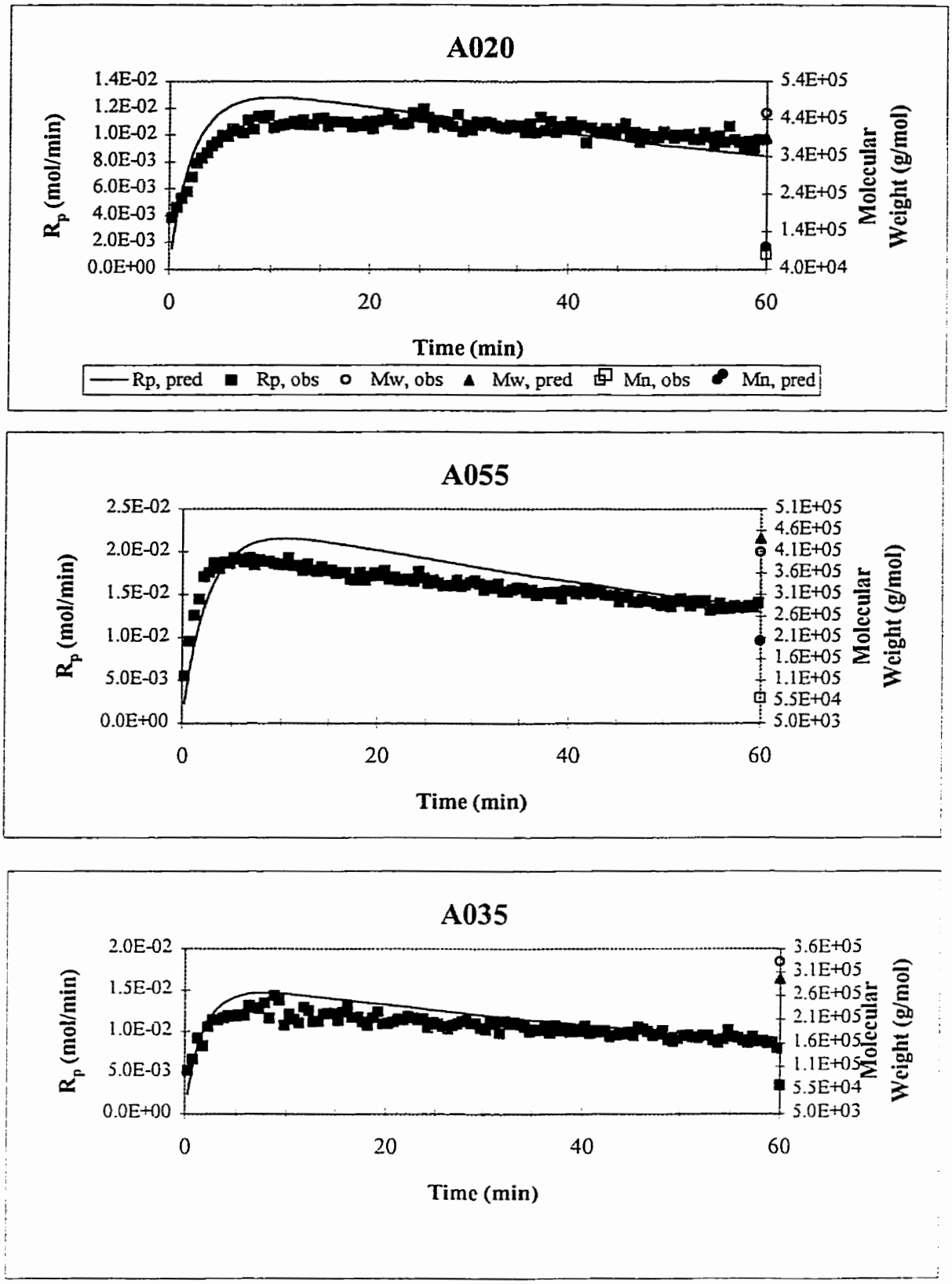

Figure 5.3. Three-response predictions for two experimental runs at each temperature group (62, 70, and 78°C) (see Appendix B for operating conditions)

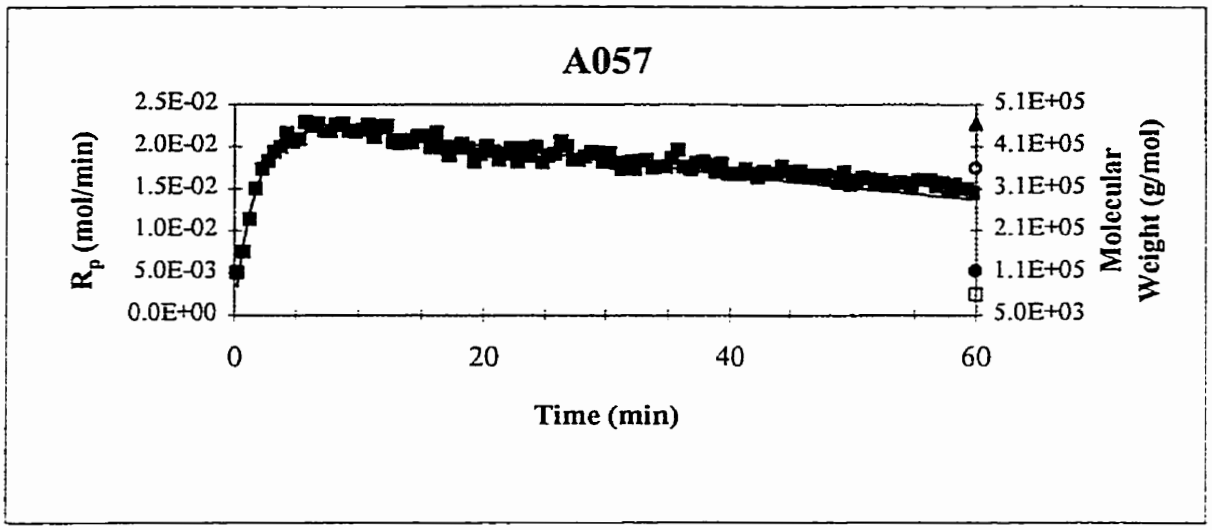

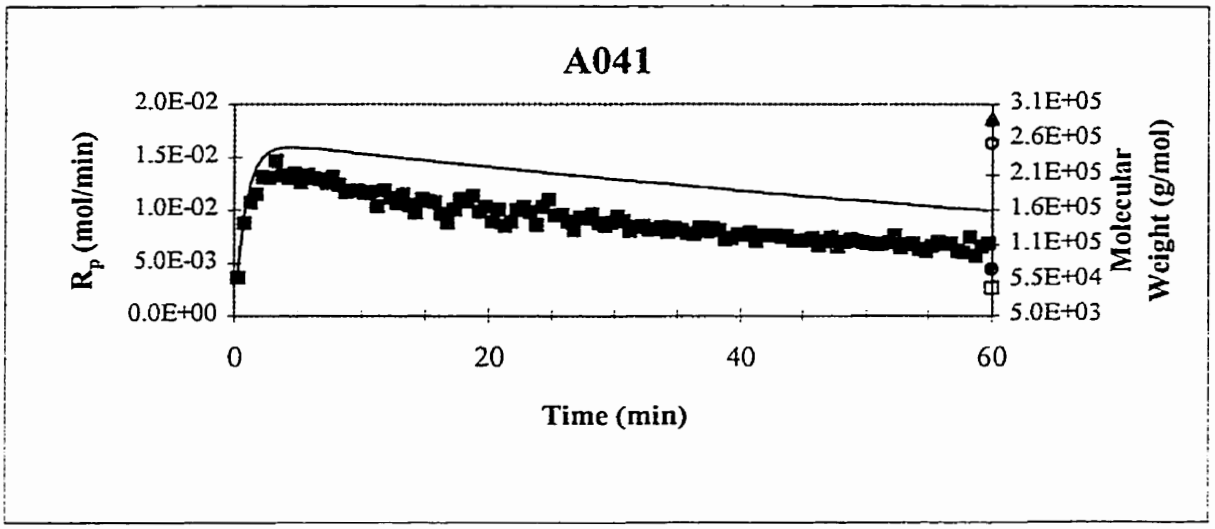

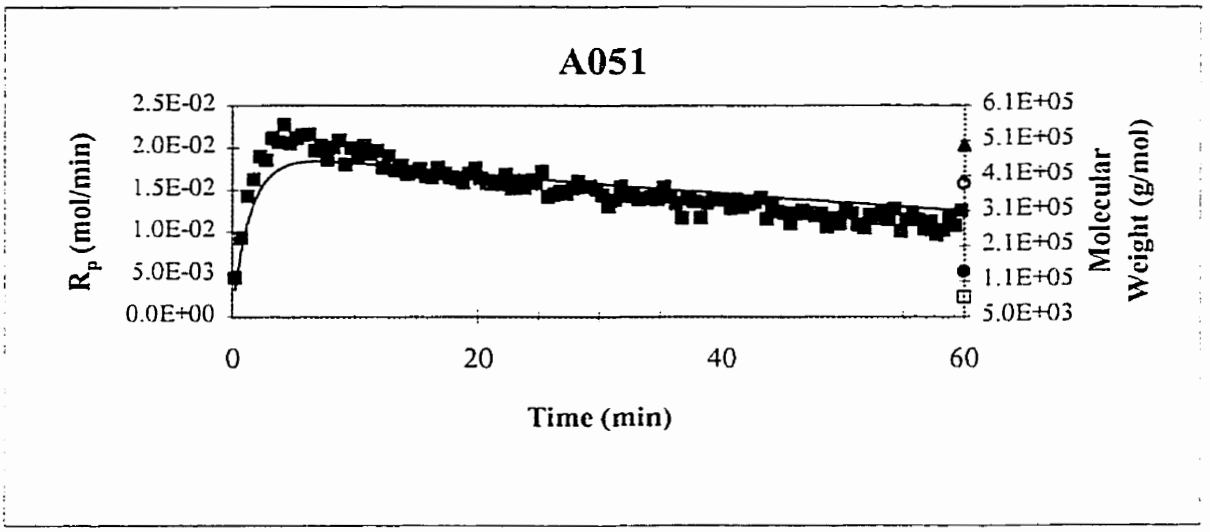

Figure 5.3. Three-response predictions for two experimental runs at each temperature group (62, 70, and 78°C), continued (see Appendix B for operating conditions)

As anticipated, the fitted model had some difficulty in predicting both $\overline{M}_w$ and $\overline{M}_n$. In this case $\overline{M}_n$ is consistently overpredicted. The estimate of the chain transfer rate constant obtained from the 30 experimental runs used to fit the model (present Section) is lower, for all temperature groups, than the estimate obtained from the 48 experimental runs (Section 5.4) ($k_{tl} = 6.48E3 \exp\left[\frac{-3.6E3}{R}\left(\frac{1}{T} - \frac{1}{343}\right)\right]$ and $k_{tl} = 6.84E3 \exp\left[\frac{-2.6E3}{R}\left(\frac{1}{T} - \frac{1}{343}\right)\right]$, respectively). With a lower k_{tl} the polymer chains propagate for a longer period of time and, consequently, a higher $\overline{M}_w$ and a higher $\overline{M}_n$ are obtained.

Chapter 6: Conclusions and Recommendations

Experimental data from Ziegler-Natta catalyzed ethylene homopolymerization reactions were fitted by various models and estimates of kinetic rate constants were obtained. From the successful parameter estimations using a missing data structure, the following conclusions can be made:

- Reactor operating data and product property data, collected at different times and frequencies during each experimental run, can be combined for parameter estimation using a missing data structure.
- Even with a severe missing data structure (5760 polymerization rate observations, 48 weight average molecular weight observations, and 48 number average molecular weight observations), significant estimates were obtained for 13 parameters in a proposed three-response model that described the non-isothermal behavior of a Ziegler-Natta catalyst with two types of sites and monomer diffusion.
- The two highest pairwise correlations between parameters in this model (k_{p0} with k_{t0} and γ_a with γ_{p0}) were found to be between parameters that should be correlated on physical grounds. Increasing both k_{p0} and k_{t0} could maintain a constant molecular and increasing γ_a while decreasing γ_{p0} could maintain a constant polymerization rate.
- The fitted model was deemed to be capable of predicting polymerization rates but had difficulty predicting both weight average molecular weights and number average molecular weights simultaneously. The estimated polydispersity values were consistently lower than the corresponding observed polydispersity values. Only 50%

of the estimated polydispersity values fell within the approximate 95% confidence intervals for the corresponding observed polydispersity values.

- Transformations of all rate constants were necessary to avoid negative estimates and to provide appropriate scaling in the isothermal and non-isothermal models with two types of sites and monomer diffusion.
- There is not enough information in the data used in this thesis to estimate certain parameters in the two types of sites models. For example, only one spontaneous deactivation rate constant (k_{sd}) could be found for both types of sites in the isothermal single-response model with two types of sites and monomer diffusion. Furthermore, two parameters (k_{ah}, k_{sd}) were found to be unnecessary in the isothermal and non-isothermal three-response models with two types of sites and monomer diffusion, as their values, along with the terms with which they were involved in the differential equations, were extremely small.

The following recommendations are made for future work:

- The number of potential active sites should be determined experimentally in order to avoid the need to estimate it since it is highly correlated with the propagation rate constant.
- An analysis of the MWDs should be conducted to determine the number of types of catalyst sites present in the Ziegler-Natta catalyst used. If there are more than two types of sites, the model should be modified to include all site types. This should produce better fits to the product property data.

- Modifications should be made to the reactor to enable polymer samples to be removed during an experimental run. Removing even a few samples during each experimental run and analyzing them to determine their product properties would diminish the severity of the missing data structure and improve the fits of the proposed models. This option would be less costly than running experimental runs for various lengths of time to characterize the polymer properties.
- The proposed model could be expanded to take into account all of the information in the molecular weight distribution (MWD). Since $\overline{M}_w$ and $\overline{M}_n$ are just two values obtained from a MWD, a complete MWD would provide a more accurate picture of the molecular weight behavior.

References

Armijo, L., "Minimization of Functions Having Lipschitz-Continuous First Partial Derivatives", Pacific J. Math., Vol. 16, 1-3 (1966)

Bard, Y., "Nonlinear Parameter Estimation", Academic Press, New York (1974)

Bartlett, M.S., "Properties of Sufficiency and Statistical Test", Proc. Roy. Soc. Series A, Vol. 160, 268 (1937)

Bates, D.M. and Watts, D.G., "Parameter Transformations for Improved Approximate Confidence Regions in Nonlinear Least Squares", The Annals of Statistics, Vol. 9, No. 6, 1152-1167 (1981)

Bates, D.M. and Watts, D.G., "Nonlinear Regression Analysis and its Applications", Wiley, New York (1988)

Biegler, L.T., Damiano, J.J., and Blau, G.E., "Nonlinear Parameter Estimation: a Case Study Comparison", AIChE Journal, Vol. 32, No. 1, 29-45 (1986)

Bilardello, P., Joulia, X., LeLann, J.M., Delmas, H., and Koehret, B., "A General Strategy for Parameter Estimation in Differential-Algebraic Systems", Computers chem. Engng, Vol. 17, No. 5/6, 517-525 (1993)

Böhm, L.L., "Reaction Model for Ziegler-Natta Catalyst Polymerization Processes", Polymer, Vol. 19, 545-552 (1978a)

Böhm, L.L., "Ethylene Polymerization Process with a Highly Active Ziegler-Natta Catalyst: 1. Kinetics", Polymer, Vol. 19, 553-561 (1978b)

Box, G.E.P. and Draper, N.R., "The Bayesian Estimation of Common Parameters from Several Responses", Biometrika, Vol. 52, 355-365 (1965)

Box, G.E.P. and Tiao, G.C., "Bayesian Inference in Statistical Analysis", Addison-Wesley, Reading, MA (1973)

Box, M.J., "A New Method of Constrained Optimization and a Comparison with Other Methods", Comput. J., Vol. 8, 42-52 (1965)

Box, M.J. and Draper, N.R., "Estimation and Design Criteria for Multiresponse Non-linear Models with Non-homogeneous Variance", Applied Statistics, Vol. 31, 13-24 (1972)

Box, M.J., Draper, N.R., and Hunter, W.G., "Missing Values in Multiresponse Nonlinear Model Fitting", Technometrics, Vol. 12, No. 3, 613-620 (1970)

Brandolin, A., Capiati, N.J., Farber, J.N., and Valles, E.M., "Mathematical Model for High-Pressure Tubular Reactor for Ethylene Polymerization", Ind. Eng. Chem. Res., Vol. 27, 784-790 (1988)

Brenan, K.E., Campbell, S.L., and Petzold, L.R., "Numerical Solution of Initial-Value Problems in Differential-Algebraic Equations", North-Holland, New York (1989)

Bukatov, G.D., Shepelev, S.H., and Zakharov, V.A., Sergeev, S.A., and Yermakov, Y.I., "Propylene Polymerization on Titanium-Magnesium Catalysts Determination of the Number of Active Centers and Propagation Rate Constants", Makromol. Chem., Vol. 183, 2657-2665 (1982)

Chien, J.C.W. and Hsieh, J.T.T., "Supported Catalysts for Stereospecific Polymerization of Propylene", J. Polym. Sci.: Part A, Vol. 14 (1976)

Chien, J.C.W. and Kuo, C-I., "Magnesium Chloride Supported High-Mileage Catalysts for Olefin Polymerization. X. Effect of Hydrogen and Catalytic Site Deactivation", Journal of Polymer Science –Polym. Chem. Ed., Vol. 24, 2707-2727 (1986)

deCarvalho, A.B., Gloor, P.E., and Hamielec, A.E., "A Kinetic Mathematical Model for Heterogeneous Ziegler-Natta Copolymerization", Polymer, Vol. 30, 280-296 (1989)

Draper, N.R. and Smith, H., "Applied Regression Analysis", Wiley, New York (1981)

Dusseault, J.J.A. and Hsu, C.C., "$MgCl_2$ Supported Ziegler-Natta Catalysts", Journal of Macromolecular Science, Reviews in Macromolecular Chemistry and Physics, C33(2), 103-145 (1993)

Edgar, T.F. and Himmelblau, D.M., "Optimization of Chemical Processes", McGraw Hill, Inc., New York (1988)

Floyd, S., Heiskanen, T., Taylor, T.W., Mann, G.E., and Ray, W.H., "Polymerization of Olefins through Heterogeneous Catalysis. VI. Effect of Particle Heat and Mass Transfer on Polymerization Behavior and Polymer Properties", Journal of Applied Polymer Science, Vol. 33, 1021-1065 (1987)

Fuguitt, R.E. and Hawkins, J.E., "The Liquid-Phase Thermal Isomerization of α-Pinene", J. of the Amer. Chem. Soc., Vol. 67, 242 (1945)

Galvan, R. and Tirrell, M., "Molecular Weight Distribution Predictions for Heterogeneous Ziegler-Natta Polymerizations Using a Two-Site Model", Chem. Eng. Sci., Vol. 41, 2385-2393 (1986)

Gear, G.W., "Numerical Initial Value Problems in Ordinary Differential Equations", Prentice-Hall, New Jersey (1971)

Grippo, L., Lampariello, F., and Lucidi, S., "A Non-monotone Line Search Technique for Newton's Method", SIAM Journal on Numerical Analysis, Vol. 23, 707-716 (1986)

Hindmarsh, A.C., LLNL Report UCRL-88007 (1982)

Hoel, E.L., Cozewith, C., and Byrne, G.D., "Effect of Diffusion on Heterogenous Ethylene Propylene Copolymerization", AIChE Journal, Vol. 40, No. 10, 1669-1684 (1994)

Keii, T., "Kinetics of Ziegler-Natta Polymerization", Kodansha Ltd., Tokyo (1972)

Kim, I., Kim, J.H., and Woo, S.I., "Kinetic Study of Ethylene Polymerization by Highly Active Silica Supported $TiCl_4/MgCl_2$", Journal of Applied Polymer Science, Vol. 39, 837-854 (1990a)

Kim, I. and Woo, S.I., "Kinetic Study for the Decay of Ethylene Polymerization Catalyzed Over Silica Supported $TiCl_4/MgCl_2$ Catalysts", Korean J. Chem. Eng., Vol. 7, 95-99 (1990b)

Kim, J.H., Kim, I., and Woo, S.I., "Computer Simulation Study of Ethylene Polymerization Rate Profile Catalyzed over Highly Active Ziegler-Natta Catalysts", Ind. Eng. Chem. Res., Vol. 30, No. 9, 2074-2079 (1991)

Kissin, Y.V., "Isospecific Polymerization of Olefins with Heterogeneous Ziegler-Natta Catalysts", Springer-Verlag, New York (1985)

Lorenzini, P., Bertrand, P., and Villermaux, J., "Modélisation de la copolymérisation éthylène α-oléfine par catalyse Ziegler-Natta", The Canadian Journal of Chemical Engineering, Vol. 69, 682-697 (1991)

Lorenzini, P., Pons, M., and Villermaux, J., "Free-Radical Polymerization Engineering – IV. Modelling Homogeneous Polymerization of Ethylene: Determination of Model Parameters and Final Adjustment of Kinetic Coefficients", Chemical Engineering Science, Vol. 47, No. 15-16, 3981-3988 (1992)

Marques, M.M.V., Nunes, C.P., Tait, P.J.T., and Dias, A.R., "Transition Metals and Organometallics as Catalysts for Olefin Polymerization", Springer-Verlag, Berlin (1988)

McAuley, K.B., MacGregor, J.F. and Hamielec, A.E., "A Kinetic Model for Industrial Gas-Phase Ethylene Copolymerization", AIChE Journal, Vol. 36, No. 6, 837-850 (1990)

Montgomery, D.C and Runger, G.C., "Applied Statistics and Probability for Engineers", Wiley, New York (1994)

Pacha, J. and Nowakowska, M., "Supported Titanium-Magnesium Catalyst for Ethylene Polymerization", Polymer Science U.S.S.R., Vol. 27, No. 9, 2067-2072 (1985)

Petzold, L.R., Sandia National Laboratories, Report SAN 808230, Livermore (1980)

Ponnuswamy, S.R. and Penlidis, A., "Batch Solution Polymerization of Methyl Methacrylate: Parameter Estimation", The Chemical Engineering Journal, Vol. 39, 175-183 (1988)

Powell, M.J.D., "Method for Minimizing a Sum of Squares of Nonlinear Functions without Calculating Derivatives", Comput. J., Vol. 7, 303 (1964)

Pritchard, D.J. and Bacon, D.W., "Prospects of Reducing Correlations Among Parameter Estimates in Kinetic Models", Chemical Engineering Science, Vol. 33, 1539-1543 (1978)

Rincon-Rubio, L.M., Wilen, C-E., and Lindfors, L-E. "A Kinetic Model for the Polymerization of Propylene Over a Ziegler-Natta Catalyst", Eur. Polym. J., Vol. 26, No. 2, 171-176 (1990)

Shariati, A., "Kinetic Modelling of Slurry Polymerization of Ethylene with a Polymer Supported Ziegler-Natta Catalyst", Ph.D. Thesis, Department of Chemical Engineering, Queen's University, Kingston, Ontario, Canada (1996)

Staha, R.L., Ph.D. Thesis, University of Texas at Austin (1973)

Stewart, W.E., "GREG: A Fortran Subroutine for Nonlinear Regression and Experimental Design; User's Manual", University of Wisconsin (1995)

Stewart, W.E., Caracotsios, M., and Sørensen, J.P., "Parameter Estimation from Multiresponse Data", AIChE Journal, Vol. 38, No. 5, 641-650 (1992)

Stewart, W.E., Caracotsios, M., and Sørensen, J.P., "Appendix A. DDASAC Software Package Documentation", University of Wisconsin, May 26 (1994)

Stewart, W.E. and Sørensen, J.P., "Bayesian Estimation of Common Parameters From Multiresponse Data with Missing Observations", Technometrics, Vol. 23, No. 2, 131-141 (1981)

Vela Estrada, J.M., and Hamielec, A.E., "Modelling of Ethylene Polymerization with Cp_2ZrCl_2/MAO Catalyst", Polymer, Vol. 35, No. 4, 808-818 (1994)

Williams, C.H., "Commissioning of an Ethylene-1-Butene Co-polymerization Reactor", M.Sc., Department of Chemical Engineering, Queen's University, Kingston, Ontario, Canada (1996)

Watts, D.G., "Estimating Parameters in Nonlinear Rate Equations", The Canadian Journal of Chemical Engineering, Vol. 72, 701-710 (1994)

Xie, T., McAuley, K.B., Hsu, C.C., and Bacon, D.W., "Gas Phase Ethylene Polymerization: Production Processes, Polymer Properties and Reactor Modeling", Ind. Eng. Chem. Res., Vol. 33, 449 (1994)

Zakharov, V.A., Bukatov, G.D., and Yermakov, Yu. I., "Coordination Polymerization", Vol. 19, Plenum Press, New York (1983)

Zhou, J.L. and Tits, A.L., "Non-monotone Line Search for Minimax Problems", Journal of Optimization Theory and Applications, Vol. 76, No. 3, 455-476 (1993)

Nomenclature

[A]	Cocatalyst concentration, mol/L
C	Number of potential active sites, mol
C_d	Deactivated catalyst site, mol
C_{0j}^*	Number of active sites of type j without monomer attached, mol
D_m	Diffusivity constant for monomer diffusion, cm^2/min
D_n	Dead polymer chain of length n, mol
E	Activation energy, cal/mol
e_j^T	Transposed error vector
e_{ui}	Errors for response i at time u (y_{ui} - $f(x_{ui},\theta)$)
F	Objective function
$f(x_u,\theta)$	Model evaluated at the values of independent variables for time u
G	Objective function
[H]	Hydrogen concentration, mol/L
k_{aj}	Activation rate constant for active sites of type j, L/mol min
k_{ah}	Rate constant for activation by hydrogen, L/mol min
k_c	Transformation rate constant, min^{-1}
k_{dj}	Deactivation rate constant for active sites of type j, L/mol min
k_i	Pseudo-rate constant of active center formation, s^{-1}
k_{pj}	Propagation rate constant for active sites of type j, L/mol min
k_{pi}	Pseudo-rate constant for species i, i=1,2, $min^{-1}psi^{-1}$
k_{sdj}	Spontaneous deactivation rate constant for active sites of type j , min^{-1}
k_{st}	Site transformation rate constant, L/mol min
k_{tj}	Chain transfer rate constant for active sites of type j, L/mol min
k_0	Rate constant at centering temperature
$\ell(\theta,\Sigma\|\mathbf{Y})$	Likelihood function
m	Total number of responses
[M]	Monomer concentration, mol/L
$[\overline{M}]$	Average monomer concentration, mol/L
$[M]_0$	Initial monomer concentration, mol/L
M_c	Catalyst load, mg
$\overline{M}_n$	Number average molecular weight, g/mol
$\overline{M}_w$	Weight average molecular weight, g/mol
MW	Molecular weight of ethylene (repeat unit)
$\overline{M}_z$	z-average molecular weight, g/mol
n	Number of experimental runs
N_c	Number of structural characteristics
n_i	Number of times response i is measured
$N_{p,i}$	Number of points used in the MWD for run i
N_{10}^*	Initial molar mass of active species of type 1, mol
p	Number of parameters
P	Pressure, psi
$\sum P_n^*$	Concentration of active sites, mol
$p(\theta,\Sigma)$	Prior density function

$p(\theta,\Sigma\|\mathbf{Y})$	Posterior density function
$p(\theta,\mathbf{Y}^{mis}\|\mathbf{Y}^{exp})$	Marginal density distribution
R	Universal gas constant, cal/mol/K
r_p	Radius of polymer particles, cm
R_p	Rate of polymerization, mol/min
$S(\theta)$ or $S(\varphi)$	Objective function
s_i^2	Sample variance for response i
t	Time, min
T	Temperature, K
T_0	Reference temperature, K
U	Bartlett's test statistic
$\mathbf{x}_u$	Independent variables for time u
Y_{uj}	Measured response j at time u
$\mathbf{W}$	Weighting matrix
z_i	Axial position for temperature measurement i

Greek Symbols

α	Armijo constant
δ_{ij}	Element ij from the unit matrix
δ_j	Weighting coefficient
δ_{MWD}	Weighting coefficient
$\Delta\upsilon_i$	Activation volume, m^3/mol
$\Im$	Fisher's information matrix
γ_i	Ratio of k_{i2} to k_{i1}, where i can be replaced by a, d, p, or t
ζ	Proportionality constant (equation 4.6), mol/mg-catalyst
λ	Relaxation factor (for GREG)
λ	Live moment of the MWD, mol
Λ	Dead moment of the MWD, mol
ρ_{P_2}	Density of polyethylene, 960 g/L
σ_i^2	Variance for response i
σ^{ij}	Element of the inverse of the covariance matrix with $i \geq j$
Σ	Covariance matrix
Σ^{-1}	Inverse covariance matrix
Σ_u	Covariance matrix obtained from Σ by inserting unit matrix element δ_{ij} when either Y_{ui} or Y_{uj} is missing
θ	Model parameter vector
θ_c	Current value of the parameter vector
θ_i^0	Frequency factor
υ	Degrees of freedom
υ_{ij}	Sums of squares and cross products of errors
φ	Vector of the model parameters and covariance matrix elements
$\omega(k)$	Weight fraction of polymer in the k^{th} fraction of the MWD

ACRONYMS

ATOL	Absolute tolerance
BNDLW	Lower boundary
BNDUP	Upper boundary
CHMAX	Maximum allowable change
CSTR	Continuously-stirred-tank reactor
DDASAC	Double precision Differential-Algebraic Sensitivity Analysis Code
'exp'	Experimental
GPC	Gel permeation chromatography
GREG	Generalized REGression analysis FORTRAN 77 subroutine
HPD	Highest posterior density
IDPROB	Problem identification variable
INFO( )	Variables set by the user in DDASAC
IR	Infrared spectroscopy
'mod'	Model
MWD	Molecular weight distribution
NMR	Nuclear magnetic resonance
PD	Polydispersity ($\overline{M}_w / \overline{M}_n$)
RPTOL	Step size tolerance
RSTOL	Objective function tolerance
RTOL	Relative tolerance
TEA	Triethylaluminum
TREF	Temperature-rising elution fractionation

Appendix A: GREG Modification

The following modification was made to the original GREG code in order to use DDASAC at *level* 22. In the subroutine GREG2X there is an IF statement which reads as follows:

IF(ITNO.EQ.1.OR.(.NOT.ALLFDD).AND.IDPROB.NE.2) THEN

The condition ".AND.IDPROB.NE.2" was removed from the IF statement since the model equations are solved numerically with DDASAC and IDPROB is equal to 2 (Section 3.3).

Furthermore, the results given at *level* 22 do not include the observations, fitted values, or residuals for the response variables. In order to display those values, a COMMON statement is required to pass the fitted values from the MODEL subroutine to the main program. The following lines were added in the main program after the call to the GREG subroutine:

```
      IF (LEVEL.EQ.22) THEN
       DO 191 K=1,NRESP
            WRITE(LUN,192) K
192         FORMAT(/5X,'RESPONSE: ',I3,//13X,'OBSERVED VALUES',
     +      8X,'PREDICTIONS',10X,'RESIDUALS')
            DO 193 I=1,NEXP
             INDEX = K+(I-1)*NRESP
             IF(PRE(K,I).NE.0.0D0) THEN
                  ERR = OBS(INDEX)-PRE(K,I)
                  WRITE(LUN,194) I,OBS(INDEX),PRE(K,I),ERR
             ENDIF
194         FORMAT(4X,I6,3X,1PD13.7,8X,1PD14.8,8X,1PD14.6)
193         CONTINUE
191    CONTINUE
      ENDIF
```

Appendix B. Polymerization conditions for ethylene homopolymerization experiments

Appendix B1. Polymerization conditions for the experimental runs at 62^0C

Run	Catalyst Load (mg)	Cocatalyst Load (mL)	Monomer Partial Pressure (atm)	Hydrogen Partial Pressure (atm)	Particle Size (μm)	Estimated Potential Active Sites (mol)
A020	8.2	1.5	2.26	0.36	325	5.8E-07
A025	12.0	0.9	2.26	0.36	325	8.5E-07
A026	12.1	0.9	1.36	0.12	325	8.5E-07
A029	12.0	0.9	2.26	0.20	177	8.5E-07
A031	8.0	0.9	1.36	0.12	177	5.6E-07
A034	12.0	1.5	2.26	0.20	325	8.5E-07
A037	8.0	1.5	2.26	0.20	177	5.6E-07
A040	8.0	0.9	2.26	0.36	177	5.6E-07
A042	12.0	0.9	1.36	0.20	177	8.5E-07
A043	12.0	1.5	1.36	0.12	177	8.5E-07
A050	8.0	1.5	1.36	0.12	325	5.6E-07
A053	8.0	0.9	2.26	0.20	325	5.6E-07
A054	8.0	0.9	1.36	0.20	325	5.6E-07
A055	12.0	1.5	2.26	0.36	177	8.5E-07
A058	12.0	1.5	1.36	0.20	325	8.5E-07
A061	8.0	1.5	1.36	0.20	177	5.6E-07

Appendix B. Polymerization conditions for ethylene homopolymerization experiments

Appendix B2. Polymerization conditions for the experimental runs at 70^0C

Run	Catalyst Load (mg)	Cocatalyst Load (mL)	Monomer Partial Pressure (atm)	Hydrogen Partial Pressure (atm)	Particle Size (μm)	Estimated Potential Active Sites (mol)
A023	10.1	2.0	2.0	0.24	250	7.1E-07
A024	14.9	1.2	2.0	0.24	250	1.1E-06
A035	10.0	1.2	2.0	0.40	250	7.1E-07
A036	10.0	1.2	1.0	0.12	250	7.1E-07
A038	9.9	0.4	2.0	0.24	250	7.0E-07
A039	10.0	1.2	2.0	0.24	250	7.1E-07
A045	10.1	1.2	2.0	0.24	420	7.1E-07
A048	5.3	1.2	2.0	0.24	250	3.7E-07
A049	10.0	1.2	2.0	0.24	250	7.1E-07
A056	9.9	1.2	2.0	0.24	250	7.0E-07
A057	10.0	1.2	3.0	0.36	250	7.1E-07
A059	10.0	1.2	2.0	0.24	125	7.1E-07
A060	10.0	1.2	2.0	0.24	250	7.1E-07
A064	10.0	1.2	2.0	0.10	250	7.1E-07
A065	10.0	1.2	2.0	0.24	250	7.1E-07
A069	9.9	1.2	2.0	0.24	250	7.0E-07

Appendix B. Polymerization conditions for ethylene homopolymerization experiments

Appendix B3. Polymerization conditions for the experimental runs at 78^0C

Run	Catalyst Load (mg)	Cocatalyst Load (mL)	Monomer Partial Pressure (atm)	Hydrogen Partial Pressure (atm)	Particle Size (μm)	Estimated Potential Active Sites (mol)
A021	8.4	1.5	2.72	0.24	325	5.9E-07
A022	12.0	1.5	2.72	0.24	177	8.5E-07
A027	12.0	0.9	1.63	0.15	177	8.5E-07
A028	8.2	1.5	2.72	0.44	177	5.8E-07
A030	12.0	0.9	2.72	0.24	325	8.5E-07
A032	8.0	1.5	1.63	0.26	325	5.6E-07
A033	12.0	1.5	1.63	0.15	325	8.5E-07
A041	12.0	1.5	1.63	0.26	177	8.5E-07
A044	12.3	1.5	2.72	0.44	325	8.7E-07
A046	8.2	0.9	2.72	0.44	325	5.8E-07
A047	7.9	0.9	1.63	0.26	177	5.6E-07
A051	8.0	0.9	2.72	0.24	177	5.6E-07
A062	12.0	0.9	1.63	0.26	325	8.5E-07
A063	12.0	0.9	2.72	0.44	177	8.5E-07
A066	8.0	1.5	1.63	0.15	177	5.6E-07
A068	8.1	0.9	1.63	0.15	325	5.7E-07

Appendix C

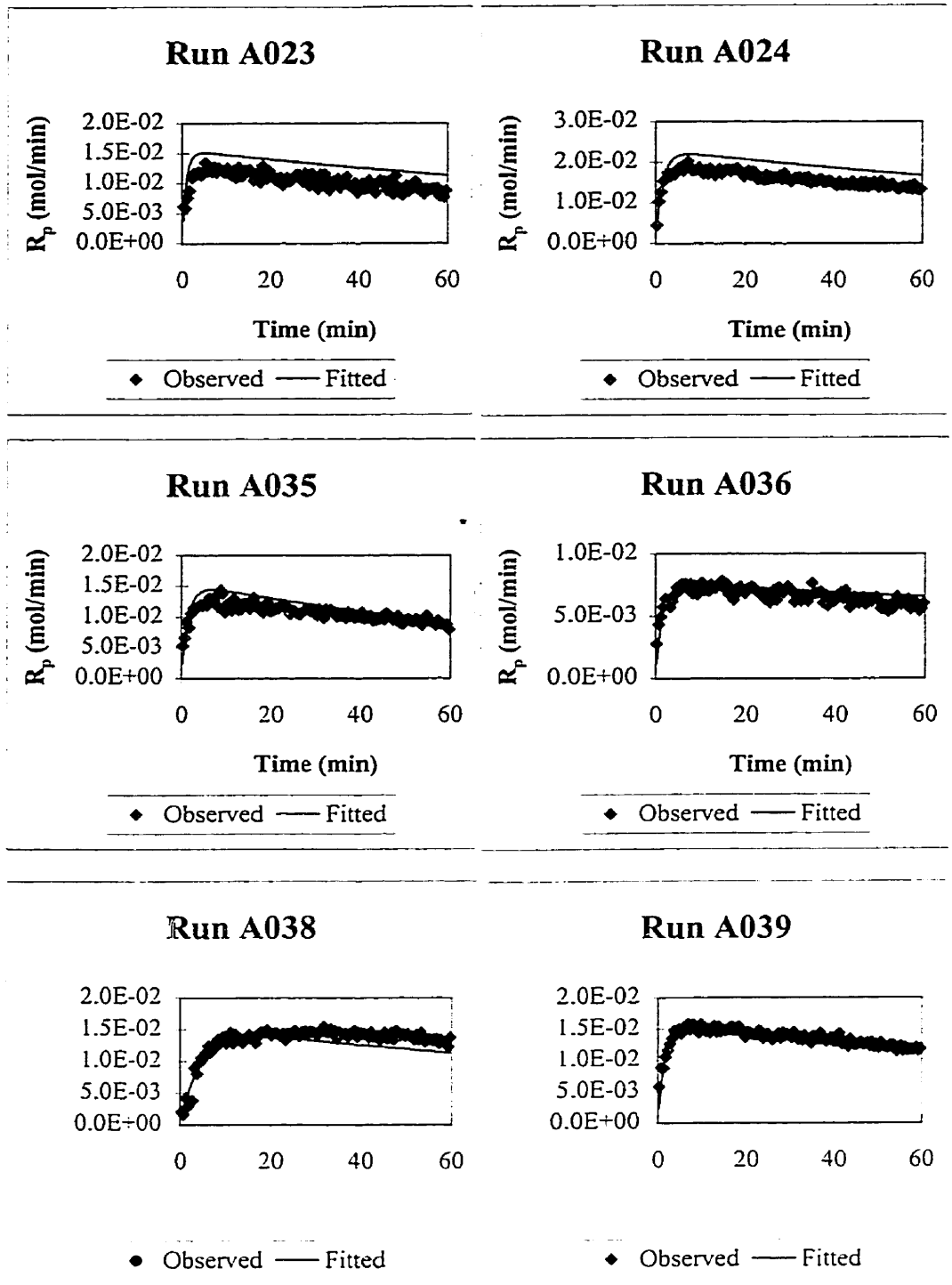

Figure C1. Fitted and observed polymerization rate values for the single response model with one type of site and no monomer diffusion at 70^{0}C

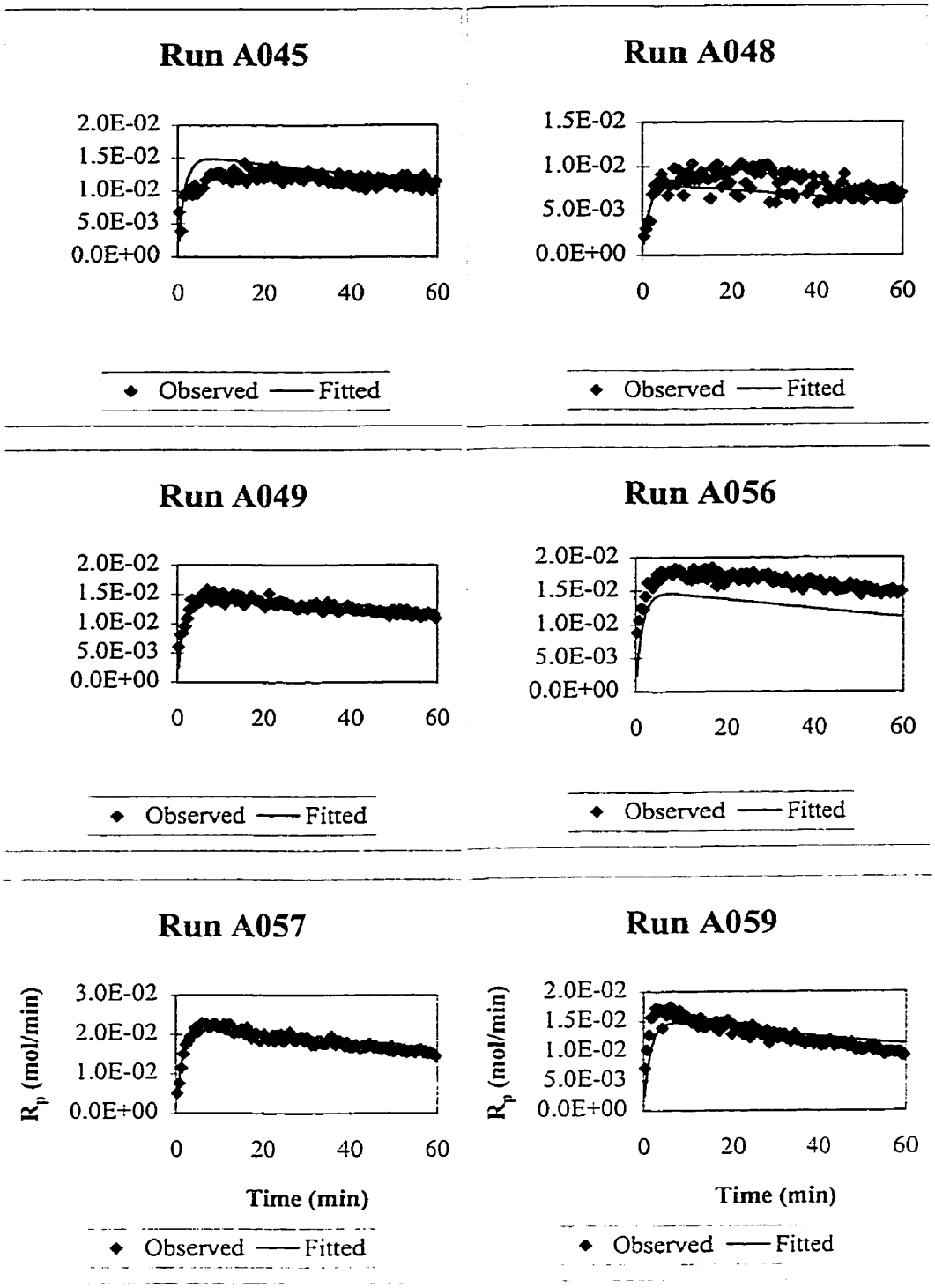

Figure C1. Fitted and observed polymerization rate values for the single response model with one type of site and no monomer diffusion at 70^{0}C (continued)

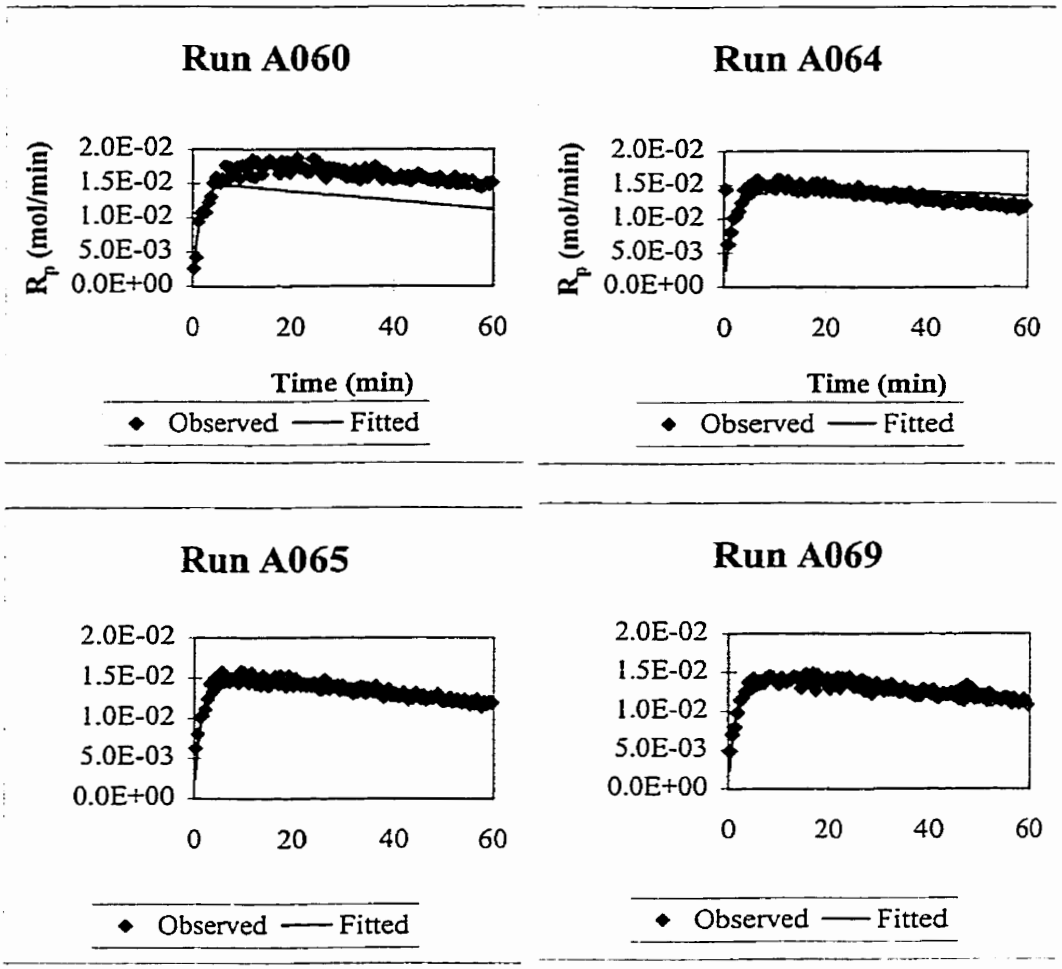

Figure C1. Fitted and observed polymerization rate values for the single response model with one type of site and no monomer diffusion at 70^0C (continued)

Appendix D

Appendix D1. Correlation matrix for the parameter estimates from a single response model at 70°C with two types of sites and monomer diffusion (corresponding to Table 5.3a)

Parameter	k_{al}	γ_a	k_{dl}	γ_d	k_{pl}	γ_p	k_{sd}	k_{ah}	k_{st}
k_{al}	1.00								
γ_a	-0.04	1.00							
k_{dl}	-0.08	0.13	1.00						
γ_d	-0.03	0.84	-0.26	1.00					
k_{pl}	-0.46	-0.08	-0.25	0.21	1.00				
γ_p	0.13	-0.81	0.18	-0.90	-0.33	1.00			
k_{sd}	0.09	-0.62	0.60	-0.88	-0.40	0.77	1.00		
k_{ah}	-0.05	0.35	-0.83	0.65	0.40	-0.68	-0.86	1.00	
k_{st}	-0.16	-0.94	0.06	-0.86	0.22	0.72	0.67	-0.41	1.00

Appendix D2. Correlation matrix for the parameter estimates from a single response model at 62°C with two types of sites and monomer diffusion (corresponding to Table 5.3b)

Parameter	k_{al}	γ_a	k_{dl}	γ_d	k_{pl}	γ_p	k_{sd}	k_{ah}	k_{st}
k_{al}	1.00								
γ_a	-0.36	1.00							
k_{dl}	-0.41	-0.28	1.00						
γ_d	-0.16	0.76	-0.49	1.00					
k_{pl}	-0.67	0.40	0.66	0.18	1.00				
γ_p	0.63	-0.79	-0.09	-0.37	-0.56	1.00			
k_{sd}	-0.31	-0.25	0.55	-0.66	0.20	-0.34	1.00		
k_{ah}	0.42	-0.88	0.27	-0.88	-0.41	0.74	-0.86	1.00	
k_{st}	-0.19	0.34	-0.42	0.70	0.01	-0.22	0.67	-0.71	1.00

Appendix E

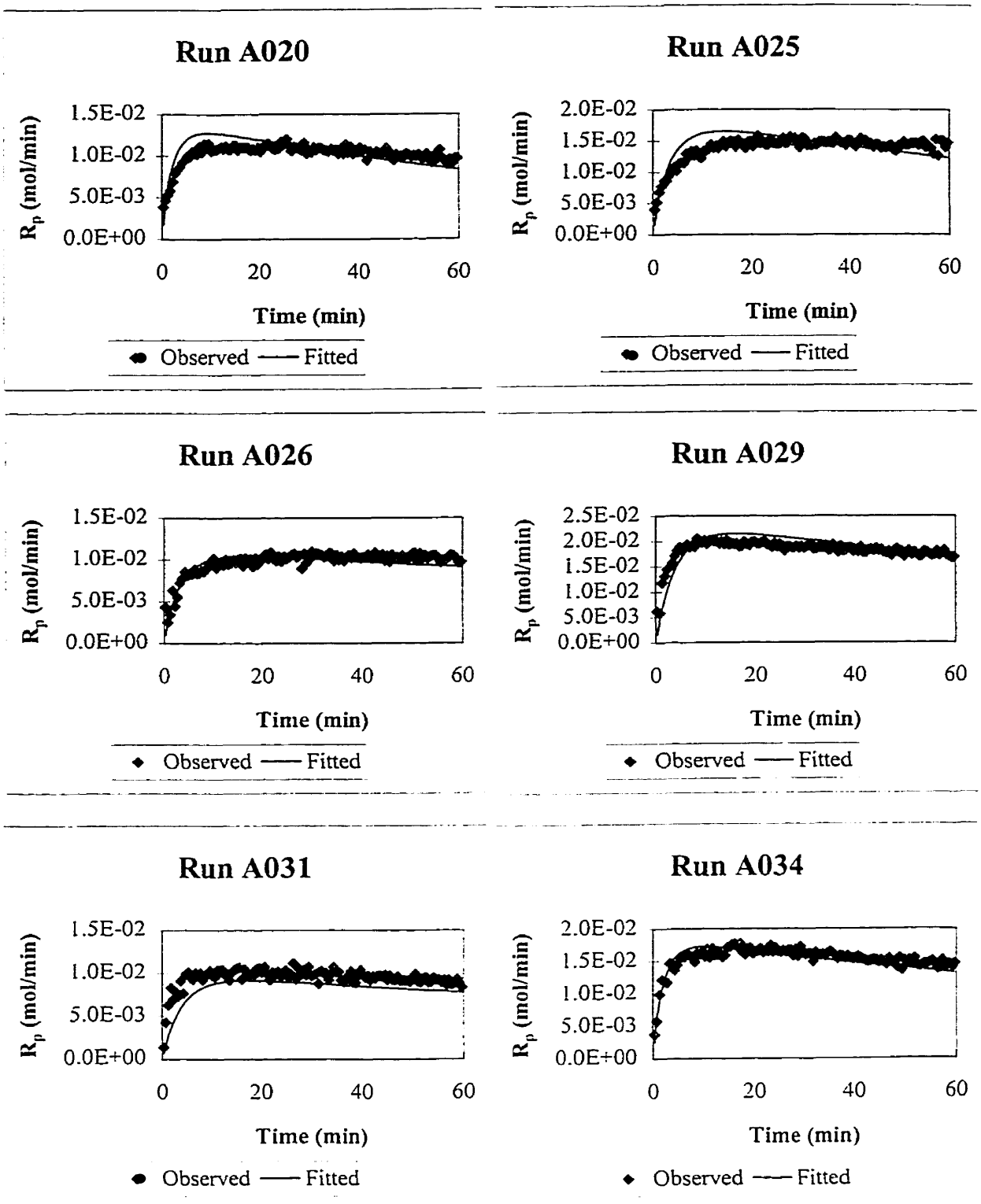

Figure E1. Fitted polymerization rate response values for the non-isothermal three-response model (R_p, M_n, and M_w) with two active site types and monomer diffusion, assuming a known diagonal covariance matrix (62^0C)

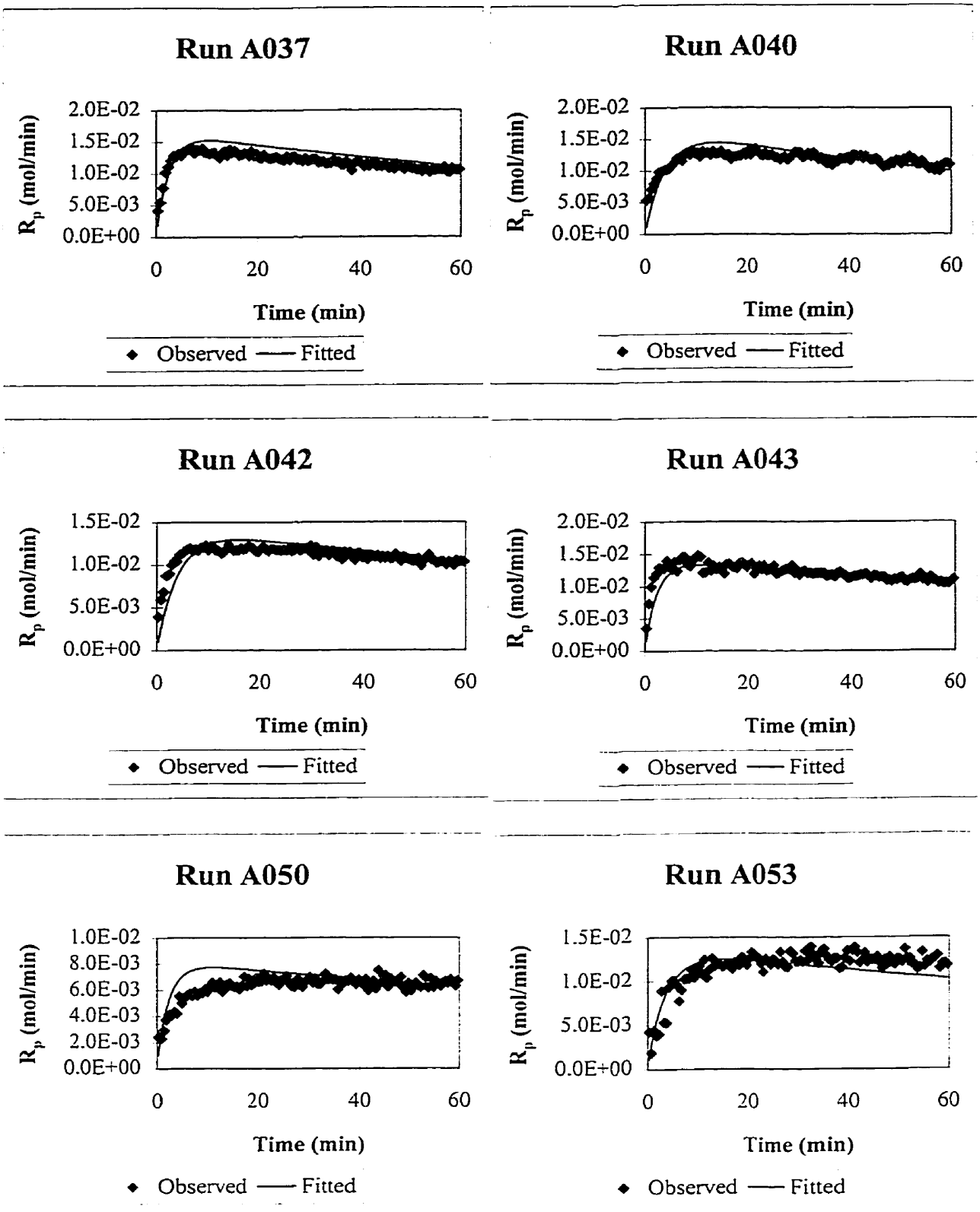

Figure E1. Fitted polymerization rate response values for the non-isothermal three-response model (R_p, M_n, and M_w) with two active site types and monomer diffusion, assuming a known diagonal covariance matrix (62^0C, continued)

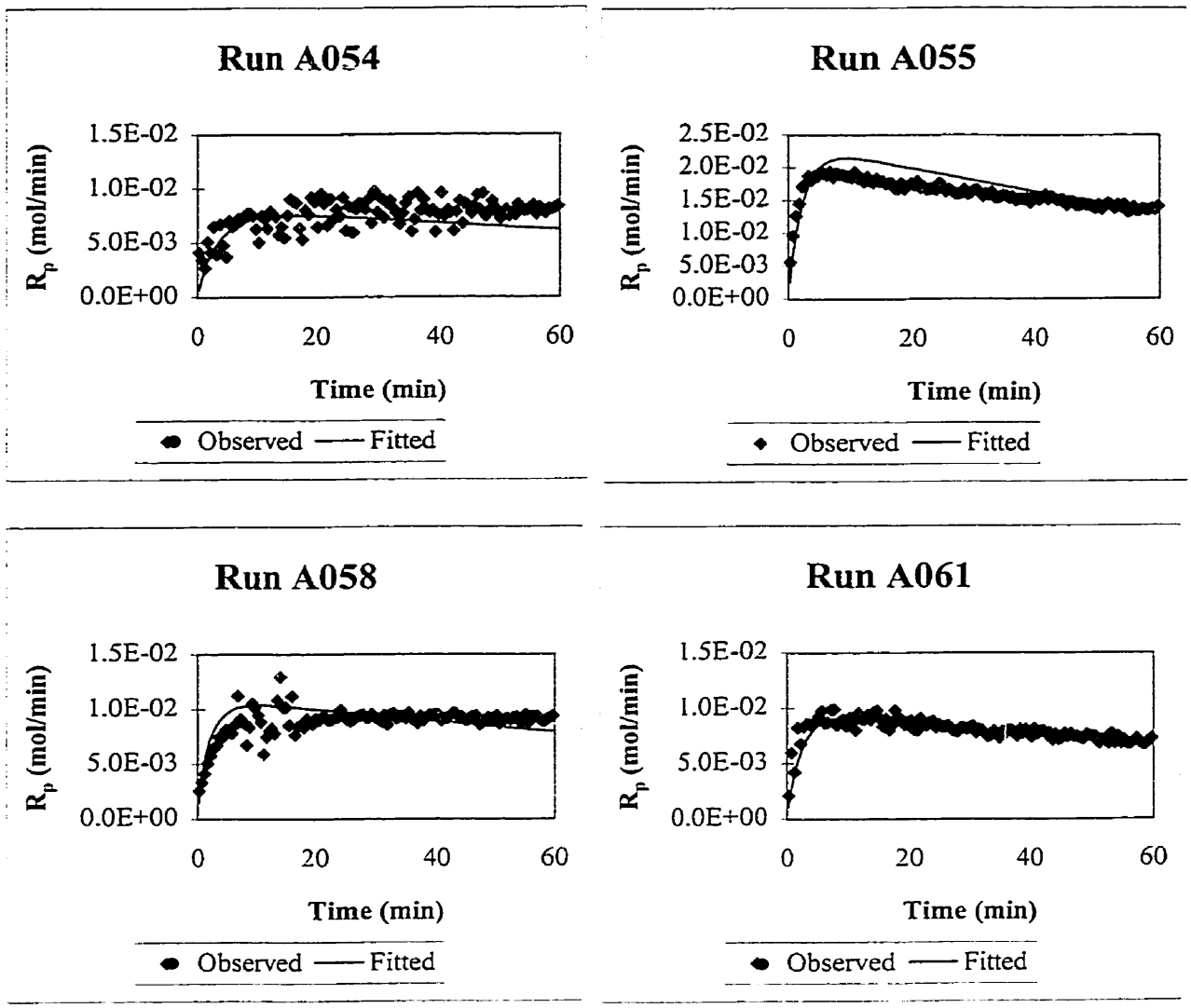

Figure E1. Fitted polymerization rate response values for the non-isothermal three-response model (R_p, M_n, and M_w) with two active site types and monomer diffusion, assuming a known diagonal covariance matrix (62^0C, continued)

Appendix E

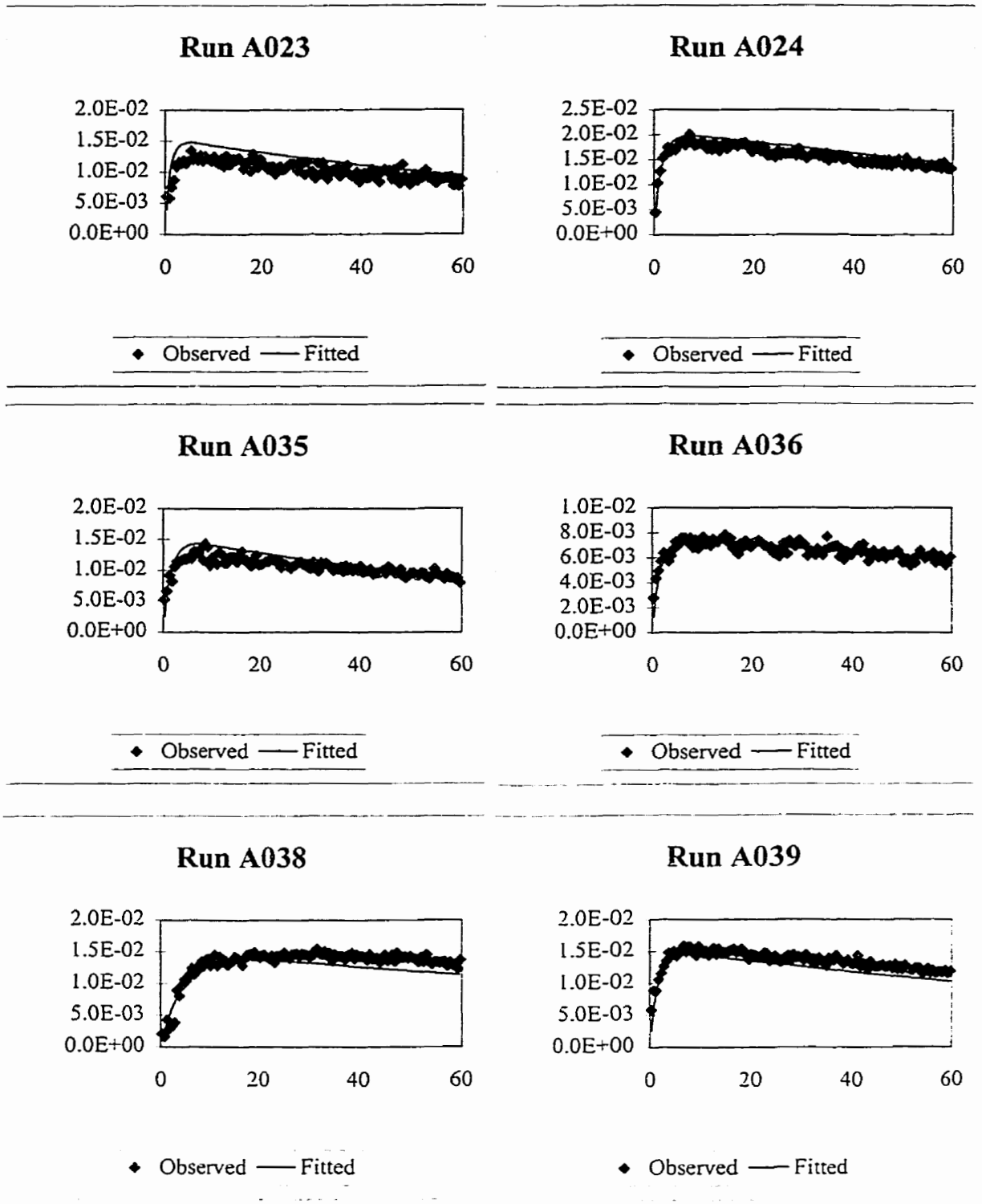

Figure E1. Fitted polymerization rate response values for the non-isothermal three-response model (R_p, Mn, and M_w) with two active site types and monomer diffusion, assuming a known diagonal covariance matrix (70^0C)

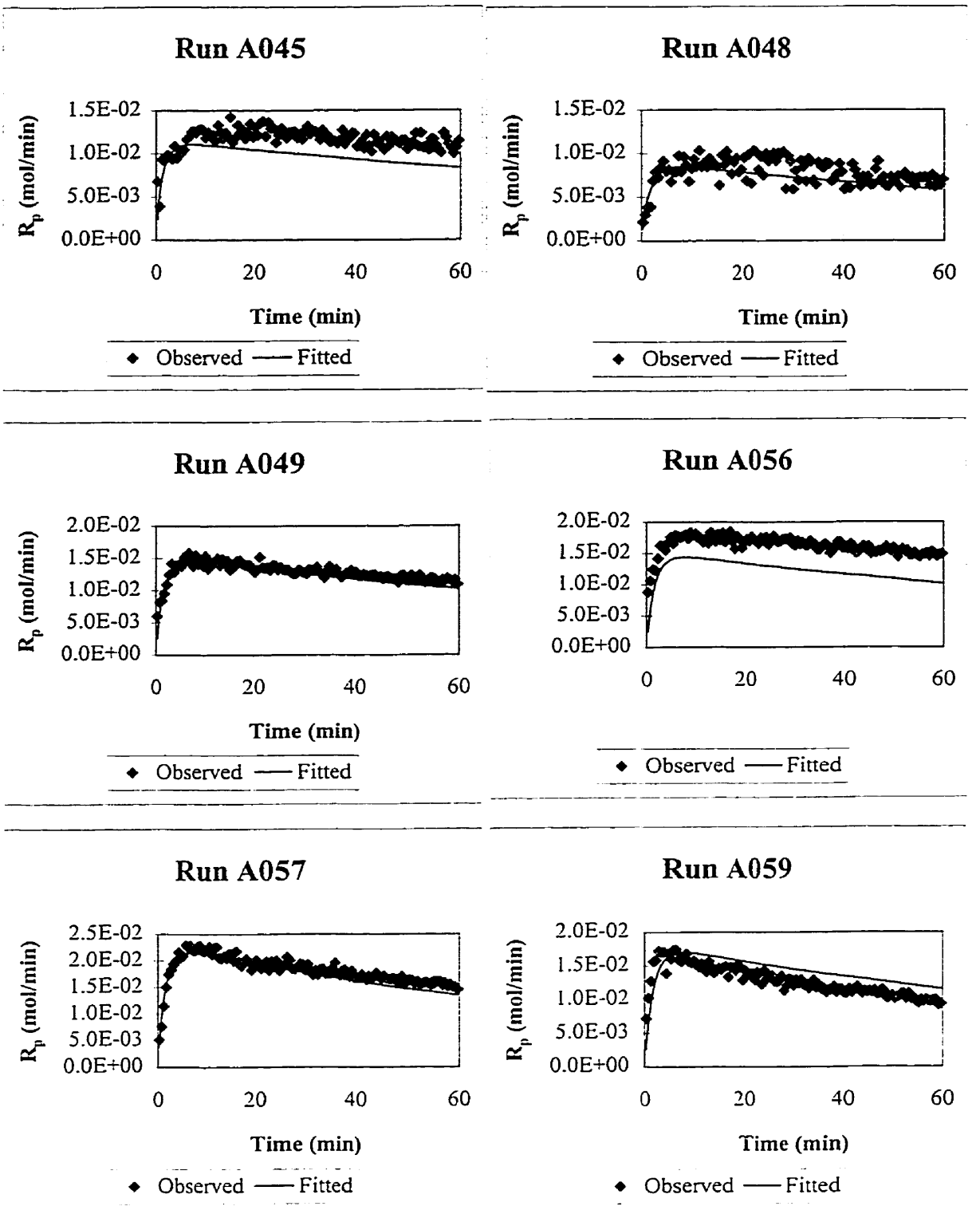

Figure E1. Fitted polymerization rate response values for the non-isothermal three-response model (R_p, Mn, and M_w) with two active site types and monomer diffusion, assuming a known diagonal covariance matrix (70^0C, continued)

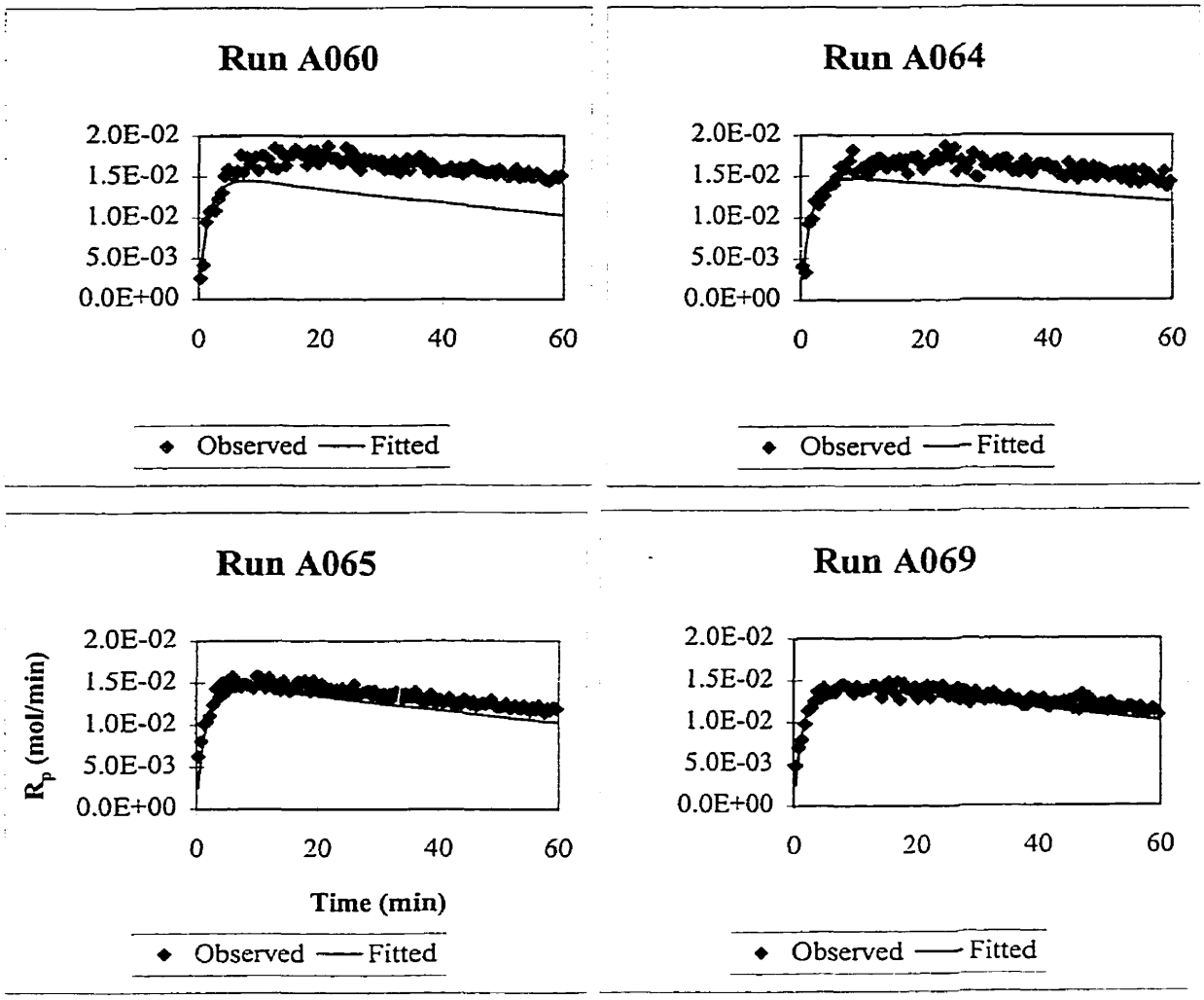

Figure E1. Fitted polymerization rate response values for the non-isothermal three-response model (R_p, Mn, and M_w) with two active site types and monomer diffusion, assuming a known diagonal covariance matrix (70^0C, continued)

Appendix E

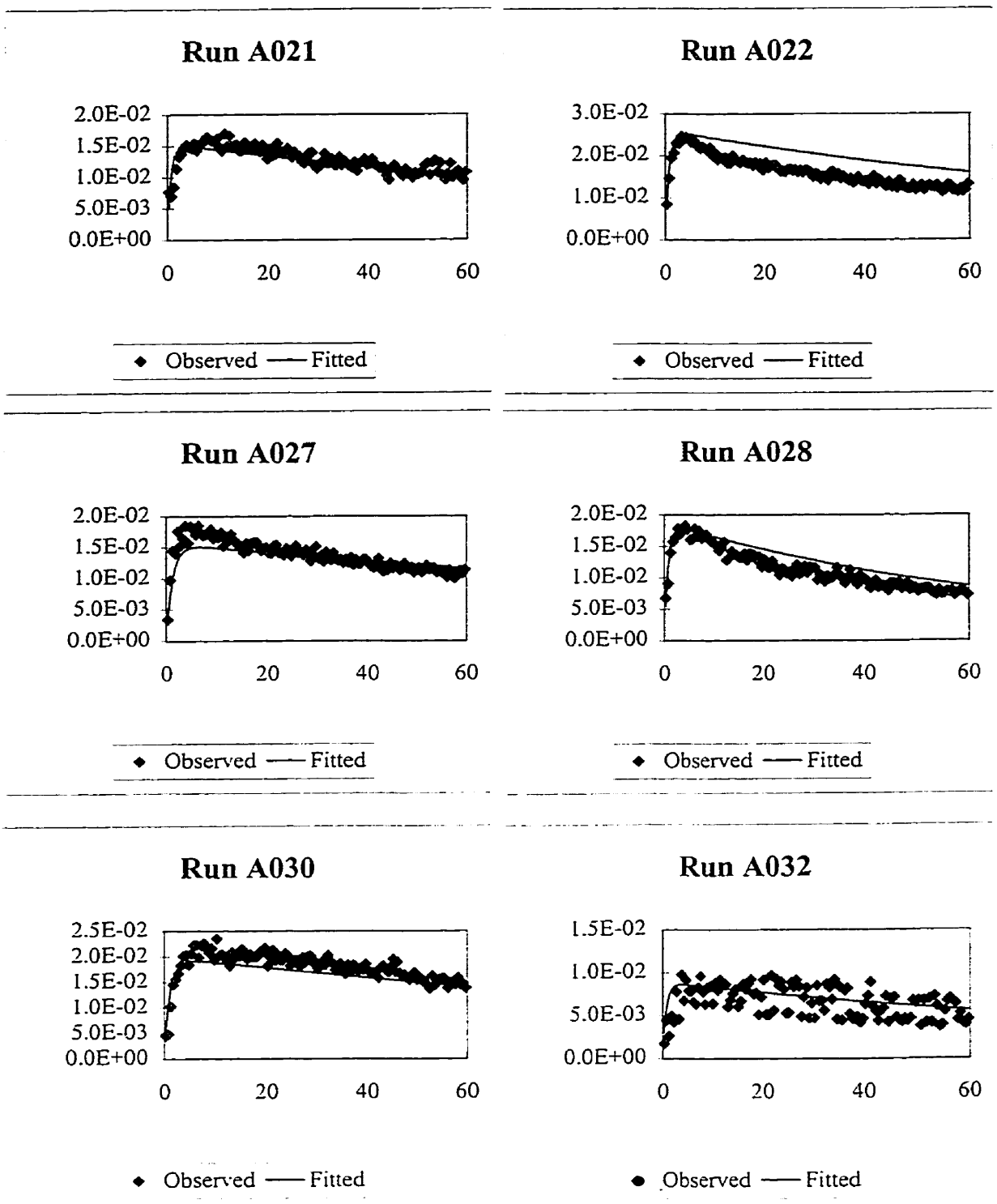

Figure E1. Fitted polymerization rate response values for the non-isothermal three-response model (R_p, M_n, and M_w) with two active site types and monomer diffusion, assuming a known diagonal covariance matrix (78^0C)

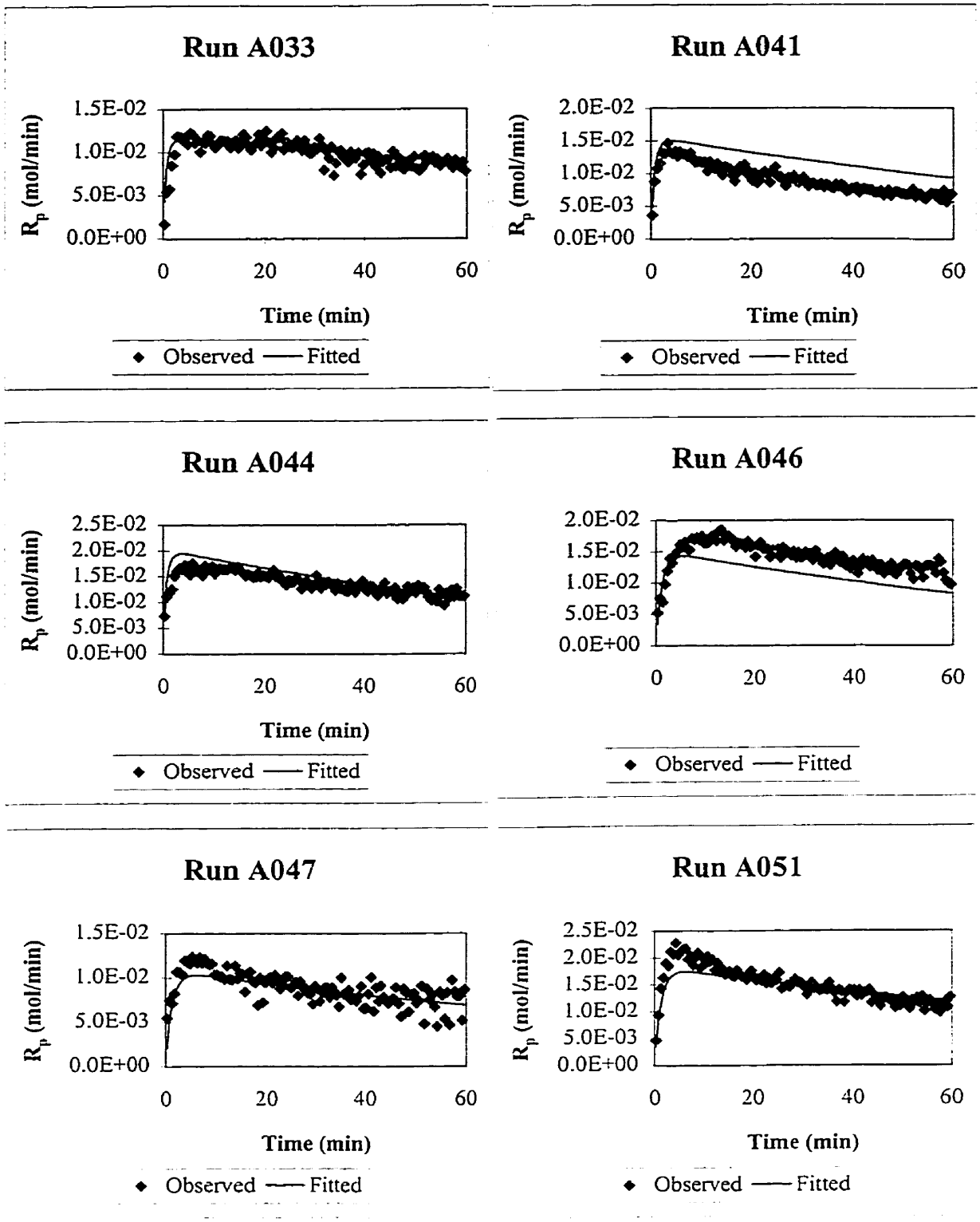

Figure E1. Fitted polymerization rate response values for the non-isothermal three-response model (R_p, M_n, and M_w) with two active site types and monomer diffusion, assuming a known diagonal covariance matrix (78^0C, continued)

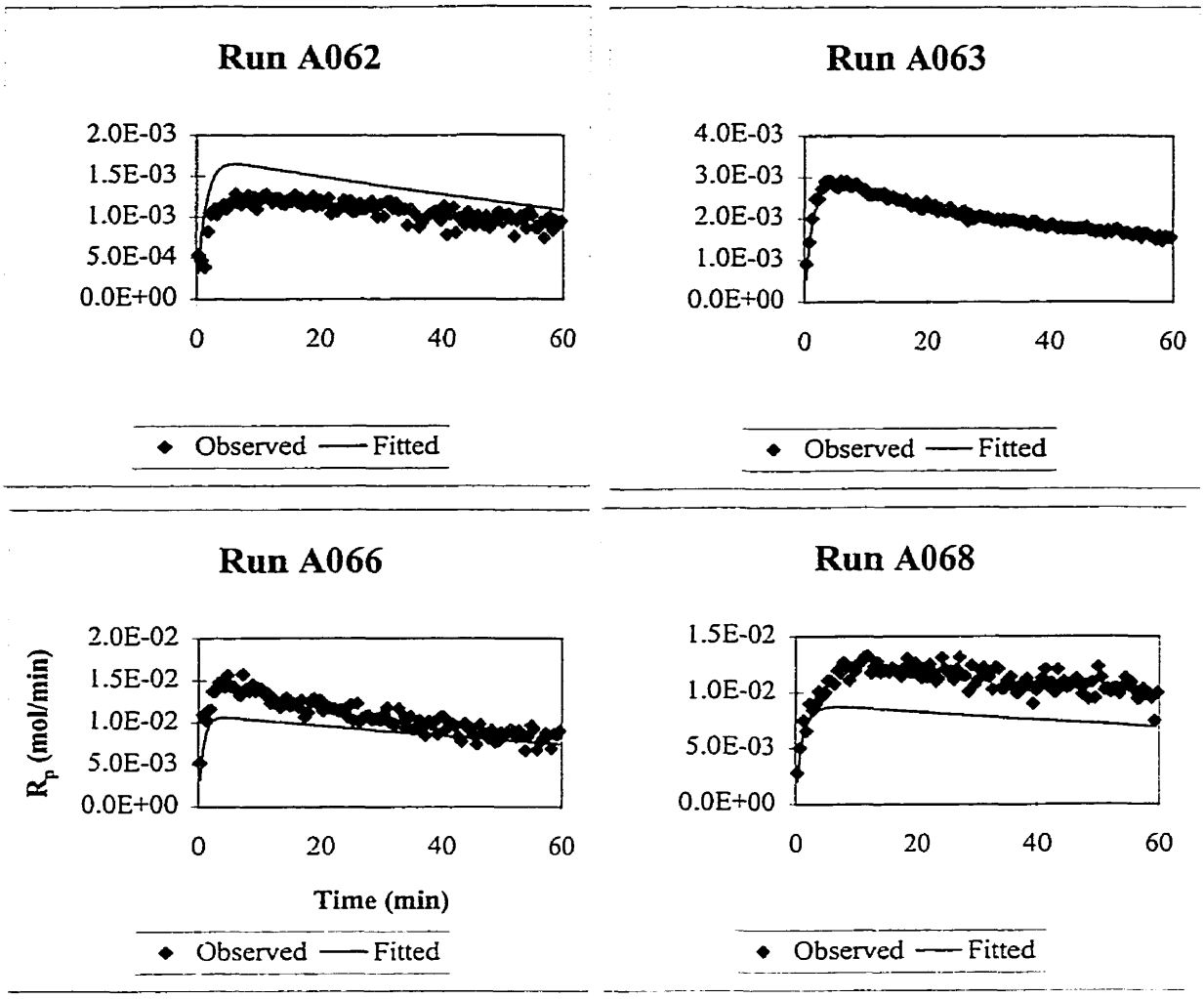

Figure E1. Fitted polymerization rate response values for the non-isothermal three-response model (R_p, M_n, and M_w) with two active site types and monomer diffusion, assuming a known diagonal covariance matrix (78^0C, continued)

Appendix F

The following were the experimental runs used to estimate the model parameters in Section 5.5.

62°C	70°C	78°C
A025	A023	A021
A026	A024	A027
A031	A036	A028
A034	A038	A032
A037	A039	A044
A042	A045	A046
A043	A048	A047
A050	A060	A062
A053	A064	A066
A054	A069	A068

The remaining eighteen experimental runs were used for the response predictions.

62°C	70°C	78°C
A020	A035	A022
A029	A049	A030
A040	A056	A033
A055	A057	A041
A058	A059	A051
A061	A065	A063

Appendix G

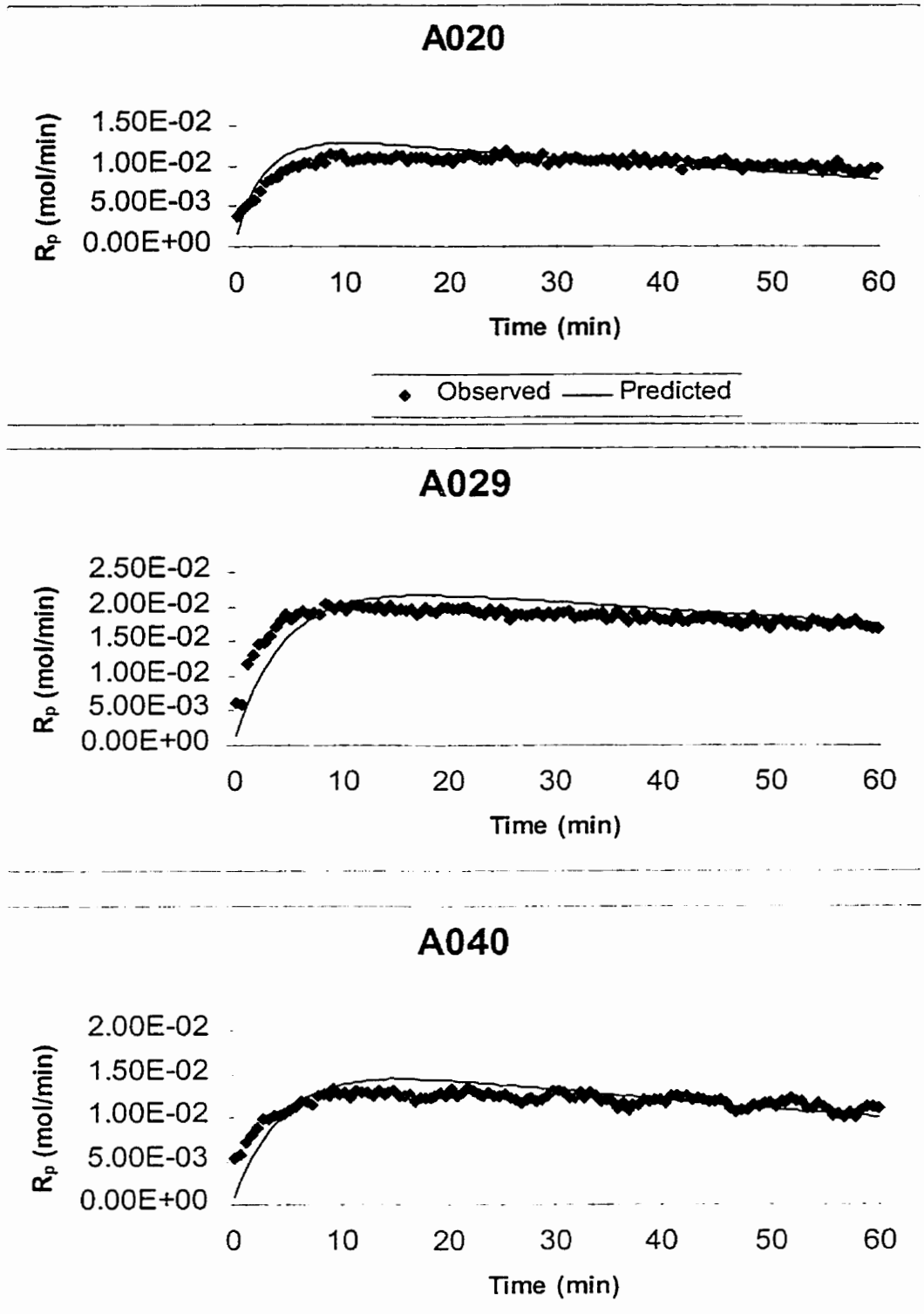

Figure G1. Predicted polymerization rate values for the non-isothermal three-response model (R_p, $\overline{M}_n$, and $\overline{M}_w$) with monomer diffusion, assuming a known diagonal covariance matrix (62°C)

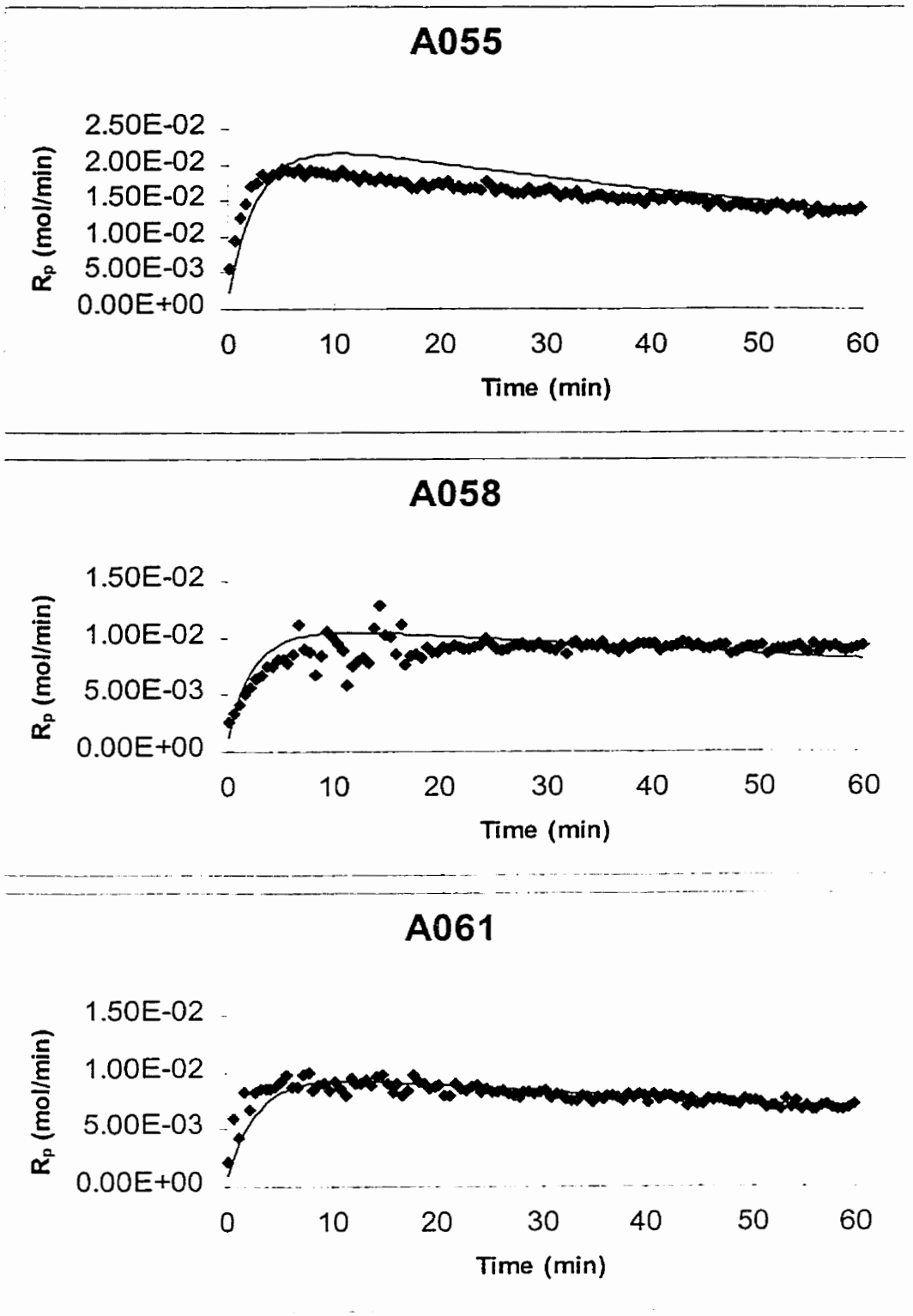

Figure G1. Predicted polymerization rate values for the non-isothermal three-response model (R_p, $\overline{M}_n$, and $\overline{M}_w$) with monomer diffusion, assuming a known diagonal covariance matrix (62°C, continued)

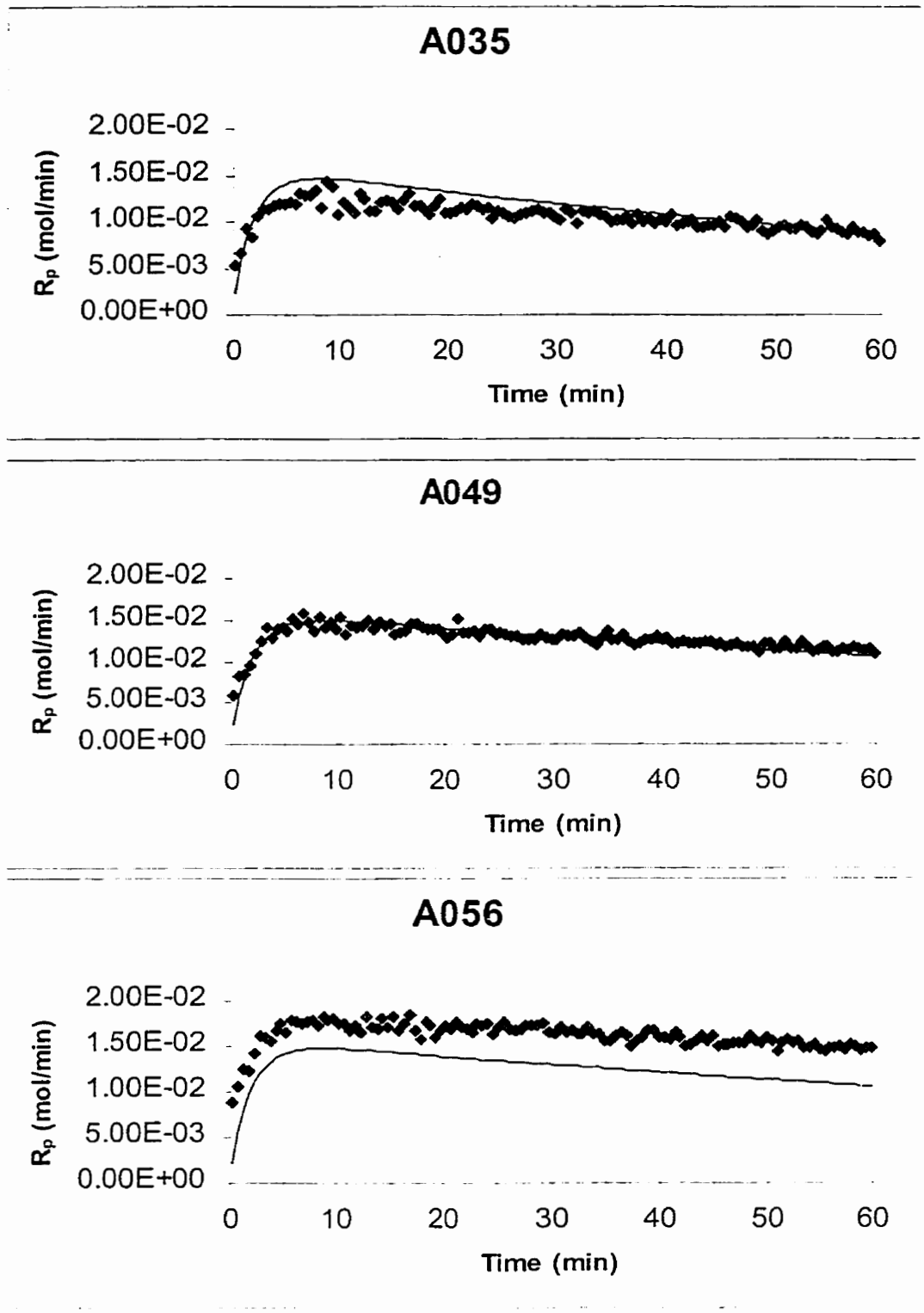

Figure G1. Predicted polymerization rate values for the non-isothermal three-response model (R_p, $\overline{M}_n$, and $\overline{M}_w$) with monomer diffusion, assuming a known diagonal covariance matrix (70°C)

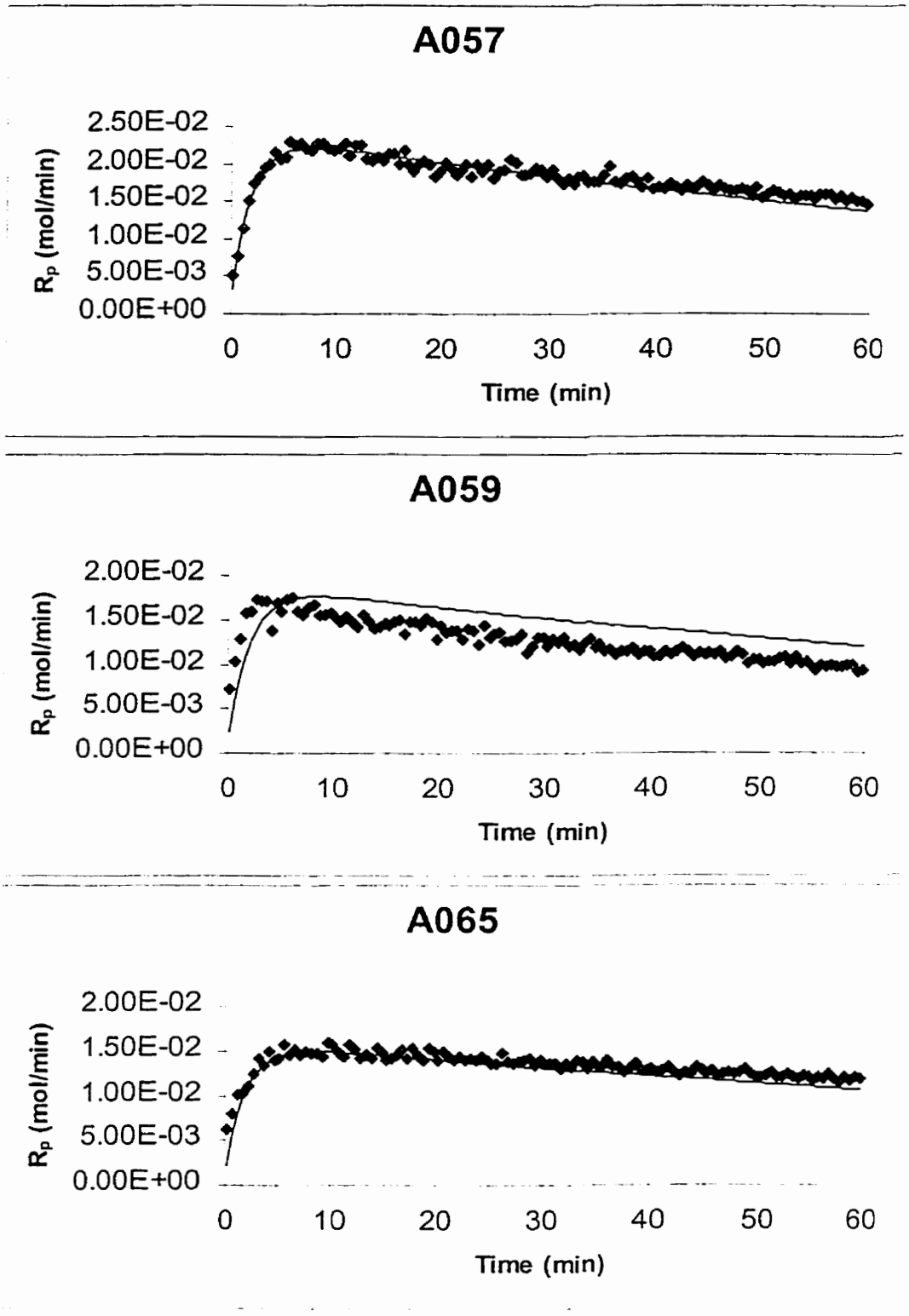

Figure G1. Predicted polymerization rate values for the non-isothermal three-response model (R_p, $\overline{M}_n$, and $\overline{M}_w$) with monomer diffusion, assuming a known diagonal covariance matrix (70°C, continued)

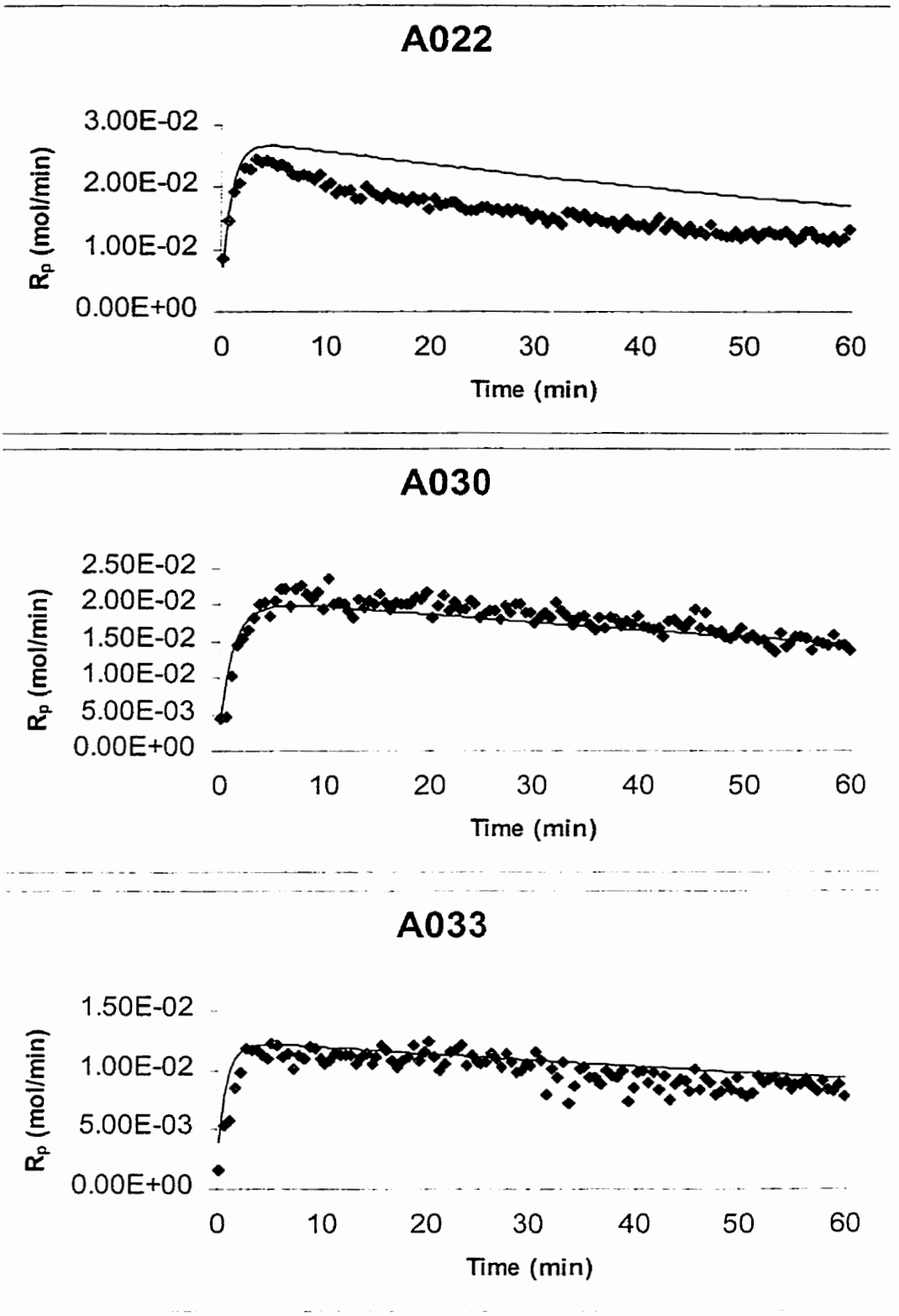

Figure G1. Predicted polymerization rate values for the non-isothermal three-response model (R_p, $\overline{M}_n$, and $\overline{M}_w$) with monomer diffusion, assuming a known diagonal covariance matrix (78°C)

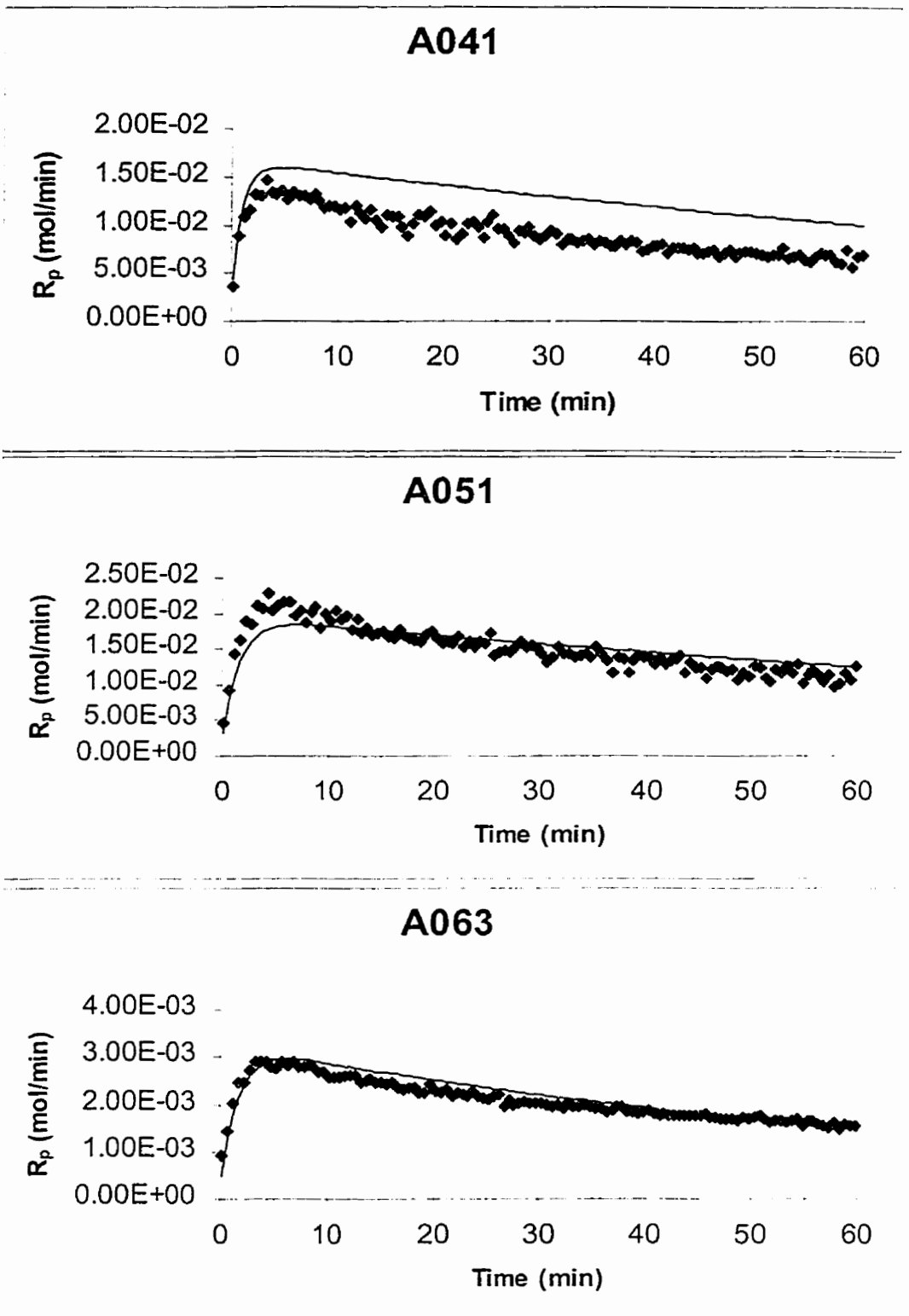

Figure G1. Predicted polymerization rate values for the non-isothermal three-response model (R_p, $\overline{M}_n$, and $\overline{M}_w$) with monomer diffusion, assuming a known diagonal covariance matrix (78°C, continued)

Appendix G

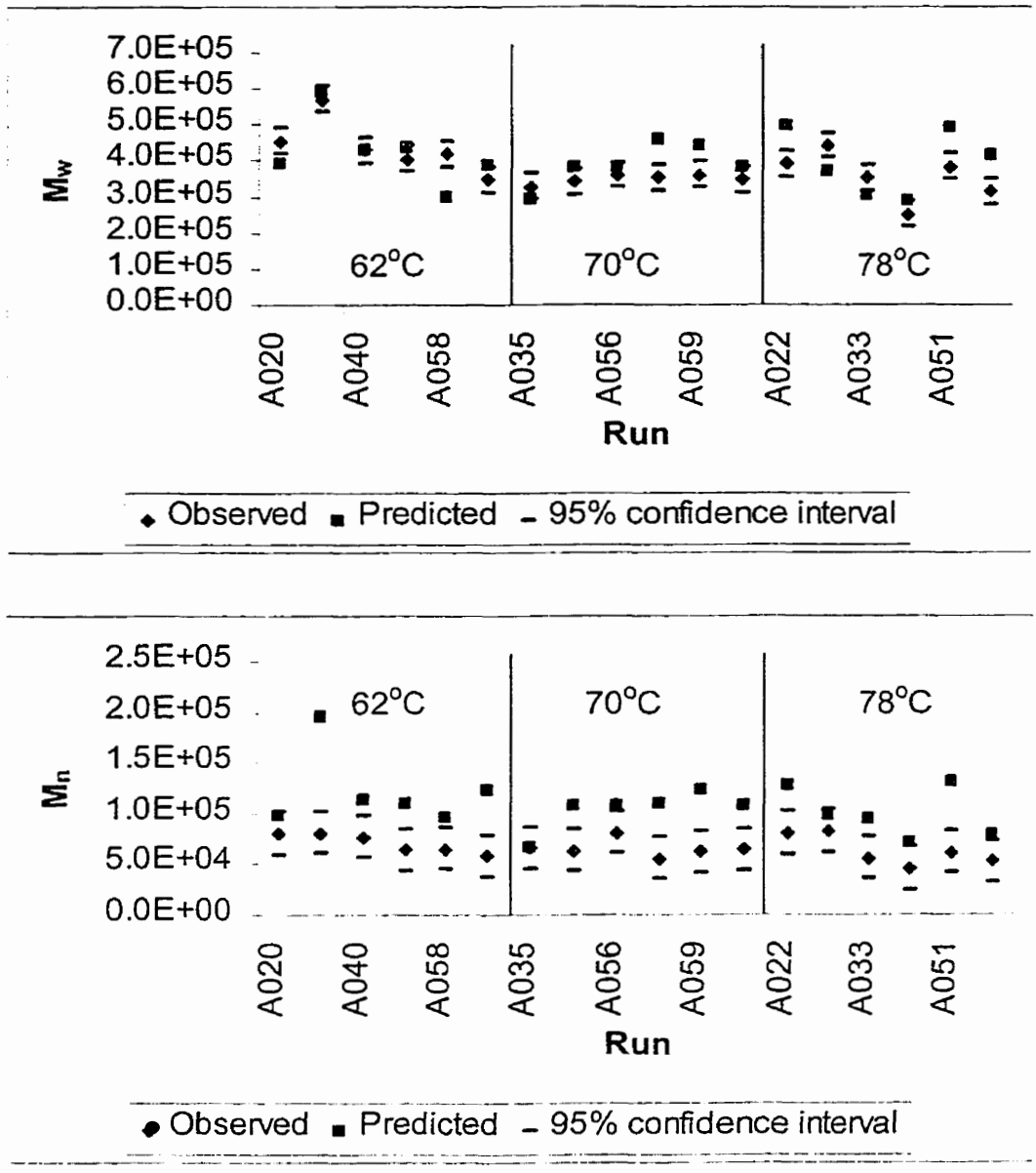

Figure G2. Predicted molecular weight values for the non-isothermal three-response model (R_p, $\overline{M}_n$, and $\overline{M}_w$) with monomer diffusion, assuming a known diagonal covariance matrix